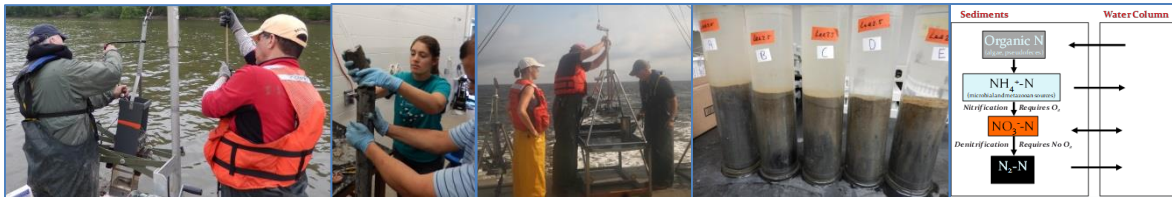


# **Exhibit 20**

# The Impact of Conowingo Particulates on the Chesapeake Bay: Assessing the Biogeochemistry of Nitrogen and Phosphorus in Reservoirs and the Chesapeake Bay

---



Investigators:

Jeffrey Cornwell, Michael Owens, Hamlet Perez, and Zoe Vulgaropulos

University of Maryland Center for Environmental Science, Horn Point Laboratory, 2020 Horn Point Road, Cambridge MD 21613

UMCES Contribution TS-703-17

Final Report to Exelon Generation and Gomez and Sullivan

July 28, 2017

# Table of Contents

- List of Tables ..... iv
- List of Figures ..... v
- Executive Summary..... x
- Introduction ..... 1
  - Program Objectives/Report Overview ..... 1
  - Background: Biogeochemical Cycling of Nitrogen and Phosphorus in Aquatic Sediments ..... 2
    - Aquatic/Estuarine N Cycling..... 2
    - Estuarine P Cycling ..... 4
- Study Chronology ..... 5
- Methods ..... 6
  - Sediment Collection ..... 6
  - Sediment-Water Exchange Experiments ..... 9
  - Pore Water and Solid Phase Chemistry ..... 10
- The Chemistry of Conowingo Deep Cores ..... 11
  - Solid Phase Chemistry..... 12
  - Pore Water Chemistry..... 20
  - Adsorbed Ammonium ..... 23
- Spatial and Seasonal Patterns of Nitrogen and Oxygen Sediment From Sediments Behind the Conowingo Dam, Maryland, USA. (Dr. Hamlet Perez) ..... 25
  - Introduction ..... 25
  - Material and Methods ..... 26
    - Study area ..... 26
    - Experimental design..... 26
    - Sediment water exchange incubation techniques..... 26
    - Solute and gas analysis ..... 27
    - Calculations ..... 27
    - Statistics and Presentation ..... 27
- Results ..... 28
  - Solid phase chemistry ..... 28
  - Sediment oxygen fluxes ..... 31

Sediment Nitrogen cycling .....	31
Discussion.....	35
Stoichiometric relationship of net sediment fluxes .....	35
Effects of Reservoir Processes on Nutrient Balances .....	37
Lake Clarke and Lake Aldred Sediment Biogeochemical Measurements .....	38
Introduction .....	38
Solid Phase and Pore Water Chemistry .....	38
Sediment-Water Exchange Rates.....	40
Sediment-Water Exchange Rates – Chesapeake Bay Fluxes.....	41
Reservoir scour as a major source of bioavailable phosphorus to a coastal plain estuary? (Zoe Vulgaropulos) .....	44
Introduction .....	44
Materials and Methods.....	46
Study Site .....	46
Reservoir Sampling .....	47
Sediment-Water Exchange Methods .....	47
Solid Phase Analyses .....	47
Flux Data Synthesis .....	47
Results.....	49
Discussion.....	56
Experimental Addition of Conowingo Sediment to Bay Sediments .....	59
2015 Experiment.....	59
Methods.....	59
Results and Discussion .....	63
Carbon and Nitrogen Production Rates - Anaerobic Diagenesis .....	66
Methods.....	67
Results and Discussion .....	68
Conowingo Biogeochemistry in Perspective.....	72
Comparison to other studies .....	72
Nitrogen Cycling – Reservoirs to the Bay.....	74
Comparative Rates.....	79

Dredging - Biogeochemical Considerations .....	80
Monitoring Recommendations .....	81
Summary .....	81
Acknowledgements.....	82
Literature Cited .....	83

## List of Tables

Table 1. Listing of major field activities for the UMCES Conowingo bottom sediment biogeochemistry program. ....	5
Table 2. Locations and sampling dates for sediment-water exchange cores in lower Susquehanna River reservoir locations. ....	7
Table 3. Locations and sampling dates for sediment-water exchange cores at Chesapeake Bay locations. ....	9
Table 4. Pore water analytical techniques .....	10
Table 5. Solid phase analyses .....	11
Table 6. Long core mean, standard deviation and median values for carbon, nitrogen and the C:N ratio. ....	14
Table 7. Site characteristics and sediment-water exchange rates in the Conowingo Reservoir. Values are means $\pm$ the standard deviation. ....	28
Table 8. Statistics for chlorophyll a concentrations in Conowingo reservoir. "All Dates" is a summation of all data from all dates, while the date-specific data consists of the 6 stations that were sampled all 5 times, allowing a fair comparison of the data. Only the May 2015 and December 2015 data are significantly different (Kruskal-Wallis P, 0.05), and there were no significant differences between stations.....	30
Table 9. Sediment amendments to Chesapeake Bay cores in cm. Bottom water salinity for each site is shown. ....	60
Table 10. Reservoir and river sediment-water exchange rates using techniques identical to this study. The studies were carried out by UMCES and Chesapeake Biogeochemical Associates (Cornwell and	

Owens 2002, Cornwell and Owens 2004, Owens and Cornwell 2006, 2008a, Owens and Cornwell 2008b, Owens and Cornwell 2009, Cornwell et al. 2017)..... 73

Table 11. Scaling of Conowingo Nitrogen Fluxes to Chesapeake Bay Fluxes..... 75

## List of Figures

Figure 1. Outline of UMCES Conowingo/Upper Bay Assessment Program (from proposal)..... 2

Figure 2. Outline of N cycling processes in aquatic sediments..... 3

Figure 3. Locations of short core collection for sediment-water exchange experiments. .... 8

Figure 4. Sampling gear. Soutar box corer used for deep sampling of surficial deposits in the Conowingo reservoir. The unit consists of a top part with the tripping mechanism (A), upon lowering a float is used to keep the device vertical in the water (B), upon retrieval cores are inserted into the lower unit (C) and 30 cm x 6.3 cm inner diameter cores (D) are collected after insertion into the core box. A core taken with a pole corer in shallow water is shown in panel E. Photos taken by Timothy Sullivan (May 2015).... 8

Figure 5. HAPS corer being readied for deployment on the R/V Rachel Carson. Inset on upper left shows flux core inserted into the HAPS core liner..... 9

Figure 6. Location of long cores (10') collected in 2015 from the Conowingo Reservoir..... 11

Figure 7. Percent water content of Conowingo deep cores. .... 12

Figure 8. Carbon concentrations in the Conowingo deep cores. To convert to percent carbon, divide the concentration by 10..... 13

Figure 9. Nitrogen concentrations in the Conowingo deep cores. .... 15

Figure 10. Molar C:N ratio in the Conowingo deep cores..... 16

Figure 11. Molar C:N ratio histogram. .... 17

Figure 12. Extractable Fe concentrations in Conowingo deep cores..... 18

Figure 13. Inorganic P concentrations in Conowingo deep cores..... 19

Figure 14. Pore water ammonium concentrations in the Conowingo deep cores. Poor water recovery in some coarse and low percent water sections resulted in no data. .... 20

Figure 15. Pore water SRP concentrations in the Conowingo deep cores. Poor water recovery in some coarse and low percent water sections resulted in no data..... 21

Figure 16. Pore water iron concentrations in the Conowingo deep cores. Poor water recovery in some coarse and low percent water sections resulted in no data..... 22

Figure 17. Adsorbed ammonium on a sediment volume basis (L or cubic decimeter) ..... 23

Figure 18. Box plot of adsorbed ammonium from all long core horizons. The solid line is the median ammonium concentration ( $40.7 \text{ mmol L}^{-1}$ ), the dotted line is the average concentration ( $38.7 \pm 22.5 \text{ mmol L}^{-1}$ ) . ..... 24

Figure 19. Concentrations of 0-1 cm carbon and nitrogen over time at 6 stations in the Conowingo reservoir (A, B) with box plots of seasonal C and N data (C,D). The “all data” box plots include the six sites in A and B as well as 2-7 more sites that were not sampled every time..... 29

Figure 20. Sediment chlorophyll a data. Concentrations are expressed on an areal basis. .... 30

Figure 21. Box plots of oxygen flux data from all sites over time..... 31

Figure 22. Seasonal box plots of nitrogen fluxes in Conowingo reservoir sediments in 2015 and 2016. Data from all stations are included in each box. .... 32

Figure 23. Box plots of all sediment water oxygen and nitrogen flux data from all sites and seasons. The inset table shows the mean, standard deviation and median of the data. The horizontal bars within the boxes are median values..... 33

Figure 24. Latitudinal Transects. (A) Scatter plot showing all net oxygen flux data calculated for individual sediment cores along a latitudinal transect during the sampling period of May-2015-April-2010 at the Conowingo Reservoir. (B) Scatter plot showing all net ammonium flux data calculated for individual sediment cores along a latitudinal transect during the sampling period of May-2015-April-2010 at the Conowingo Reservoir. (C) Scatter plot showing all net nitrate flux data calculated for individual sediment cores along a latitudinal transect during the sampling period of May-2015-April-2010 at the Conowingo Reservoir. (D) Scatter plot showing all net  $\text{N}_2\text{-N}$  flux data calculated for individual cores along a latitudinal transect during the sampling period of May-2015-April-2016 at the Conowingo Reservoir. .... 34

Figure 25. Sediment Flux Property Plots. (A) Relationship between net sediment  $\text{N}_2\text{-N}$  flux and net sediment oxygen flux for the individual cores. The 100 % line represents a Redfield ratio of  $\text{O}_2\text{:N}$  (6.6:1). (B) Relationship between the sum of all net sediment N flux ( $\text{N}_2\text{-N} + \text{NH}_4^+ + \text{NO}_3^- = \Sigma\text{N}$ ) and net sediment oxygen flux for the individual cores. The blue line represents Redfield ratio of C:N (106:16), assuming to be identical to the  $\text{O}_2\text{:N}$  ratio. (C) Relationship between the net sediment dissolved inorganic nitrogen ( $\text{DIN} = \text{NH}_4^+ + \text{NO}_3^-$ ) flux versus net sediment ammonium flux. Most of the individual cores are around the 1:1 blue line, meaning both that sediment  $\text{NO}_3^-$  fluxes were about zero or negative with a net loss to denitrification ( $\text{N}_2\text{-N}$ ). This figure also shows a strong positive Spearman correlation fit (red line) between net sediment ammonium flux and net dissolved DIN flux. (D) Relationship between

denitrification (net sediment $N_2-N$ flux) and nitrification (net sediment $N_2-N$ flux minus net sediment $NO_3^-$ flux). .....	36
Figure 26. Conowingo water discharge (USGS monitoring data). .....	37
Figure 27. Solid phase C and N concentrations and the molar C:N ratio of surficial (0-1 cm) deposits. ...	38
Figure 28. Pore water chemistry of Lake Clarke and Lake Aldred sediments.....	39
Figure 29. Sediment-water exchange rates of Lake Clarke and Lake Aldred sediments. ....	40
Figure 30. Sediment-water exchange rates from Chesapeake Bay sites, August 15, 2015. Samples were incubated at 26.4°C. Lee 3 is co-located with the long-term station Still Pond. For reference, the station locations (left to right) represent a south to north transect. ....	42
Figure 31. Sediment-water exchange rates from Chesapeake Bay sites, April 28, 2016. Samples were incubated at 14.5°C. . For reference, the station locations (left to right) represent a south to north transect. ....	43
Figure 32. Sedimentary iron (Fe), phosphorus (P), and sulfur (S) cycling in the Upper vs. Mid Chesapeake Bay. In the Upper Bay and similar oligohaline systems, iron reduction is the dominant anaerobic metabolic pathway, and P efflux is limited due to sorption to Fe oxides and precipitation of Fe(II) minerals. In contrast, in higher salinity regions such as the Mid Bay where sulfate reduction dominates, Fe is reduced by sulfides to Fe sulfides, burying Fe and allowing greater P efflux.....	45
Figure 33. Site locations for sediment-water exchange measurements. ....	48
Figure 34. Summer SRP fluxes along the Chesapeake Bay salinity gradient and Conowingo Reservoir (A) and box plots of the same flux data for each region (B).....	49
Figure 35. Relationships between summer SRP flux in the Bay mainstem and different water quality parameters: salinity, station depth, and bottom water dissolved oxygen (DO). ....	50
Figure 36. Concentration depth profiles of different phosphorus forms and iron in Conowingo Reservoir sediments.....	52
Figure 37. Relationship between concentrations of iron (Fe) and inorganic phosphorus (IP) (A) and sulfide-extractable phosphorus (sulfide-P) (B) in Conowingo Reservoir long cores. ....	53
Figure 38. Surface sediment concentrations of different P forms and iron during different seasons along the length of the Lower Susquehanna Reservoir System. ....	54
Figure 39. Spring surface sediment concentrations of total, inorganic, and sulfide-extractable P along the length of the Lower Susquehanna Reservoir System. ....	55

Figure 40. Relationship between concentrations of iron (Fe) and inorganic phosphorus (IP) (A) and sulfide-extractable phosphorus (sulfide-P) (B) in surface sediment from the Lower Susquehanna Reservoir System..... 55

Figure 41. Molar ratios of inorganic P/Fe during different seasons along the length of the Lower Susquehanna Reservoir System. .... 56

Figure 42. Site locations for the experimental cores collected August 11, 2015. .... 60

Figure 43. Cores on August 14 2015 after sediment addition. The upper cores are from Still Pond, the middle cores from Lee 2.5, and the bottom cores from S2..... 61

Figure 44. Core comparison between the initiation of the experiment on August 14 and the end on September 14..... 62

Figure 45. Time course of SRP flux from Chesapeake Bay sediment amended and control cores. .... 63

Figure 46. Molar dissolved inorganic carbon to SRP flux ratio versus depth of added Conowingo sediment for site S2. .... 64

Figure 47. Time course of SRP porewater profiles..... 65

Figure 48. Ammonium and DIC diagenesis time courses from surficial sediments (0-2 cm) collected from the Conowingo Reservoir in September 2015. Concentrations are expressed on the basis of dry mass in the incubation and are the average  $\pm$  S.D. of 4 samples. The four samples came from Sites 2, 5, 8, and 13 ..... 69

Figure 49. Ammonium and DIC diagenesis time courses from surficial sediments (0-2 cm) collected from Lake Clarke in April 2016. Concentrations are expressed on the basis of dry mass in the incubation and are the average  $\pm$  S.D. of 3 samples, one from each sample location..... 70

Figure 50. Time course of average  $\pm$  S.D. concentrations of ammonium and DIC concentrations from seven suspended samples collected in February 2016. Concentrations are expressed on the basis of dry mass in the incubation. The much higher concentrations per gram relative to sediment incubations reflects the much higher water volumes relative to the amount of sediment. .... 71

Figure 51. Sediment oxygen demand as a function of latitude in April 2016. Note the sign reversal from previous oxygen flux plots. The average rate at all sites was  $763\pm 387 \mu\text{mol m}^{-2} \text{h}^{-1}$ . Though all measurements were made in April, temperatures were different at the time of sampling, with  $T = 9.6^\circ\text{C}$  in the Conowingo Reservoir,  $T = 14.5^\circ\text{C}$  at Bay sites, and  $T = 18.0^\circ\text{C}$  at Lakes Clarke/Aldred..... 76

Figure 52. Conowingo sediment oxygen demand as a function of incubation temperature. Only sites with data from all 5 dates were used in the analysis. Each individual core is plotted. Average rates in May 2015 are almost twice the other rates at similar temperatures. .... 77

Figure 53. Spring 2016 sediment-water nitrogen exchange rates as a function of latitude. The average  $N_2-N$ ,  $NH_4^+$  and  $NO_x^-$  flux rates were  $104 \pm 54$ ,  $52 \pm 59$  and  $-34 \pm 81 \mu\text{mol m}^{-2} \text{h}^{-1}$  respectively. Though all measurements were made in April, temperatures were different at the time of sampling, with  $T = 9.6^\circ\text{C}$  in the Conowingo Reservoir,  $T = 14.5^\circ\text{C}$  at Bay sites, and  $T = 18.0^\circ\text{C}$  at Lakes Clarke/Aldred..... 78

Figure 54. Pie chart of sediment-water ammonium fluxes from reservoirs and the Maryland mainstem bay. The sum of all fluxes is  $3,604 \times 10^6 \text{ moles y}^{-1}$ , or 111,136,564 lbs N per year. In this plot, it is assumed that the annual ammonium flux per  $\text{m}^2$  in Lakes Clarke and Aldred are the same as in the Conowingo reservoir..... 79

## Executive Summary

Measurements of biogeochemical concentrations and rate processes were made in the Conowingo Reservoir, upper reservoirs (Lake Clarke, Lake Aldred) and the upper Chesapeake Bay in 2015 and 2016. The assessment program consisted of measurements of sediment-water exchange, pore water and solid phase chemical profile measurements, estimates of organic matter reactivity, and measurements of adsorbed ammonium.

Sediment-water exchange measurements were made at multiple sites in the Conowingo Reservoir on 5 occasions; modest rates of oxygen uptake, ammonium efflux and nitrate uptake were observed, with high rates of denitrification on some dates. Overall rates were comparable to measurements in the upper Chesapeake Bay. Long (10') cores showed considerable variability in grain size, carbon, nitrogen and phosphorus concentrations. Pore waters were characterized by high dissolved iron, low concentrations of soluble reactive phosphorus, and variable concentrations of ammonium. Measurements of organic matter reactivity showed modest rates of C and N regeneration, with water column particulates having a reactivity >10 times that of bottom sediments.

The sediment-water exchange rates of phosphorus in Conowingo Reservoir, Lake Clarke and Lake Aldred were very low, suggesting that the abundant iron oxides were highly efficient at P retention. Low pore water phosphorus concentrations were observed, likely from a combination of adsorption and iron phosphate mineral formation. A sulfide extraction technique was developed to simulate the diagenetic remobilization of inorganic phosphorus bound to iron oxides. The sulfide-extractable comprised ~25% of total P in Conowingo sediment deposits. With low yields of P from upper bay sediments evident from sediment-water exchange measurements, combined with only modest potential P effluxes from mid-bay sediments, these results reinforce the bay model predictions that P from scours would not have a large effect on the Chesapeake Bay.

Nitrogen recycling as ammonium in the Conowingo Reservoir would contribute <1% of the ammonium regenerated in the upper Chesapeake Bay. The Conowingo reservoir has an area < 1% of Maryland's mainstem bay, and a complete movement of the organic matter metabolism from the reservoir to the bay would result in a < 1 % increase in nutrient remineralization and flux. Observations of high adsorbed ammonium in Conowingo Reservoir sediments showed surprising high values; scour of these deposits into the Chesapeake Bay might contribute ammonium in an amount equivalent to 2% of average annual N inputs.

## Introduction

### Program Objectives/Report Overview

The motivation for this assessment program was to supplement the information in the Lower Susquehanna River Watershed Assessment (LSRWA) with new information on nitrogen and phosphorus cycling in the Conowingo Reservoir and the upper Chesapeake Bay. This additional data was requested by the Maryland Department of Natural Resources (MDDNR) and Maryland Department of the Environment (MD) to better evaluate Exelon Generation's application for a water quality certification.

The LSWRA work examined the effects of increased scour on the Chesapeake Bay. The broad premise is that infilling of the Conowingo Reservoir has led to lower trapping of suspended particulates and a dynamic equilibrium in which deposition of sediments into the reservoir is balanced by large scale scour of sediments under high flow conditions (Hirsch 2012, Cerco 2016, Zhang et al. 2016). Erosion during tropical storm Lee resulted in substantial deposition of sediments in the upper Chesapeake Bay (Palinkas et al. 2014). Input of scour scenarios in the Chesapeake Bay Model resulted in small losses of dissolved oxygen in several mid-bay model segments (Linker et al. 2016). Despite the relatively low effect of the modeling changes on oxygen, these effects were thought to create additional difficulties for achieving the Total Maximum Daily Load (TMDL) goals of the Chesapeake Bay Program. Refinement of model parameters was an important goal of the current assessment.

The UMCES program (Figure 1) was one component of the overall assessment, with substantial water quality efforts provided by Exelon and its contractors, the United States Geological Survey (USGS), and MDDNR. The University of Maryland Center for Environment Science (UMCES) program elements included biogeochemical characterization (this project), geological characterization of bed deposits, hydraulic characteristics of suspended materials, sediment modeling and modeling of sediment transport processes in the upper Chesapeake Bay.

The biogeochemistry program consisted of 4 main elements:

1. Seasonal measurement of sediment-water exchange of nutrients and oxygen ("fluxes) in the Conowingo Reservoir. In addition, flux measurements were made in the upper reservoir pools (Lake Aldred, Lake Clark) and the upper Chesapeake Bay.
2. Characterization of pore water and solid phase chemistry on short and long cores from the Conowingo Reservoir.
3. Determination of the reactivity of Conowingo sediments using anaerobic incubations of bottom and suspended sediments.
4. Experiments using Conowingo sediment additions to bay sediments.

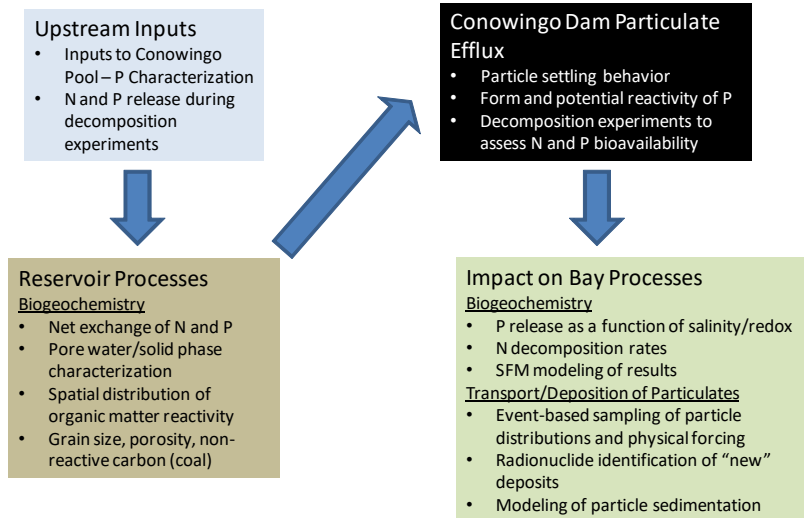


**Figure 1. Outline of UMCES Conowingo/Upper Bay Assessment Program (from proposal).**

The key part of this characterization of biogeochemical processes, in comparison to the LSWRA assessment, was the measurement of *biogeochemical rate processes*. This information is useful for assessing the impact of Conowingo bed deposits on the composition of the water flowing through the reservoir, as well as potential Chesapeake Bay impacts.

The results presented in this report are organized into sections that are complete and ready for journal submission, as well as sections dominated by data presentation. Consistent with the mission of UMCES, two of the detailed sections were written by 1) a graduate student (Zoe Vulgaropulos) and 2) a post-doctoral researcher (Dr. Hamlet Perez) who had previously carried out similar sediment flux work in a hypereutrophic lagoon as part of his work at the University of Puerto Rico Rio Piedras (Perez-Villalona et al. 2015).

## Background: Biogeochemical Cycling of Nitrogen and Phosphorus in Aquatic Sediments

The cycling of nitrogen and phosphorus in aquatic sediments depends on: the source and quality of organic matter; overlying water characteristics including pH, nutrient and dissolved oxygen concentrations; animal impacts such as bioirrigation, bioturbation and filtration; sediment grain size; dark/illuminated conditions; and temperature. Consequently, a broad range of sediment-water exchange rates are observed in lakes, reservoirs and estuaries. A broad background narrative on sediment N and P cycling follows here.

### Aquatic/Estuarine N Cycling

The sedimentary cycle of nitrogen deposited from the water column is often complex and is related to the overall rate of sediment metabolism and N regeneration (a function of organic matter loading), concentrations of overlying water nitrate, dissolved oxygen and salinity, and other factors such as

bioturbation/bioadvection of burrowing/filtering organism(Cornwell et al. 1999, Joye and Anderson 2008, Kellogg et al. 2013, Testa et al. 2013, Testa et al. 2015). The amount and reactivity of the organic matter is key to nutrient remineralization, with stable isotopes suggesting that there is a gradient of the quality of organic matter from the Conowingo Dam to the Chesapeake Bay Bridge. This gradient is generally related to a switch from terrestrial, poorer quality organic matter, to higher quality organic matter from estuarine algae (Cornwell and Sampou 1995). The erosion of sediment deposits from behind the Conowingo Dam may increase N deposition during floods, but the biogeochemical effect depends very much on the organic matter quality. This program is designed to identify the bioavailability of organic C and N.

The remineralization of organic nitrogen from algal or other sources is a key first step in sediment nitrogen cycling, and ammonium ( $\text{NH}_4^+\text{-N}$ ) is the initial inorganic product of organic matter breakdown (Figure 2). Under aerobic conditions, ammonium can be nitrified, with nitrate as an end product. This nitrate, as well as the nitrate influx from overlying water, can be reduced to  $\text{N}_2$  gas, a process generally referred to as denitrification. This process is a major nitrogen removing process in aquatic sediments and is generally has a positive effect in eutrophic systems. A number of alternative pathways are also observed in aquatic sediments (Koike and Hattori 1978, Risgaard-Petersen et al. 2004, Burgin and Hamilton 2007, Rich et al. 2008, Giblin et al. 2013)

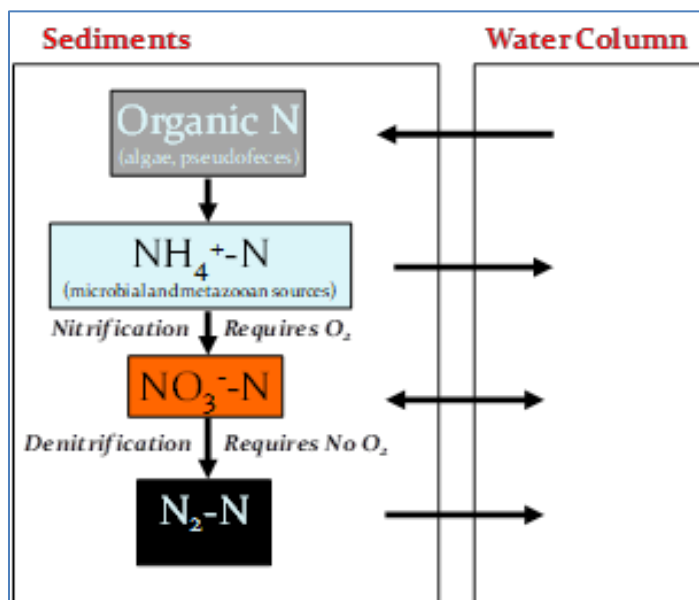


**Figure 2. Outline of N cycling processes in aquatic sediments**

A further consideration is whether the remineralization of N in the reservoir, from these same particulates, would generate the same amount of algal-available N as it would in the estuary. Reservoir and estuarine sediments either can take up or release ammonium or nitrate, with denitrification intercepting some of the remineralized N. Comparing the balance of these effluxes of bioavailable N and

inert N<sub>2</sub> gas in reservoir versus bay sediments will have a large impact of the magnitude of flood-related biogeochemical changes in the Chesapeake Bay.

### Estuarine P Cycling

In order for these larger particulate P inputs to have a large effect on P biogeochemistry and biological production, there are a number of key questions:

1. In a given bay segment, is P a key limiting factor to the growth of phytoplankton or possibly epiphytes on submerged aquatic vegetation? The role of light, N and P limitation of algal growth varies by salinity/location and season (Fisher et al. 1992, Fisher et al. 1999, Kemp et al. 2005). In the upper Chesapeake Bay, dissolved P would likely be the limiting nutrient, with light limitation also a key factor in this particulate-rich environment.
2. Since dissolved P is the substrate for algal nutrition, does suspended particulate P represent an important source of P for algae? Studies in the Chesapeake Bay suggest that algae rather than P adsorption/desorption regulates P concentrations (Conley et al. 1995), despite a paradigm that particulates and salinity-driven desorption could control dissolved P (Froelich 1988, Fox 1990, Gardolinski et al. 2004). Our work suggests that P desorption from suspended particulates is not a major control of P cycling in the Potomac estuary (Limnotech and UMCES 2007) and recent work suggests that desorption from iron oxides, a dominant form of inorganic P incorporation into particulates (Jordan et al. 2008), is not an important means of P release from suspended particulates (Spiteri et al. 2008).
3. Would sediment release of the added P result in a large production of dissolved P? Sediment-water exchange studies in the mainstem Chesapeake generally suggest that in the low salinity upper bay, sediments are highly retentive of P (Cowan and Boynton 1996), often with dissolved P uptake by the sediments. In general, P release is enhanced by anoxia in saline Chesapeake environments (Callender 1982, Cowan and Boynton 1996, Jasinski 1996, Boynton 2000) and elevated pH often associated with cyanobacterial blooms in tidal freshwater areas (Seitzinger 1991, Bailey et al. 2006, Gao et al. 2012). In addition, in mesohaline environments, we observe high rates of P release in oyster communities (Kellogg et al. 2013). In general, we expect P release from surface sediment particulates to occur under more saline condition (Cowan and Boynton 1996, Hartzell et al. 2017) in areas which are typically N limited in the summer.
4. Have experiments shown sediment P release to overlying water under different conditions? In the mainstem Chesapeake, experiments in which mesohaline sediments were driven to anoxia showed high rates of P efflux (Jasinski 1996). Our work at a proposed mesohaline dredge disposal site also showed that the addition of oxidized sediment from shipping channels resulted in high P releases under anoxia (Cornwell et al. 2000). Experimental work with Potomac and Sassafras River sediments (Gao et al. 2012) confirm previous observations of pH-driven P release.

## Study Chronology

The major activities of this project are tabulated in Table 1. Not included are the unsuccessful initial sampling efforts for long core collection and the suspended sediment collections.

**Table 1. Listing of major field activities for the UMCES Conowingo bottom sediment biogeochemistry program.**

Date	Activity	Comments
May 19, 2015	Conowingo. Short core collection for sediment-water flux measurements, pore water, diagenesis	13 sites, fluxes on all with 3 fluxes at sites replicated
July 21, 2015	Conowingo. Short core collection for sediment-water flux measurements, pore water, diagenesis	8 sites with duplicate cores
Aug 11, 2015	Upper Chesapeake Bay. Short cores collected aboard R/V Rachel Carson, fluxes at 4 sites, sediment addition experiments at 3.	
August 2015 – multiple dates	Conowingo. 5 long cores collected by Exelon. Used for solids, diagenesis, pore water	
Sept 22, 2015	Conowingo. Short core collection for sediment-water flux measurements, pore water, diagenesis	8 sites with duplicate cores
Dec 3, 2015	Conowingo. Short core collection for sediment-water flux measurements, pore water, diagenesis	6 sites with duplicate cores. Full sampling limited by high winds
April 13, 2016	Conowingo. Short core collection for sediment-water flux measurements, pore water, diagenesis	8 sites with duplicate cores
April 27, 2016	Lake Clarke, Lake Aldred. Short core collection for sediment-water flux measurements, pore water, diagenesis	3 sites with duplicate cores in each reservoir
April 28, 2016	Upper Chesapeake Bay. Short cores collected aboard R/V Rachel Carson, fluxes at 3 sites, sediment addition experiments.	

## Methods

The methods used in this project are described below. In cases when more specialized analyses were used for limited numbers of activities, they are described in the individual result/discussion sections.

### Sediment Collection

For short core collection in reservoirs, 23' or 25' outboard boats were used as a coring platform, with locations located using GPS. Exelon and UMCES safety protocols were observed in all sampling. Coring locations were initially chosen in conjunction with Exelon. In May 2015, duplicate cores were collected at sites 4, 5 and 8 and a total of 13 sites were sampled. In July 2015, September 2015 and April 2016, eight sites were sampled and all had duplicate cores at each site. In December 2015, high winds at the northern end of the Conowingo Reservoir resulted in truncation of sampling to 6 sites. Three sites were sampled in Lake Clarke and Lake Aldred in April 2016, with duplicate cores collected. The reservoir locations and sampling times are shown in Table 2 and Figure 3. At all reservoirs, a gradient of cores was collected from the dam northward.

Reservoir cores were collected using a Soutar box corer or a pole corer (Figure 4) that we have used in previous studies of aquatic sediments (Cornwell et al. 2014, Gao et al. 2014a). The box corer was deployed by hand using a davit and 6.3 cm id flux cores were inserted into the core box. Cores that were disturbed in the coring process were rejected and the corer was deployed a second time. In addition to flux cores, extra cores were collected at each site for Ms. Emily Russ in support of Dr. Cindy Palkas' characterization program. At selected sites, an extra core was collected for pore water analysis or for collection of sediment for diagenesis experiments. The pole corer was effective at shallow depths and was able to collect relatively coarse sediment deposits.

On two occasions (Table 3), sediments were collected in the Chesapeake Bay using the R/V Rachel Carson. A HAPS corer (KC Denmark, <http://www.kc-denmark.dk/products/sediment-samplers/haps-corer/haps-core.aspx>) was used for sediment collection, with the 13.6 cm id stainless steel tube sub-cored with our flux cores (Figure 5). The R/V Carson used differential GPS with dynamic positioning to maintain exact position during the coring operation. Cores for a final sediment addition experiment were collected in the Chesapeake mid-bay on one occasion using the Soutar corer.

At each reservoir station, surface and deep measurements of conductivity, temperature, and dissolved oxygen were made using a YSI multiparameter sonde. Similar measurements were made at bay stations, including salinity. Water was collected via pump from two reservoir locations for use in sediment incubations and from multiple locations in the Chesapeake Bay.

After collection, cores were placed upright in large insulated containers full of site water; this mode of containment helped maintain ambient temperatures during transport to the incubation facility at Horn Point Laboratory.

**Table 2. Locations and sampling dates for sediment-water exchange cores in lower Susquehanna River reservoir locations.**

Site ID	Lat N	Long W	May 19 2015	July 22 2015	Sept 22 2015	Dec 3 2015	April 13 2016	April 27 2016
Conowingo Reservoir								
1	39.77340	76.26538	X					
2	39.77679	76.25802	X	X	X	X	X	
3	39.76044	76.24958	X	X	X		X	
4	39.75986	76.24252	X					
5	39.74719	76.24574	X	X	X	X	X	
6	39.72934	76.23305	X					
7	39.72224	76.23582	X	X	X		X	
8	39.69210	76.21880	X	X	X	X	X	
9	39.69676	76.21145	X	X	X	X	X	
10	39.66166	76.18556	X					
11	39.66305	76.18528	X	X	X	X	X	
12	39.66582	76.18250	X					
13	39.66916	76.18111	X	X	X	X	X	
Lake Clarke								
LC1	39.92560	76.41412	Dec					X
LC2	39.93180	76.43603	April					X
LC3	39.96837	76.47240						X
Lake Aldred								
LA4	39.84358	76.35012						X
LA5	39.85738	76.35657						X
LA6	39.87347	76.37805						X

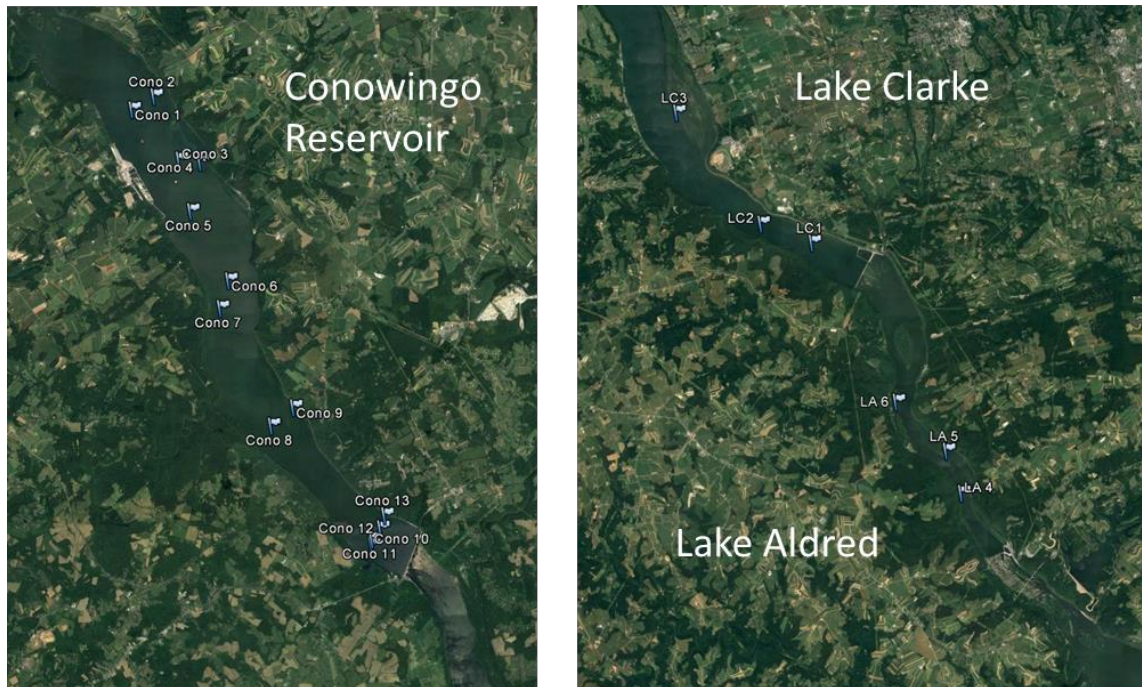


**Figure 3. Locations of short core collection for sediment-water exchange experiments.**

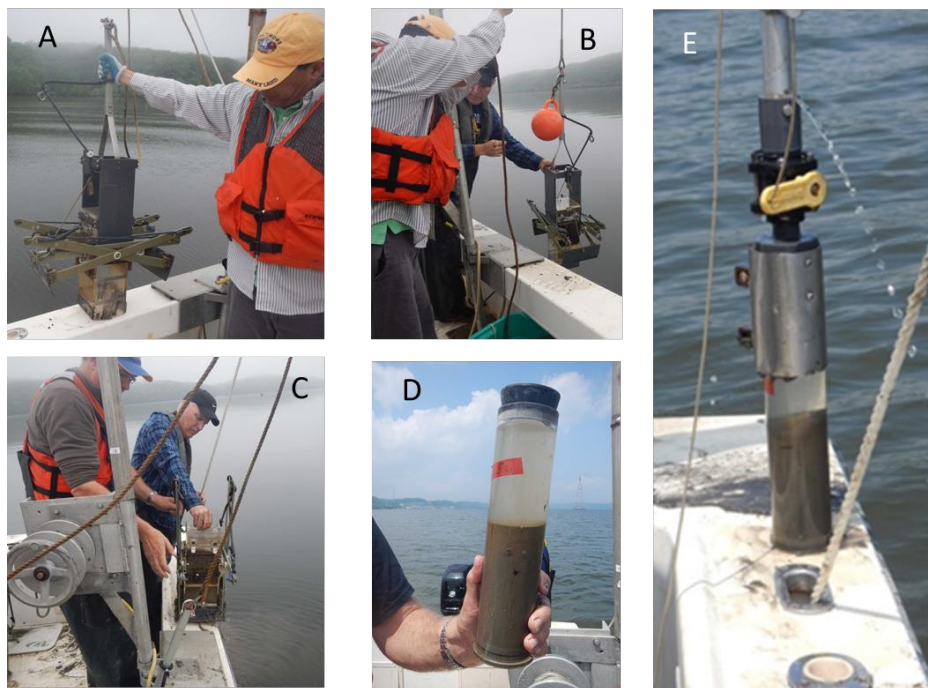


**Figure 4. Sampling gear. Soutar box corer used for deep sampling of surficial deposits in the Conowingo reservoir. The unit consists of a top part with the tripping mechanism (A), upon lowering a float is used to keep the device vertical in the water (B), upon retrieval cores are inserted into the lower unit (C) and 30 cm x 6.3 cm inner diameter cores (D) are collected after insertion into the core box. A core taken with a pole corer in shallow water is shown in panel E. Photos taken by Timothy Sullivan (May 2015).**

**Table 3. Locations and sampling dates for sediment-water exchange cores at Chesapeake Bay locations.**

Site ID	Lat N	Long W	August 11, 2015	April 28, 2016
Lee 7	39.41392	76.0794	X	X
Still Pond "Lee 5"	39.3479	76.1812	X	X
Lee 2.5	39.1966	76.3109	X	X
Lee S 2	38.7568	76.4727	X	

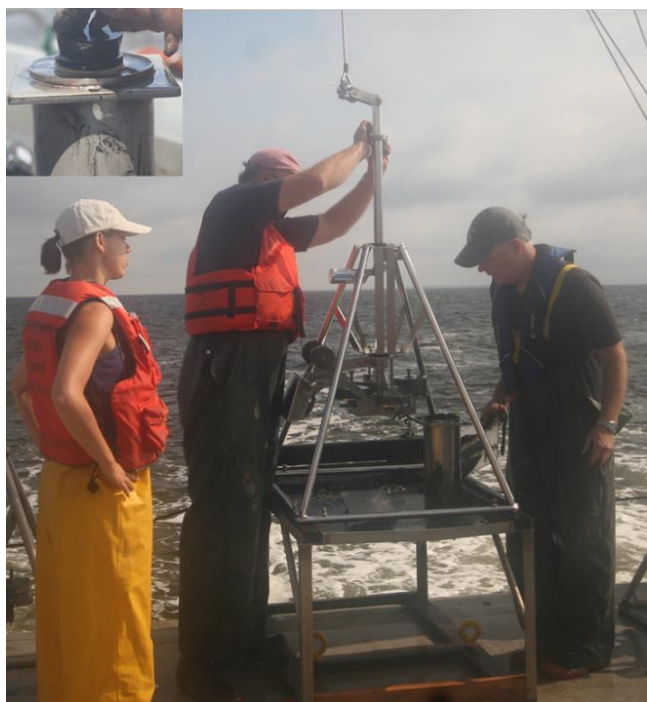


**Figure 5. HAPS corer being readied for deployment on the R/V Rachel Carson. Inset on upper left shows flux core inserted into the HAPS core liner.**

## Sediment-Water Exchange Experiments

Incubation procedures followed our published methodology (Cornwell et al. 2014, Owens and Cornwell 2016) and are briefly described here. A video-based technique presentation is available at

<https://www.jove.com/video/54098/the-benthic-exchange-o2-n2-dissolved-nutrients-using-small-core>.

Cores were transported to the laboratory at UMCES-HPL (University of Maryland Center for Environmental Science – Horn Point Laboratory) on the day of collection, maintaining aerobic conditions at bottom water temperatures during transit. A temperature-controlled incubation chamber was used for experiments, with temperature set at field values. Cores were put into an incubation “tub” and submerged with site water. The water within the cores was exchanged incubation water and bubbled with air to maintain oxygen saturation prior to incubation. At the beginning of the incubation phase, stirring lids were attached to the cores and a time course of overlying water chemistry was determined initially under dark conditions for 4-6 hours. Additional site-water-only “blank” incubations were set up from each aerobic coring site to correct for biogeochemical processes occurring in the water. Water analyses included gas ratio (O<sub>2</sub>:Ar, N<sub>2</sub>:Ar) analysis via MIMS - membrane inlet mass spectrometry (Kana et al. 1994), and nutrients (nitrate plus nitrite - NO<sub>x</sub><sup>-</sup>, ammonium – NH<sub>4</sub><sup>+</sup> and soluble reactive phosphorus - SRP) using conventional colorimetric methods (Parsons et al. 1984, Garcia-Robledo et al. 2014). Gas and nutrient flux rates were calculated from core area and volume and the slope of solute/gas versus time. At the end of the incubations, the overlying water volumes were recorded and surface 0-1 cm samples were collected for solid phase analysis of total carbon, nitrogen and pigments.

## Pore Water and Solid Phase Chemistry

For pore water collection, cores were placed into a glove bag filled with N<sub>2</sub> to minimize oxidation artifacts (Bray et al. 1973) and sectioned. The short cores were sectioned into the following depth intervals: 0.0–0.5 cm, 0.5–1.0 cm, 1–2 cm, 2–3 cm, 3–5 cm, and 8–10 cm. The long cores (10') were extruded from their metal liner and sampled with a cut off 50 mL syringe. The syringe was capped with rubber stopper and transferred to a glove bag for processing. Sediment in 50-mL centrifuge tubes were spun at 2000 G for 10 minutes, and the supernatant water was filtered with 0.45-µm syringe filters. Water is collected in 7-mL vials and the pore water rapidly distributed into vials for immediate hydrogen sulfide analysis. Pore water was diluted using calibrated pipets. Pore water analytes included ammonium, soluble reactive phosphorus, hydrogen sulfide, and iron, all analyzed colorimetrically (Table 4).

**Table 4. Pore water analytical techniques**

Analyte	Technique
NH <sub>4</sub> <sup>+</sup>	(Parsons et al. 1984)
Fe	Ferrozine colorimetry (Gibb 1979)
ΣH <sub>2</sub> S	Colorimetry (Parsons et al. 1984)
SRP	Phosphomolybdate colorimetry (Parsons et al. 1984)

Solid phase characterization (Table 5) included total carbon, total nitrogen, total P, inorganic P, HCl-extractable Fe and chlorophyll a. Percent water was determined on samples by drying at 65°C.

**Table 5. Solid phase analyses**

Analyte	Technique
CHN	CHN analyzer (Cornwell et al. 1996)
HCl-extractable Fe	HCl extraction, flame AAS (Leventhal and Taylor 1990)
Chlorophyll a	Acetone extraction, fluorometry (Parsons et al. 1984)
Total, Inorganic P	HCl extraction of ashed, unashed sediment (Aspila et al. 1976)

## The Chemistry of Conowingo Deep Cores

The sediment biogeochemistry program received 5 long cores for analysis from Exelon’s contractor in August 2015. The samples were stored in steel tubes that were 2’ in length, with 5 tubes per site. A parallel core was also collected for geotechnical and geological workup by AECOM and Cindy Palinkas at UMCES. The five sites span the length of the reservoir, from above the Peach Bottom nuclear facility to near the face of the Conowingo dam (Figure 6). A report on the sampling and characterization of the materials is available elsewhere (AECOM Project No. 60389146). The data in this section is briefly described and discussion will be largely presented in other sections of the report.

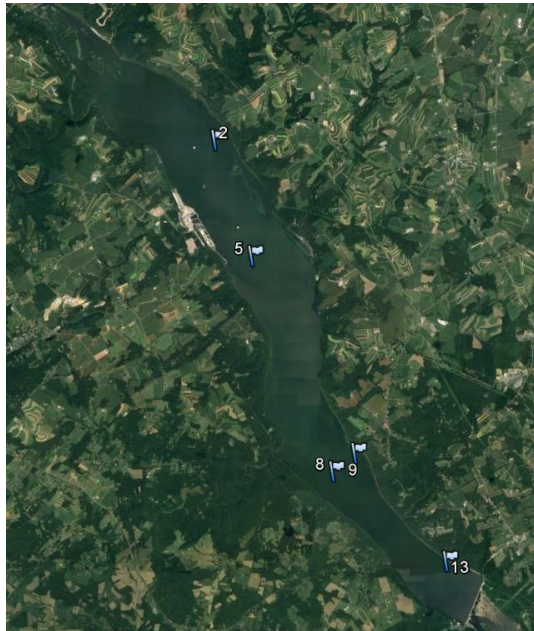


**Figure 6. Location of long cores (10’) collected in 2015 from the Conowingo Reservoir.**

### Solid Phase Chemistry

The water content of the long cores varied widely (Figure 7), with somewhat higher values in the three lower sampling sites that had fine-grained sediment in all sediment horizons. Site 2 varied the most in this sample set with a pronounced minimum at mid depths, largely corresponding to coarse horizons.

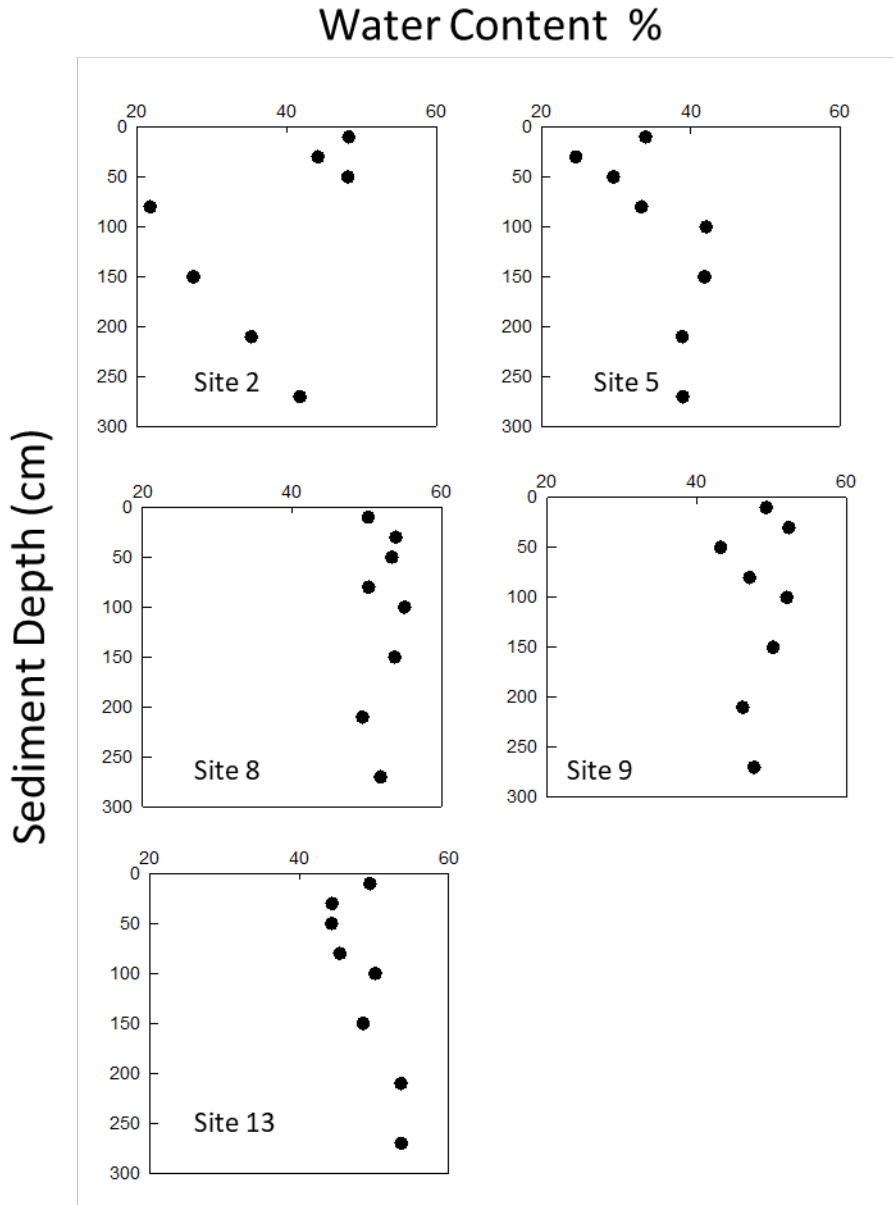
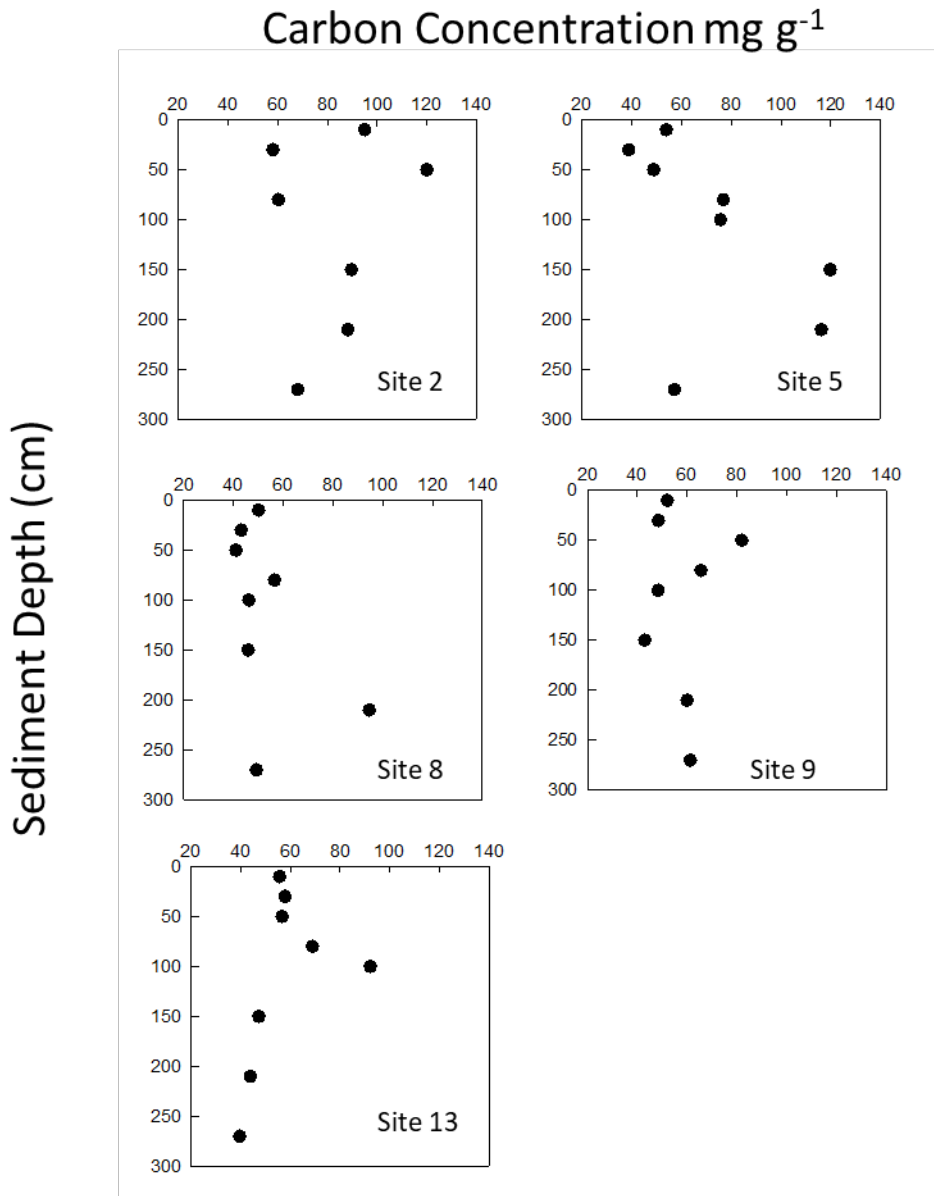


Figure 7. Percent water content of Conowingo deep cores.

The carbon concentrations in the long cores varied with depth in the long cores from sites 2 and 5 (Figure 8). The average concentration of data from each core was also higher at those two sites, averaging  $82.8 \pm 22.1$  and  $73.4 \pm 30.3$   $\text{mg g}^{-1}$  for sites 2 and 5 respectively (Table 6). The C concentrations in the lower 3 sites (8, 9, 13) ranged from  $53$ - $58$   $\text{mg g}^{-1}$ , concentrations similar to fine-grained sediments in the upper Chesapeake Bay (Kerhin et al. 1988, Cornwell and Sampou 1995).



**Figure 8. Carbon concentrations in the Conowingo deep cores. To convert to percent carbon, divide the concentration by 10.**

**Table 6. Long core mean, standard deviation and median values for carbon, nitrogen and the C:N ratio.**

Analyte	Core	Mean	Std. Dev	Median
Carbon mg g <sup>-1</sup>	2	82.8	22.1	88.2
	5	73.4	30.3	66.5
	8	53.3	17.3	47.7
	9	57.6	12.5	56.0
	13	57.8	16.6	56.2
Nitrogen mg g <sup>-1</sup>	2	2.77	0.69	2.80
	5	2.45	0.82	2.40
	8	3.76	0.50	3.83
	9	3.43	0.22	3.35
	13	3.10	0.58	3.10
C:N Ratio molar	2	35.5	8.1	36.3
	5	34.8	5.9	34.7
	8	16.6	4.5	14.4
	9	19.8	5.0	18.9
	13	22.5	6.9	25.7

Nitrogen concentrations were generally 2-4 mg g<sup>-1</sup> (Figure 9). While in general they showed similar downcore changes as did the carbon, there were some key differences. The proportional variation in nitrogen was smaller than for carbon. These differences suggest that there might be differences in the source of carbon in the reservoir. The presence of coal (Edwards 2006) has been noted in previous studies; this would enhance the carbon concentrations without substantial increases in nitrogen. We observed coal particles in coarser-grained sediments, particularly in upper reservoir locations.

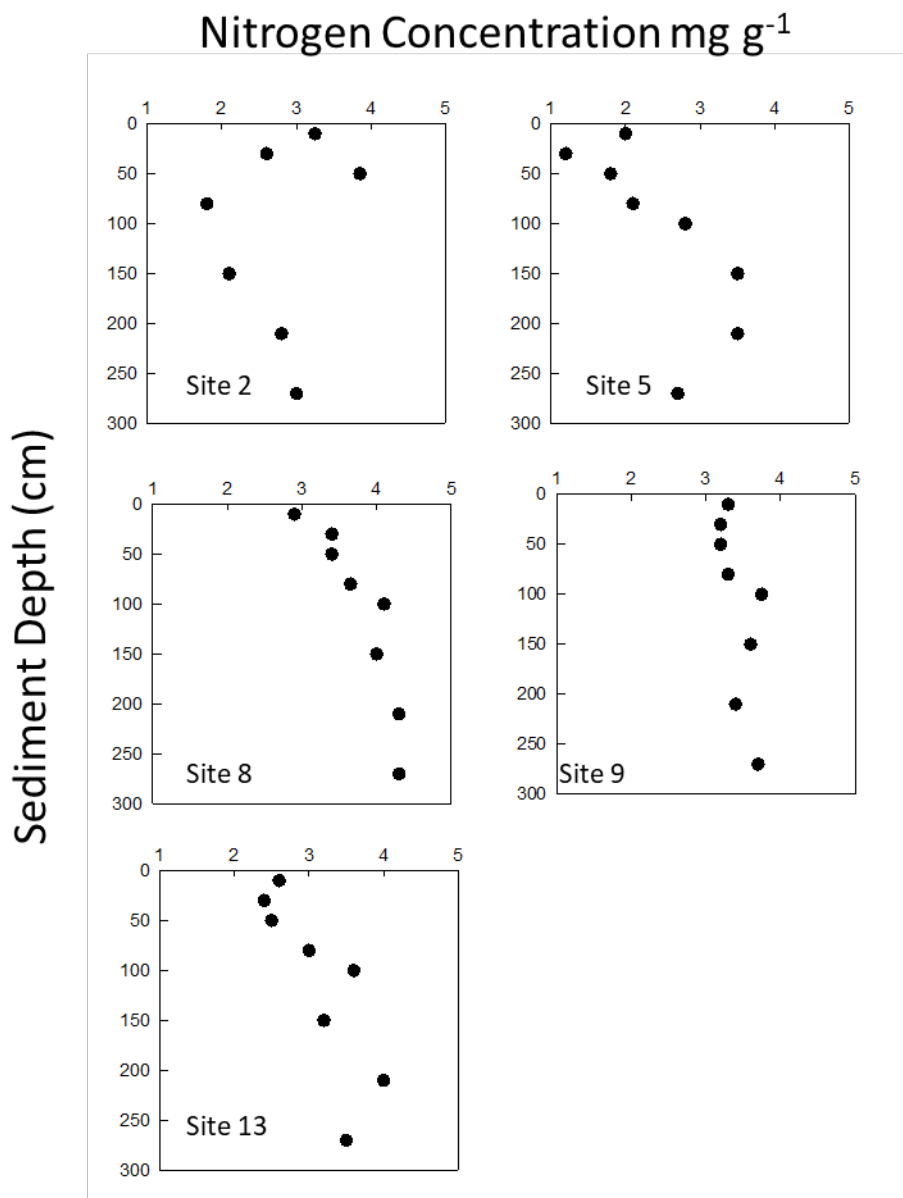


**Figure 9. Nitrogen concentrations in the Conowingo deep cores.**

The molar C:N ratios were highly variable (Figure 10), with sites 8 and 9 having somewhat lower average ratios. Site 13 had C:N ratios higher in the upper 5 sections. Interpreting the C:N ratio for terrestrial versus algal sources of organic matter can be difficult (Thornton and McManus 1994), but in general higher ratios suggest sources of organic matter that might include terrestrial plants and/or coal. If we

examine all core data, there is a considerable amount of data that would span algal through coal sources of material (Figure 11).

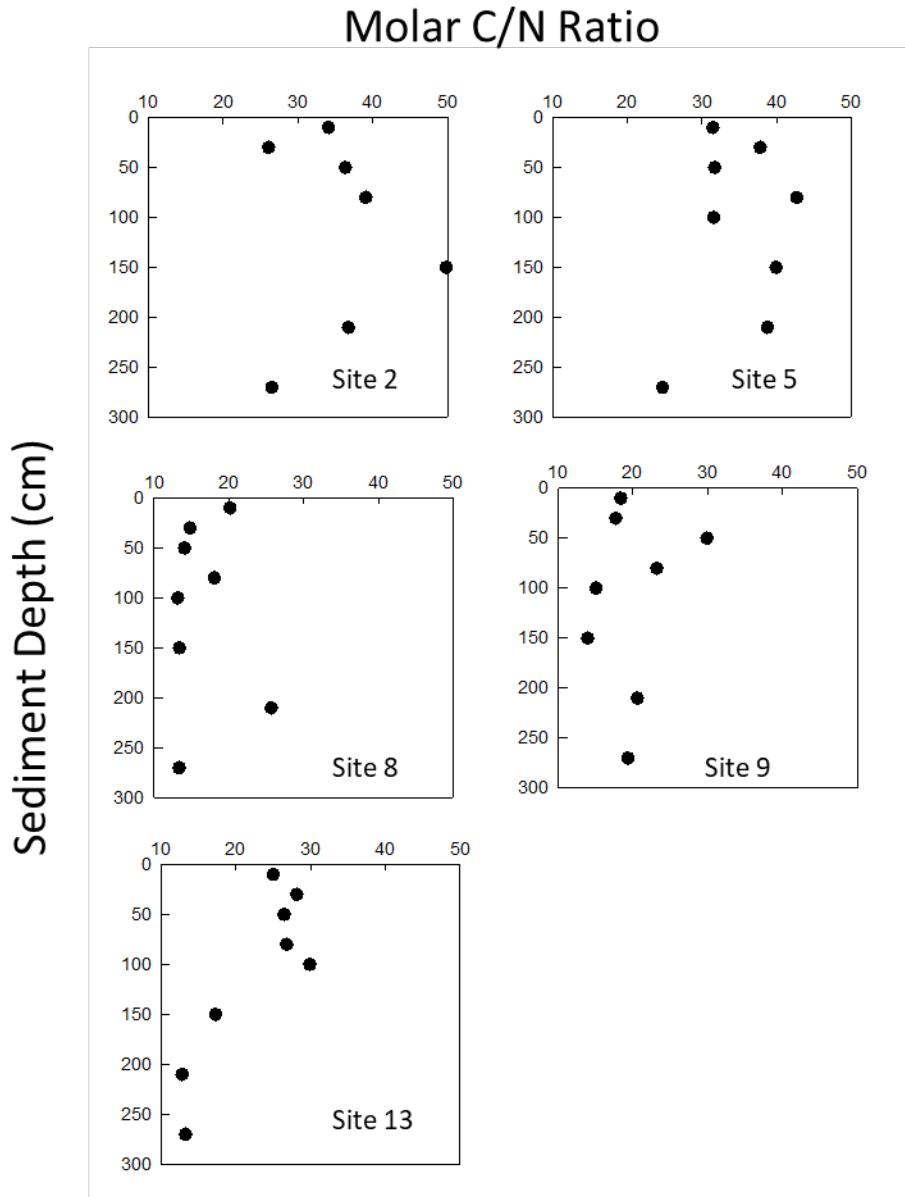
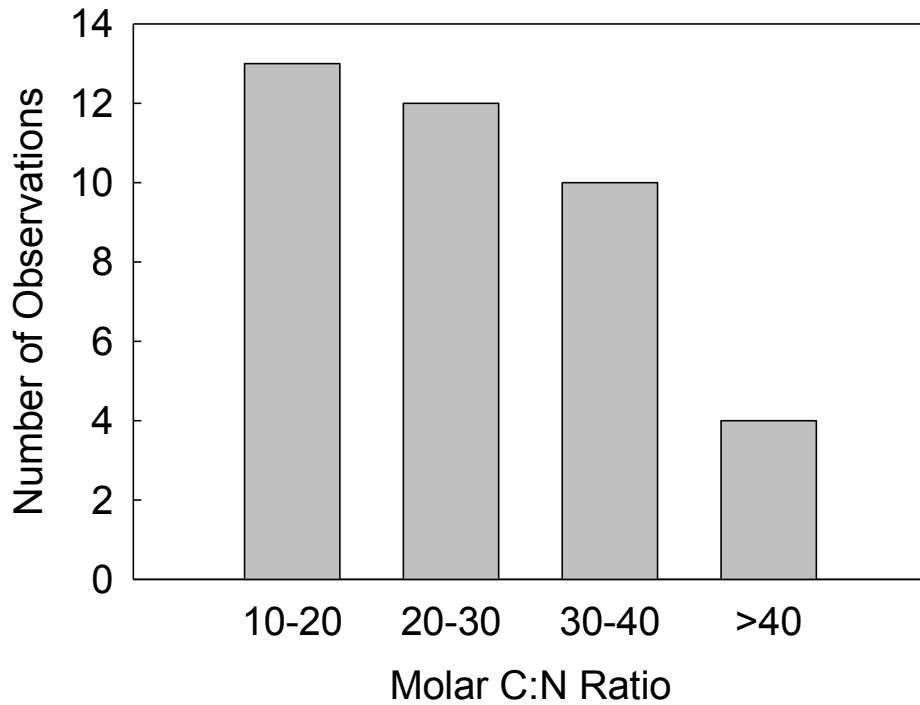


Figure 10. Molar C:N ratio in the Conowingo deep cores.



**Figure 11. Molar C:N ratio histogram.**

Solid phase HCl-extractable iron concentrations (Figure 12) had considerable variability at each site, and were similar to data from the upper Chesapeake Bay (Cornwell and Sampou 1995). Iron can remobilize in sediments and be focused into distinct sediment layers (Anthony 1977, Cornwell and Kipphut 1992); however in coastal sediments it can also be related to grain size (Daskalakis and O'Connor 1995). Different patterns of iron concentration were observed, with higher values observed at greater depths at site 13 and lower values at depth at site 9. Inorganic P (Figure 13), generally considered to be a combination of iron-associated P or P in apatite minerals, has similar profile to nitrogen. Since it is likely that much of the inorganic P was deposited from fluvial inputs, rather than remineralization of organic P, the key driver in inorganic P concentration likely is the grain size of the sampled horizon.

# HCl- Extractable Iron Concentration $\text{mg g}^{-1}$

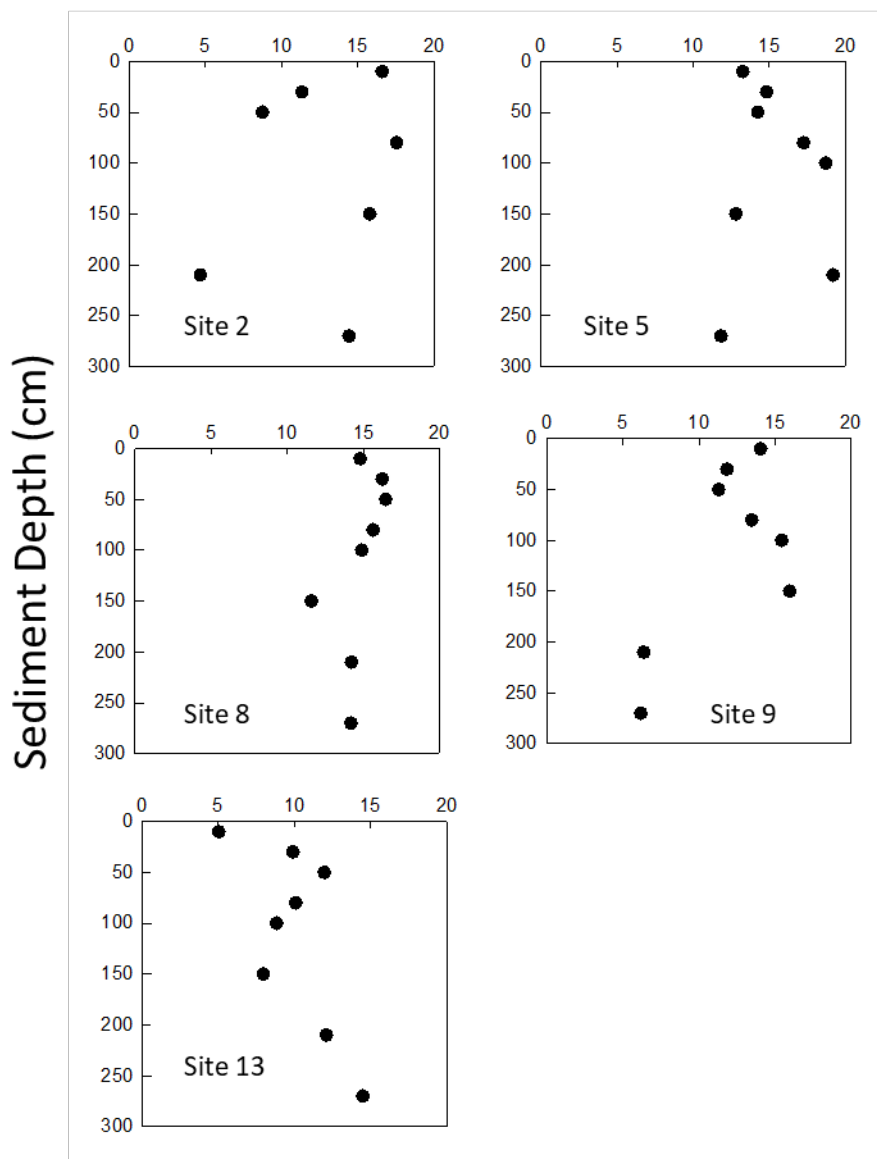


Figure 12. Extractable Fe concentrations in Conowingo deep cores

# Inorganic Phosphorus Concentration $\text{mg g}^{-1}$

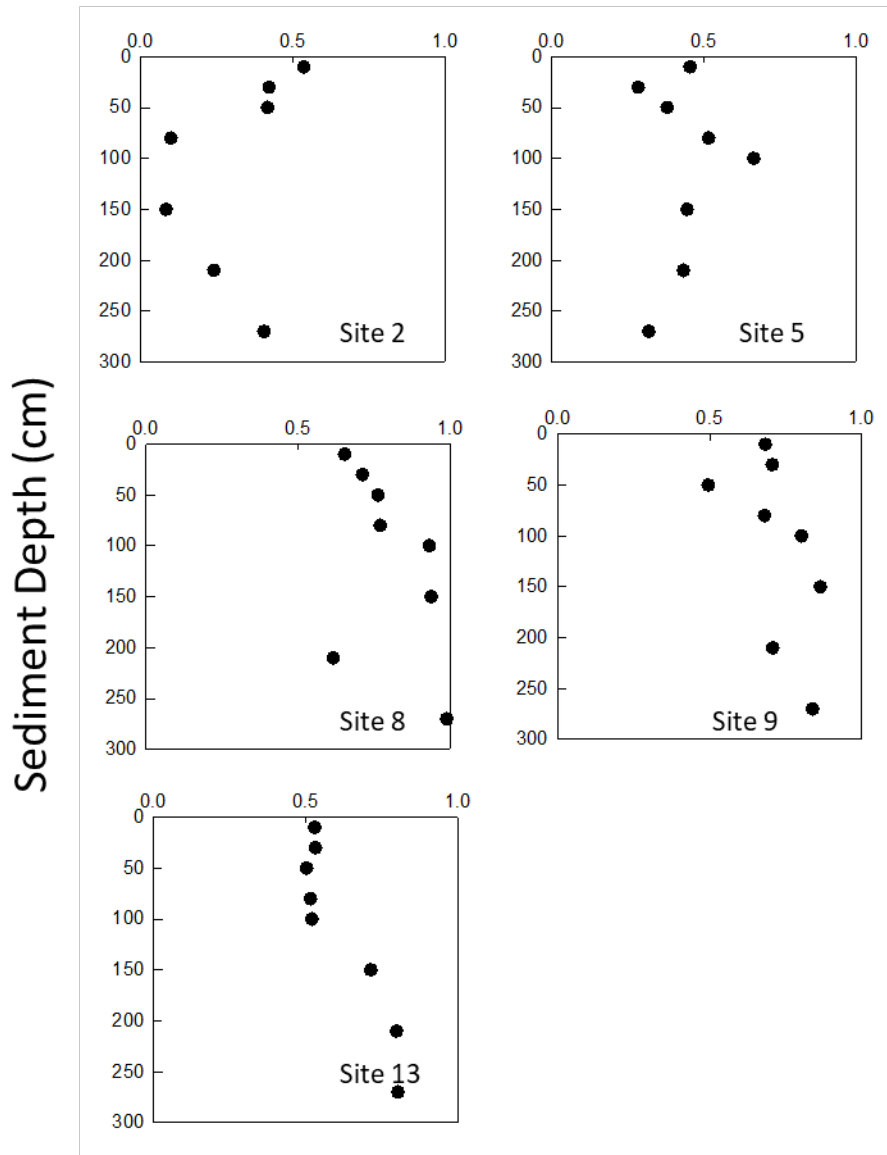


Figure 13. Inorganic P concentrations in Conowingo deep cores

### Pore Water Chemistry

The presence of coarse grained sediment layers, as well as relatively low water content in compacted fine grained sediments, made obtaining pore water for chemical analysis difficult for some sediment horizons. Extraction of as little as 1 mL of water typically can yield analysis for ammonium and iron, but in many cases even these analyses were not possible. Concentrations of ammonium ranged from very low to  $> 5,000 \mu\text{mol L}^{-1}$  (Figure 14), with site 8 showing the largest down core increase.

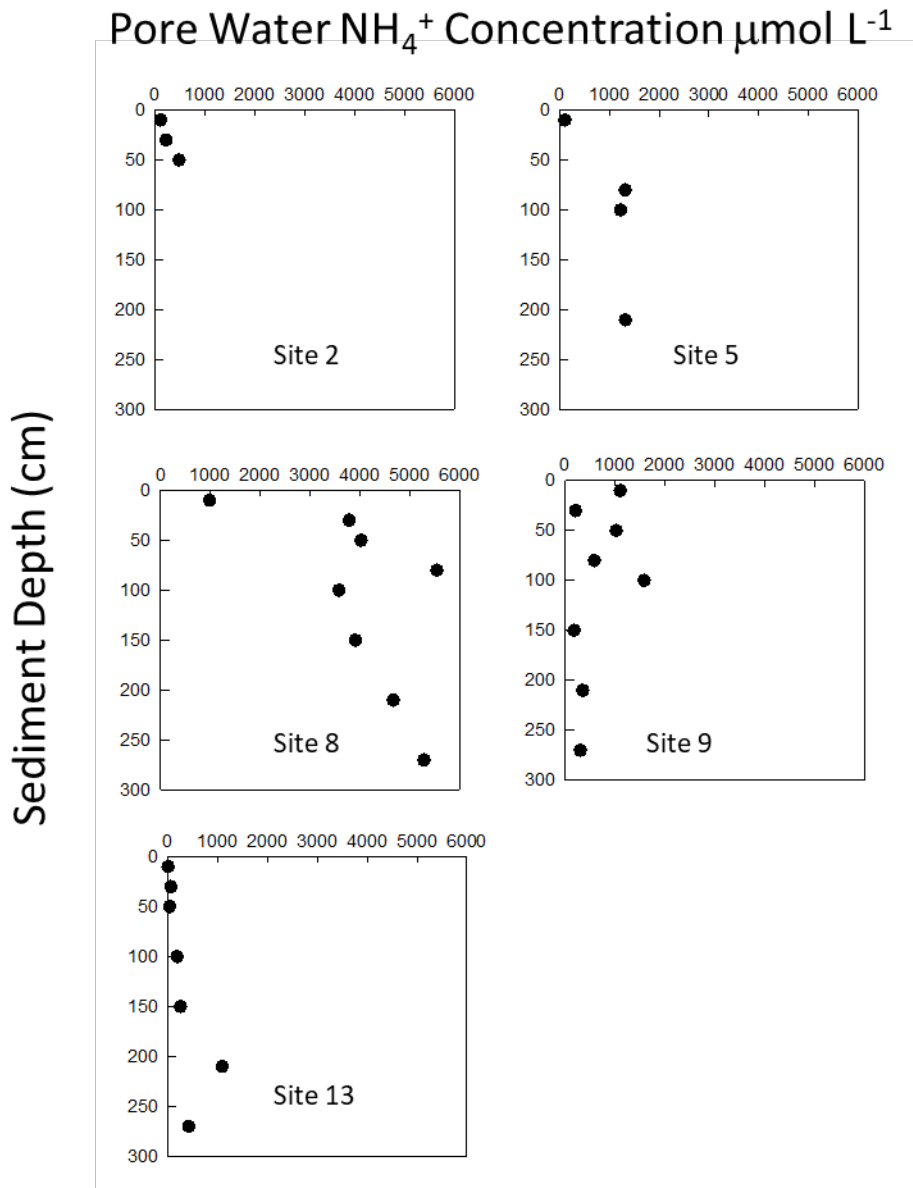


Figure 14. Pore water ammonium concentrations in the Conowingo deep cores. Poor water recovery in some coarse and low percent water sections resulted in no data.

Pore water SRP concentrations were  $< 10 \mu\text{mol L}^{-1}$  (Figure 15), a strong contrast to concentrations observed in the mid-bay area of the Chesapeake Bay (Cornwell unpublished). In the absence of sulfate reduction which reduced iron oxide binding of P through formation of iron sulfide minerals (Lehtoranta et al. 2009, Hartzell et al. 2017), the adsorption of SRP to iron oxides and the formation of discrete iron phosphate minerals (Hearn et al. 1983, Cornwell 1987) likely limits SRP concentrations.

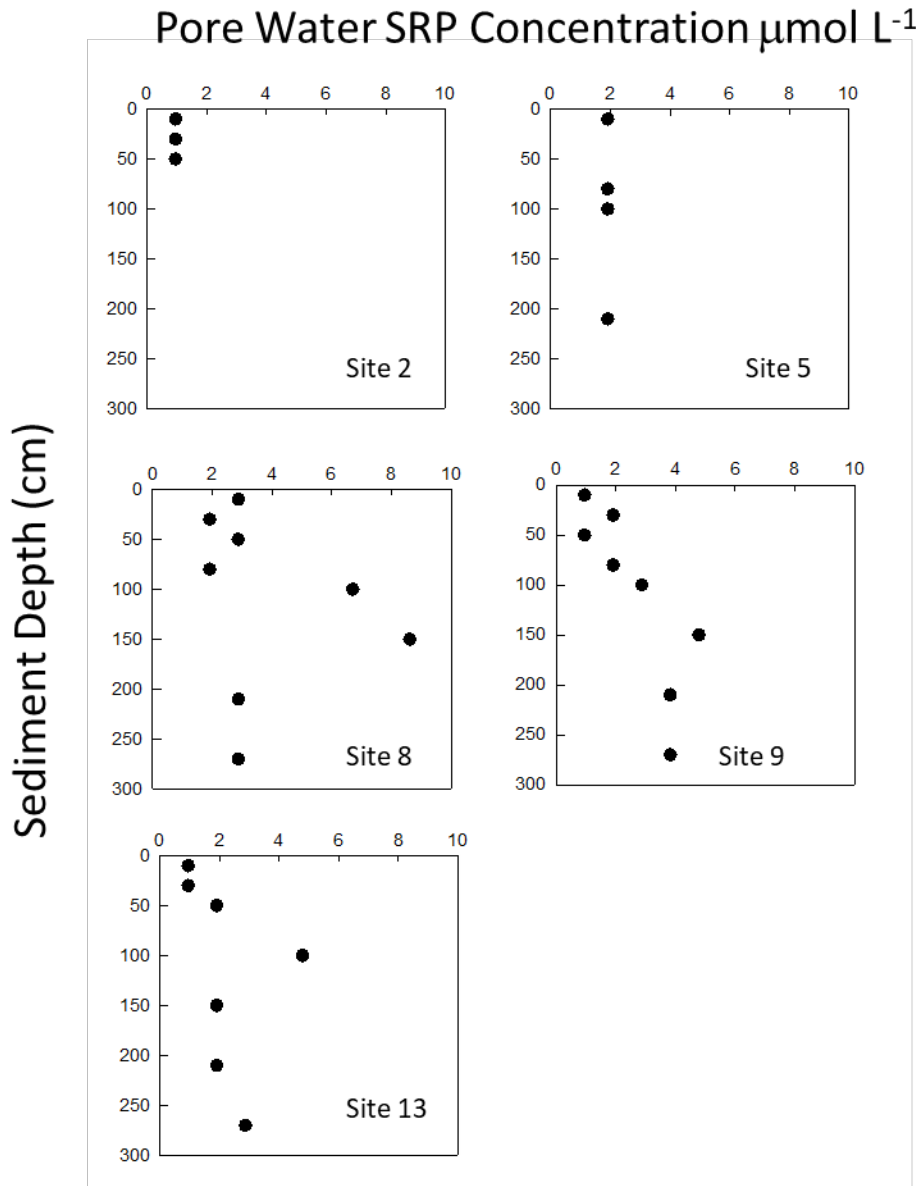
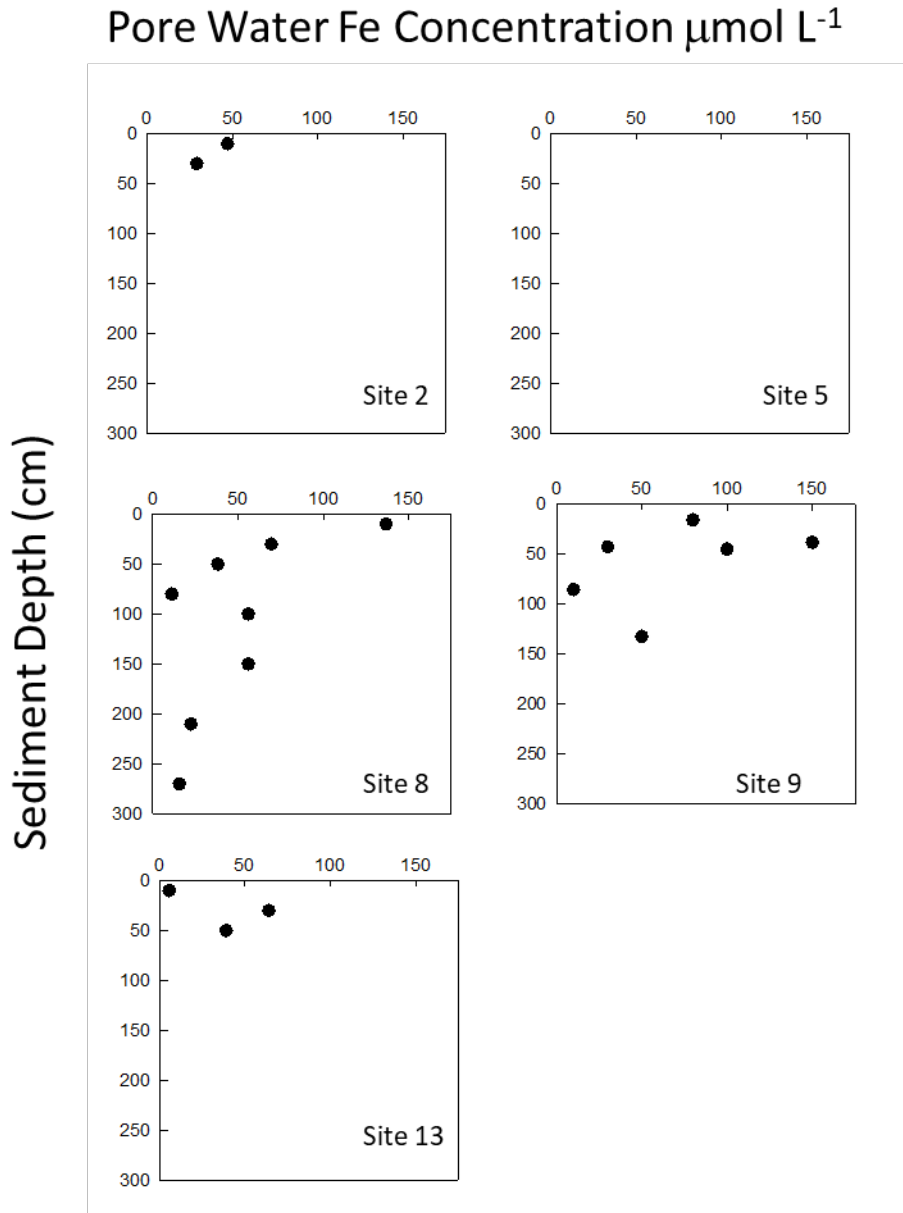


Figure 15. Pore water SRP concentrations in the Conowingo deep cores. Poor water recovery in some coarse and low percent water sections resulted in no data.

The concentrations of iron in pore water was volume limited in many cases, but the key finding of the deep core work is that relatively high concentrations of iron are found throughout the sediment profiles (Figure 16). Dissolved iron at the observed concentrations are likely in the form of Fe(II) and subject to rapid oxidation when exposed to oxygen (Stumm and Morgan 1981).



**Figure 16. Pore water iron concentrations in the Conowingo deep cores. Poor water recovery in some coarse and low percent water sections resulted in no data.**

### Adsorbed Ammonium

The limitations of obtaining pore water in many sections resulted in incomplete ammonium profiles. The extractable ammonium concentrations were not limited however, and the displacement of ammonium with potassium provides an assessment of the total ammonium within the sediment (Weston et al. 2010, Cornwell and Owens 2011). Down core increases in adsorbed ammonium were observed in all cores (Figure 17).

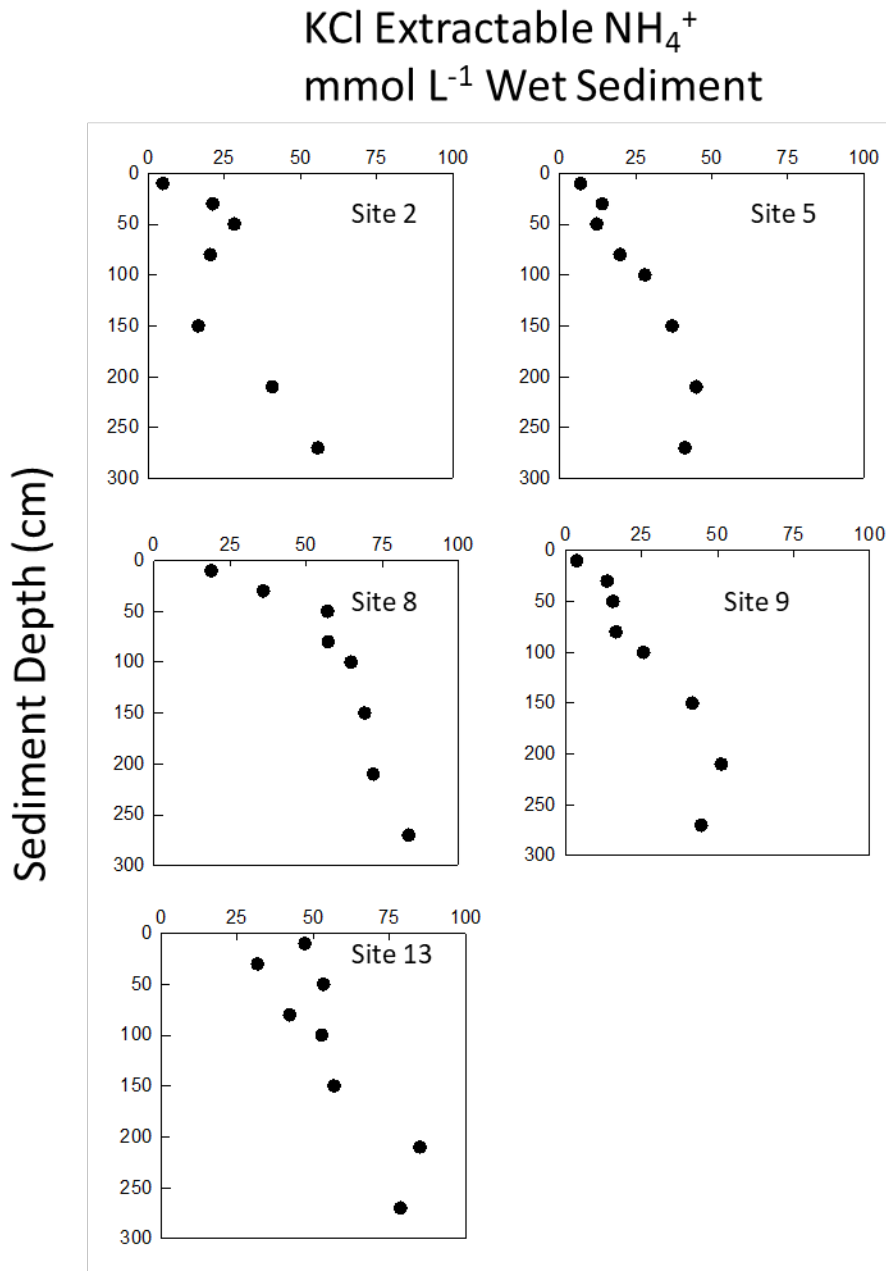


Figure 17. Adsorbed ammonium on a sediment volume basis (L or cubic decimeter)

Using all extractable ammonium data (Figure 18), the average concentration of extractable ammonium was  $38.7 \pm 22.5 \text{ mmol L}^{-1}$  where volume (L) was of whole wet sediment. In Chesapeake Bay shipping channels (Cornwell and Owens 2011), observations were generally in the range of  $5\text{-}18 \text{ mmol L}^{-1} \text{ NH}_4^+$ . The amount of adsorbed ammonium generally is much higher in freshwater sediments (Seitzinger et al. 1991) such as the Conowingo because the adsorption coefficients are much higher at lower salinities (i.e. lower  $\text{K}^+$  concentrations). In addition, in the Conowingo reservoir, the sediments are much more compacted and there are more solids and more surface area per unit sediment volume. In both Chesapeake shipping channels and in the Conowingo reservoir, the “burial” of dissolved and adsorbed ammonium is enhanced by high sedimentation rates (Cornwell and Owens 2011).

In order to “bury” so much ammonium at depth, sedimentation rates need to be high so that burial of ammonium-producing organic matter is fast. Literature burial rates showed high ( $2\text{-}7 \text{ cm y}^{-1}$ ) accretion rates (McLean et al. 1991). If the organic matter is of medium reactivity, such as might be expected from organic matter from terrestrial sources, it may produce ammonium slowly over many years in the sediments. The combination of accretion and slow ammonium production from the relatively high organic matter pools in sediments likely leads to high adsorbed ammonium.

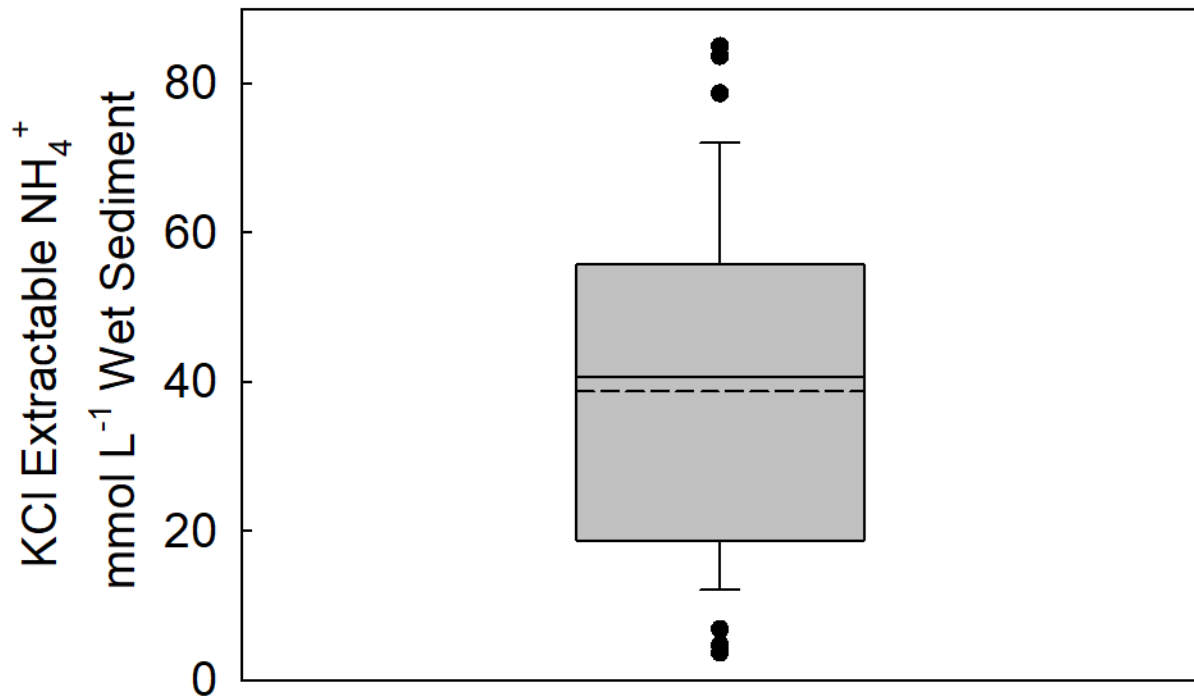


Figure 18. Box plot of adsorbed ammonium from all long core horizons. The solid line is the median ammonium concentration ( $40.7 \text{ mmol L}^{-1}$ ), the dotted line is the average concentration ( $38.7 \pm 22.5 \text{ mmol L}^{-1}$ ).

# Spatial and Seasonal Patterns of Nitrogen and Oxygen Sediment From Sediments Behind the Conowingo Dam, Maryland, USA. (Dr. Hamlet Perez)

## Introduction

Currently, there are about 800,000 artificial lakes and large dams (height > 15 m) in operation worldwide, which occupy approximately 3% of the land surface (Friedl and Wuest 2002). The primary effect of dam construction is the segmentation of rivers and the formation of reservoirs behind their walls, which represents a transition between lentic and lotic ecosystems sometimes called “river-lake hybrids” (Kimmel et al. 1990). Consequently, reservoirs can have a profound effect on water quality by changing the water residence time, reducing turbulence, increasing sedimentation, changing temperature resulting in vertical stratification, and in some cases, anoxia (Nilsson and Berggren 2000, Friedl and Wuest 2002, Burford et al. 2012). Reservoir sediments affect biogeochemical material balances due to their high area-specific nutrient recycling and high rates of carbon burial (Downing et al. 2008, Harrison et al. 2009). When located upstream of coastal ecosystems, reservoirs may attenuate the nutrient loads moving downstream that may contribute to coastal eutrophication (Rabalais et al. 2002, Cook et al. 2010).

Relatively few studies have examined sediment nitrogen cycling in reservoir sediments. Denitrification, the microbial reduction of nitrate to  $N_2O$  or  $N_2$ , is of particular importance because it permanently removes available N from the ecosystem (Burgin and Hamilton 2007). The role of denitrification appears to be variable among reservoirs. For instance, Koszelnik et al. (2007) and Grantz et al. (2012) reported 16-25% of N removed by denitrification in Polish and Arkansas, (USA) reservoirs. Denitrification has reported to account for 50% of N removal in an Illinois reservoir David et al. (2006).

The Conowingo Reservoir has diminished storage capacity and sediment trapping efficiency (Cerco 2016). This reservoir is similar to many worldwide reservoirs where sediment and nutrient export may be detrimental to downstream ecosystems (Hirsch 2012, Zhang et al. 2013). In the Conowingo Reservoir, sediments and associated particulate nutrients may pass downstream due to both the reduced storage capacity and seasonal high flow events such as tropical storms. Scour under high flow may export sediments and particulate N and P to the Chesapeake Bay in a relatively short period of time (Palinkas et al. 2014), with sediment loads from the watershed and potential scour from all three dams. The purpose of this study is to quantify the exchange of nitrogen and other biogeochemical parameters between the sediment and water column of the Conowingo Reservoir, and determine whether reservoir denitrification exerts an important control of nitrogen inputs to the Chesapeake Bay.

## Material and Methods

### Study area

The Susquehanna River drains an area of 71,000 km<sup>2</sup> and includes south-central New York state, southern Pennsylvania and northeastern Maryland. It is the 16<sup>th</sup> largest river of USA and the largest source of freshwater, sediment suspended sediment and nutrient to Chesapeake Bay (LSRWA, US EPA 2010). About 63 percent of the Susquehanna drainage area is covered by forest in the northern and western areas, while agricultural and urban areas (southern) cover 26 and 9.3 percent of its drainage area, respectively (USGS 1997). The Conowingo hydroelectrical dam was constructed in 1929 and the Conowingo Reservoir straddles the Maryland-Pennsylvania border. Upstream, the Holtwood and Safe Harbor dams form two reservoirs, Lake Aldred and Lake Clarke. Decreasing sediment storage capacity at the Conowingo Dam has been observed, from initial water storage capacity of  $3.7 \times 10^8 \text{ m}^3$  to about  $2.1 \times 10^8 \text{ m}^3$  (Whaley 1960; Reed and Hoffiman 1997). The Conowingo reservoir may be close to reaching its maximum storage capacity (Langland 2009) and an increasing trend in particulate nitrogen, total phosphorus loads and suspended sediment export has been noted at the Conowingo outfall (Hirsch 2012).

### Experimental design

Five cruises were conducted in the Conowingo Reservoir in the months of May, July, September, December 2015 and April 2016. A total of 13 sampling sites were established at the Conowingo Reservoir along a longitudinal gradient varying in depth, and sediment type upstream from the Conowingo Reservoir. A total of 76 intact sediment cores were collected during the five sampling months. The intact sediment cores were collected using a pole corer in shallow sites and a Soutar type box corer in the deeper sites (Cornwell et al. 2014). Acrylic cores were stored submerged in site water in coolers and transported to the Incubation laboratory. Additional intact sediment cores were collected to perform grain size analysis by other UMCES investigators. Field temperature, conductivity, dissolved oxygen, and pH were measured using a YSI 600 XLM Multi-Parameter Water Quality Sonde.

### Sediment water exchange incubation techniques

Sediment incubation procedures followed Owens and Cornwell (2016). At the laboratory, the sediment cores were submerged in site water and bubbled overnight in an environmental chamber at ambient temperature. The next day, sediment cores were sealed with an o-ring-fitted stirring top operated at stirring speed that mixed the overlying water without resuspending the surface of the core. Water samples for gas analysis and nutrient analyses were collected as replacement water was added to the core via gravity. Four sample points were collected over 4-6 hours. Dissolved gas samples were preserved with 10  $\mu\text{L}$  of 50% saturated  $\text{HgCl}_2$ , capped, and kept submerged in water just prior to analysis. Water samples for dissolved nutrients were filtered through 0.4- $\mu\text{m}$  polycarbonate filters and frozen until analyses.

### Solute and gas analysis

Concentrations of  $\text{NH}_4^+$ , and  $\text{NO}_x$ , (i.e.  $\text{NO}_3^- + \text{NO}_2$ ) were determined via colorimetric analysis (Parsons et al. 1984; Garcia-Robledo 2014). A membrane inlet mass spectrometer was used for high precision analysis of  $\text{N}_2$ ,  $\text{O}_2$  and Ar in water (Kana et al. 1994).

### Calculations

The changes in concentrations of dissolved gases ( $\text{O}_2$ , and  $\text{N}_2$ ) in water samples were estimated using the  $\text{O}_2$ :Ar and  $\text{N}_2$ :Ar ratios (Kana et al. 1994; Kana et al. 1998). Exchange rates of  $\text{O}_2$ ,  $\text{N}_2$ ,  $\text{NH}_4^+$ , and  $\text{NO}_3^-$  were calculated as follows,

$$F = \frac{\Delta C}{\Delta t} \times \frac{V}{A}$$

Where,

F is the flux ( $\mu\text{mol m}^{-2} \text{h}^{-1}$ ),  $\frac{\Delta C}{\Delta t}$  is the slope of the analyte ( $\mu\text{mol L}^{-1} \text{h}^{-1}$ ) over time (t), V is the volume of the overlying water (L), and A is the area of the incubated cores ( $0.00317 \text{ m}^2$ ). The fluxes data included in this study were those reaching a regression coefficient greater than 0.81 using 4 time points. All the  $R^2$  regression coefficients calculated for oxygen fluxes were  $> 0.97$ , while 93 % of those for  $\text{N}_2$ -N were  $\geq 0.86$ . The ammonium and nitrate regressions, had  $R^2$  regression coefficients greater than 0.84 and 0.80 for 85 and 93% of all cores, respectively.

The budget of dissolved inorganic nitrogen presented in this study was calculated using the average water discharge, ammonium, and nitrate concentrations data reported for the years 2014 and 2015 (USGS 2016) and 2014-2016 at the Susquehanna River, Marietta Site (USGS parameter Code number 01576000), respectively, located in the Lancaster County, Pennsylvania. The fluxes of ammonium, nitrate and  $\text{N}_2$ -N at the sediment water interface presented in this study were used to calculate nutrient loads to the Conowingo reservoir

### Statistics and Presentation

Before determining the significant differences among the variables, all data sets were checked for the normality test. If the data met the assumption of normality, a parametric test was applied (One way ANOVA, T-Test), otherwise proceeded with a nonparametric test (Kruskal Wallis on Rank and Mann-Whitney Rank Sum Test). All statistic analyses and graphing were performed using a 11.0 Sigma Plot Software.

Box plots are used for presentation of data throughout this report. The median is presented as a solid line in the middle of the box; in some cases the mean is shown as a dotted line. The bottom and the top of the box represent the first and third quartiles of the data. The error bars represent the 10<sup>th</sup> and 90<sup>th</sup> percentile of the data. Dots represent outliers.

## Results

Average bottom water temperatures ranged from 8.8 in December 2015 to 26.3 in July 2015. (Table 1). Average bottom water dissolved oxygen concentrations ranged from 5.7 to 12.6 mg L<sup>-1</sup>, with the lowest values in May-September 2015. In no instances were dissolved oxygen concentrations hypoxic during this study. The bottom water NH<sub>4</sub><sup>+</sup> concentrations averaged 1.2 – 11.3 μmol L<sup>-1</sup>, while the concentrations of NO<sub>x</sub><sup>-</sup> were 37 – 75 μmol L<sup>-1</sup>.

**Table 7.** Site characteristics and sediment-water exchange rates in the Conowingo Reservoir. Values are means ± the standard deviation.

Sampling month	T	C	N	NH <sub>4</sub> <sup>+</sup>	NO <sub>3</sub> <sup>-</sup>	O <sub>2</sub>	NH <sub>4</sub> <sup>+</sup>	NO <sub>3</sub> <sup>-</sup>	N <sub>2</sub> -N
	°C	mg g <sup>-1</sup>		μmol L <sup>-1</sup>		μmol m <sup>-2</sup> h <sup>-1</sup>			
<b>May 2015</b>	23.8 ± 1.7	61 ± 16	3.8 ± 0.5	11.3 ± 2.6	37 ± 1.0	-1760 ± 742	274 ± 157	-112 ± 51	115 ± 79
<b>July 2015</b>	26.3 ± 0.4	48 ± 6	2.9 ± 0.7	1.2 ± 0.3	54 ± 3.9	-1064 ± 147	64 ± 38	-42 ± 30	99 ± 51
<b>Sept 2015</b>	25.3 ± 1.0	48 ± 9	2.9 ± 0.5	2.8 ± 0.5	60 ± 1.5	-1041 ± 169	-2 ± 44	-74 ± 26	202 ± 66
<b>Dec 2015</b>	8.8 ± 0.9	54 ± 9	3.1 ± 0.7	4.2 ± 0.2	60 ± 0.1	-380 ± 84	-5 ± 49	-10 ± 20	118 ± 50
<b>April 2015</b>	9.7 ± 0.7	51 ± 22	3.2 ± 1.3	3.1 ± 0.3	75 ± 0.4	-546 ± 213	45 ± 42	-17 ± 47	96 ± 48

### Solid phase chemistry

The mean concentrations of carbon and nitrogen in the top 1 cm of sediment averaged 51 ± 11 and 3.2 ± 0.7 mg g<sup>-1</sup> respectively, over all dates. The high degree of temporal variability was illustrated by the large seasonal changes in C and N at station 2 (Figure 19 A, B). When the median and average

concentrations of the 6 sites sampled in all five months were examined for each sample point, there were no statistical differences (Figure 19 C, D). All sediment solid phase phosphorus data is discussed in a separate section.

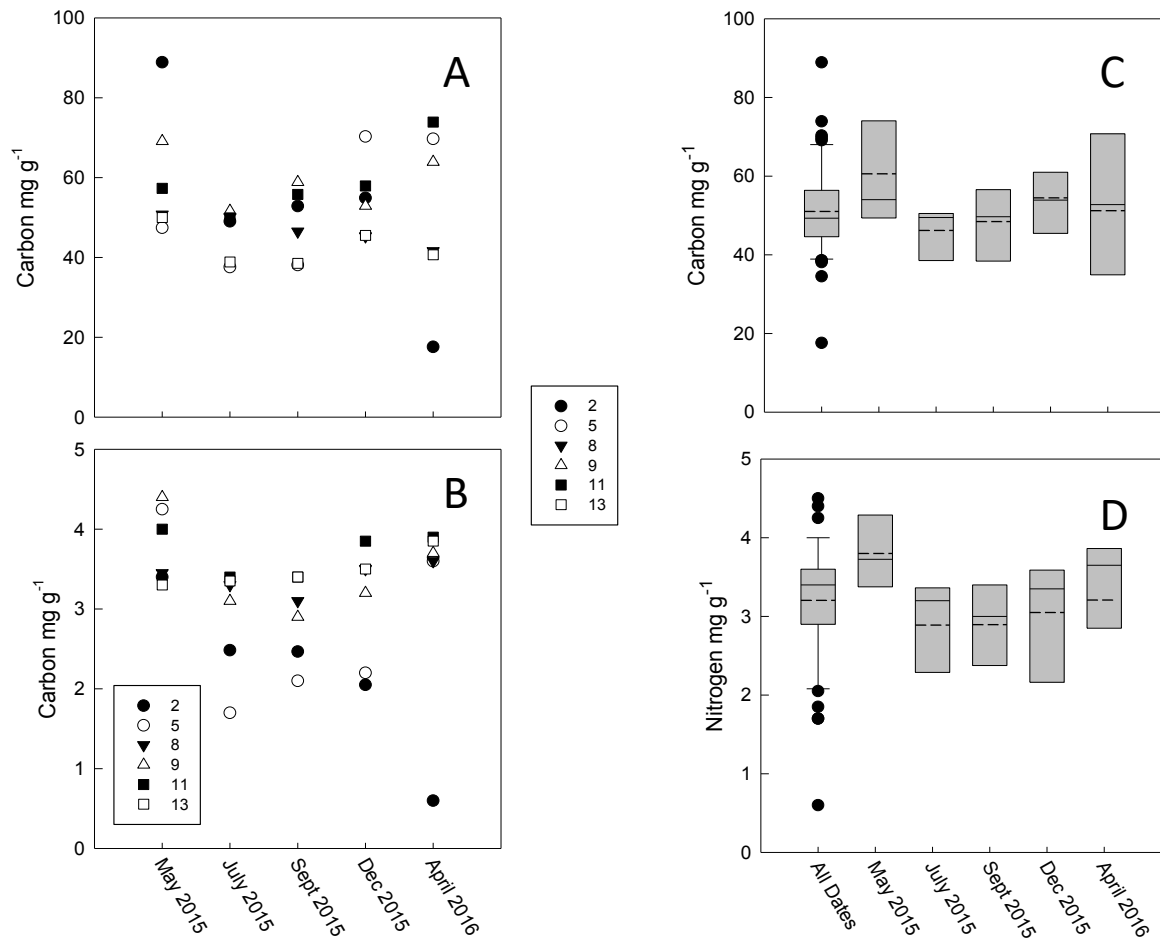


**Figure 19. Concentrations of 0-1 cm carbon and nitrogen over time at 6 stations in the Conowingo reservoir (A, B) with box plots of seasonal C and N data (C,D). The “all data” box plots include the six sites in A and B as well as 2-7 more sites that were not sampled every time.**

Sediment chlorophyll a, expressed on an areal basis, was generally high at these sites, with the mean from all samples of  $26.9 \pm 17.1 \text{ mg m}^{-2}$  (Table 8; Figure 20). The highest mean and median concentrations were observed in May 2015, with concentrations ~2 times the values for all other

months. Of the 6 stations measured over time, station 2 had both the highest and lowest concentrations. The single highest observation was 79.2 mg m<sup>-2</sup> in May 2015 for station 7.

**Table 8. Statistics for chlorophyll a concentrations in Conowingo reservoir. “All Dates” is a summation of all data from all dates, while the date-specific data consists of the 6 stations that were sampled all 5 times, allowing a fair comparison of the data. Only the May 2015 and December 2015 data are significantly different (Kruskal-Wallis P, 0.05), and there were no significant differences between stations.**

	Mean	Std Dev	Max	Min	Median
All Dates	26.9	17.1	79.2	3.1	20.3
May-15	39.9	21.3	73.4	18.6	37.6
Jul-15	17.6	5.3	25.5	9.8	17.4
Sep-15	16.8	3.7	22.8	12.4	16.6
Dec-15	15.2	4.0	19.6	8.5	15.1
Apr-16	24.3	13.9	39.9	3.1	24.9

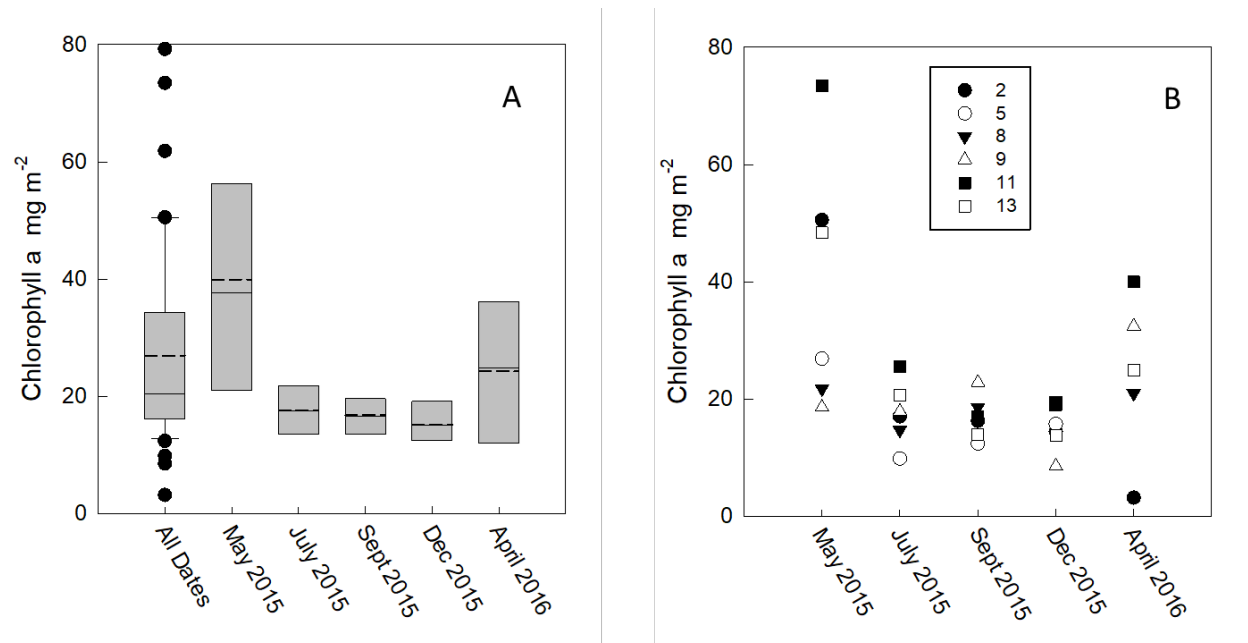


**Figure 20. Sediment chlorophyll a data. Concentrations are expressed on an areal basis.**

### Sediment oxygen fluxes

Sediment oxygen fluxes averaged  $-1007 \pm 603 \mu\text{mol m}^{-2} \text{h}^{-1}$  for all data, with the highest uptake rates in May ( $-1760 \pm 741 \mu\text{mol m}^{-2} \text{h}^{-1}$ ). Similar rates were observed in July ( $-1064 \pm 147 \mu\text{mol m}^{-2} \text{h}^{-1}$ ) and September ( $-1041 \pm 168 \mu\text{mol m}^{-2} \text{h}^{-1}$ ). December oxygen fluxes ( $-379 \pm 83 \mu\text{mol m}^{-2} \text{h}^{-1}$ ) represented the lowest SOD average calculated in this study (Figure 21). Two pairwise comparisons, July versus May and September did not yield significant differences in  $\text{O}_2$  fluxes (Kruskal Wallis,  $P > 0.05$ ). No correlations between oxygen flux and chlorophyll a concentration were observed, though the highest mean chlorophyll a and sediment oxygen fluxes both were observed in May.

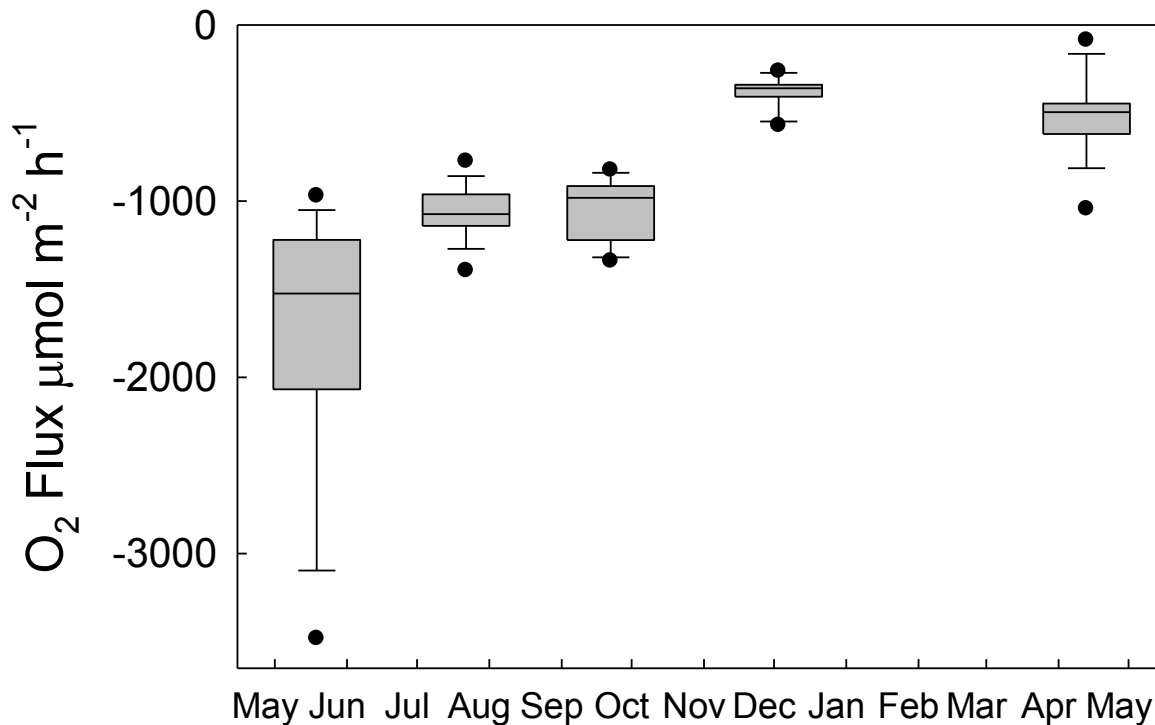


Figure 21. Box plots of oxygen flux data from all sites over time.

### Sediment Nitrogen cycling

The median ammonium flux was mostly directed out of the sediment in May ( $274 \pm 157 \mu\text{mol m}^{-2} \text{h}^{-1}$ ), July ( $64 \pm 38 \mu\text{mol m}^{-2} \text{h}^{-1}$ ), and April ( $45 \pm 42 \mu\text{mol m}^{-2} \text{h}^{-1}$ ), with uptake in September ( $-2.2 \pm 44 \mu\text{mol m}^{-2} \text{h}^{-1}$ ) and December ( $-5.4 \pm 49 \mu\text{mol m}^{-2} \text{h}^{-1}$ ; Figure 22). The ammonium flux in May was significantly higher (Kruskal Wallis,  $P < 0.001$ ) than those calculated for July, September, December, and April.

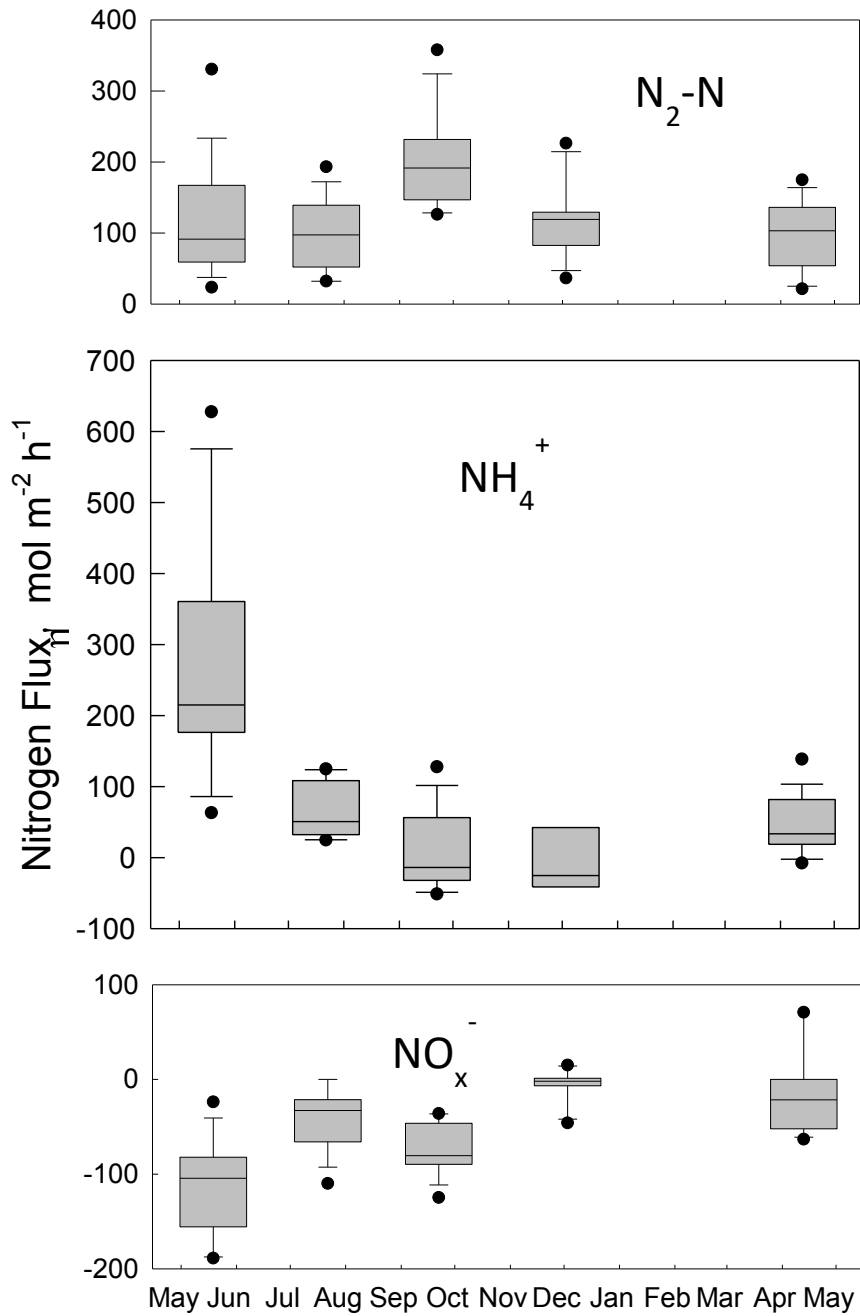
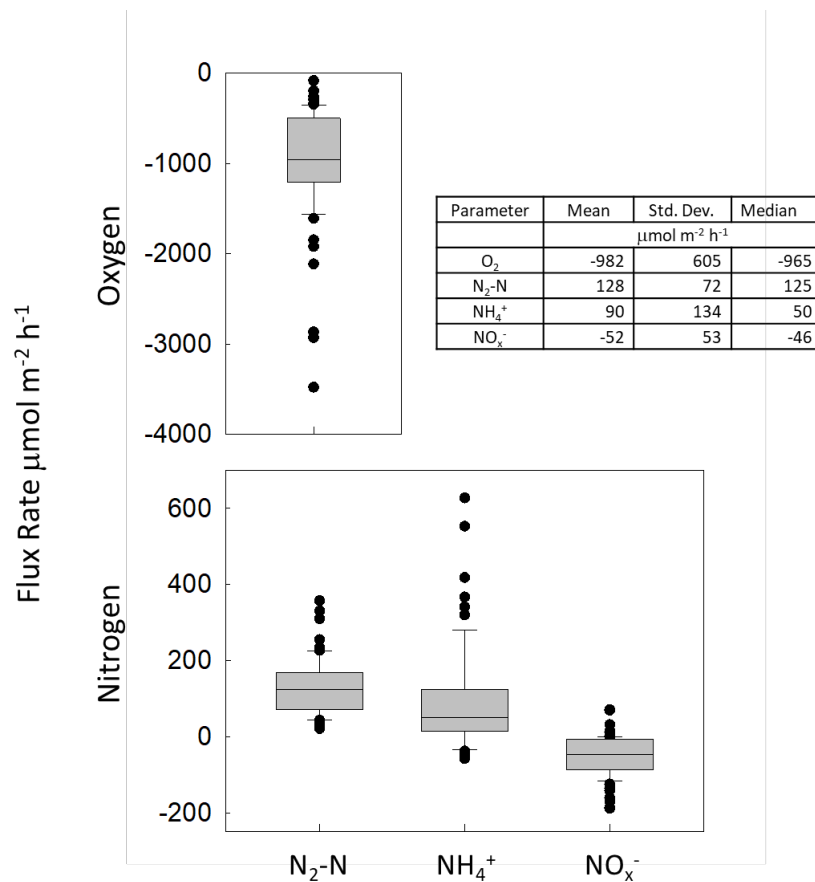


Figure 22. Seasonal box plots of nitrogen fluxes in Conowingo reservoir sediments in 2015 and 2016. Data from all stations are included in each box.

The nitrate flux was usually directed into the sediment in this study. The highest fluxes were in for May ( $-112 \pm 51 \mu\text{mol m}^{-2} \text{h}^{-1}$ ), September ( $-74 \pm 26 \mu\text{mol m}^{-2} \text{h}^{-1}$ ) and July ( $-42 \pm 30 \mu\text{mol m}^{-2} \text{h}^{-1}$ ). The lowest nitrate flux were in April ( $-17 \pm 47$ ), and December ( $-10 \pm \text{SD } 20$ ) (Figure 22). The May nitrate flux calculated was significantly higher than those calculated for December, April, and July (Kruskal Wallis,  $P > 0.001$ ). The December nitrate flux was significantly lower (Kruskal Wallis,  $P < 0.001$ ) than those of July, and September, but not for April (Kruskal Wallis,  $P > 0.001$ ). The nitrate flux calculated for July was not significantly higher than that of September or April.

Overall, the net  $\text{N}_2$  production was relatively high ( $128 \pm 79 \mu\text{mol m}^{-2} \text{h}^{-1}$ ). The highest Net  $\text{N}_2$  production was in September ( $201 \pm 66 \mu\text{mol m}^{-2} \text{h}^{-1}$ ), followed by December ( $118 \pm 72 \mu\text{mol m}^{-2} \text{h}^{-1}$ ), July ( $99 \pm 51 \mu\text{mol m}^{-2} \text{h}^{-1}$ ), and April ( $96 \pm 48 \mu\text{mol m}^{-2} \text{h}^{-1}$ ). The net  $\text{N}_2$  production in September was significantly higher than those calculated for May, July, December, and April (Kruskal Wallis,  $P < 0.001$ ). Other pairwise comparisons in net  $\text{N}_2$  production among sampling months were not significant (Kruskal Wallis,  $P > 0.001$ ). Overall an examination of all nitrogen flux data shows that  $\text{N}_2\text{-N}$  is the major constituent of nitrogen fluxes, with an average efflux  $\sim 42\%$  higher than ammonium effluxes (Figure 23).



**Figure 23. Box plots of all sediment water oxygen and nitrogen flux data from all sites and seasons. The inset table shows the mean, standard deviation and median of the data. The horizontal bars within the boxes are median values.**

The oxygen flux in May decreased towards the dam (Figure 24A). Apart from May, where a dramatic increase and decrease occurred along the downward gradient, ammonium flux showed a slight increase and relatively small peaks in the region near the Conowingo Dam (Figure 24B). A slight decreasing trend was observed in July and September in the nitrate flux, while December and May small fluctuations along the southward direction, respectively (Figure 24C). In general, net  $N_2$  flux showed a decreasing trend towards the dam (Figure 24D). This pattern was clearly shown in September and December. In May,  $N_2-N$  showed the highest effluxes upstream followed by a sharp decrease with smaller peaks near the Conowingo Dam.

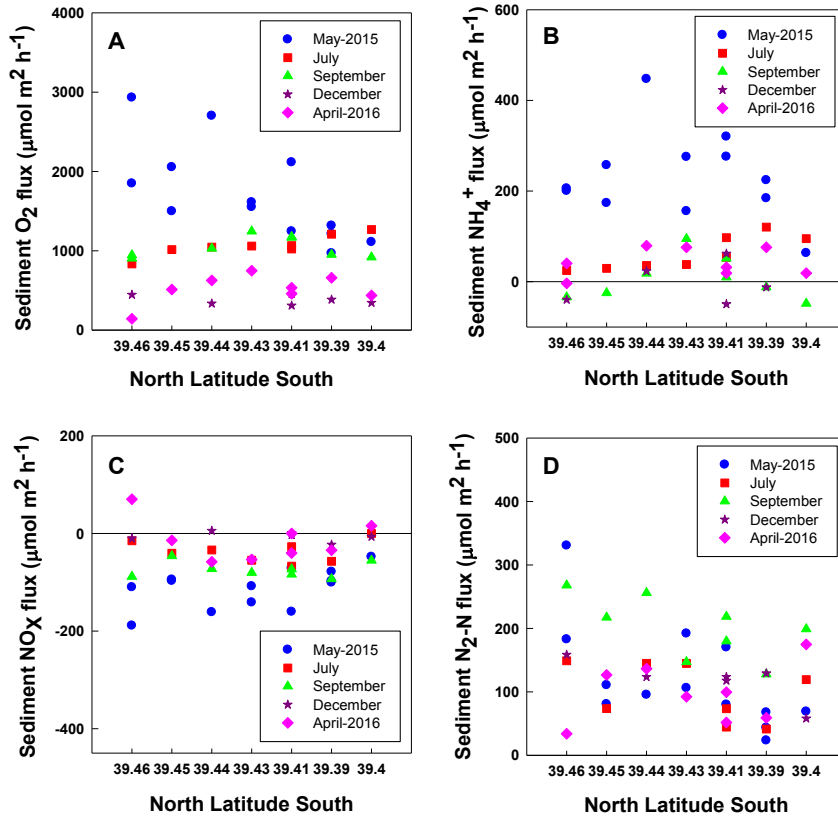


**Figure 24. Latitudinal Transects. (A)** Scatter plot showing all net oxygen flux data calculated for individual sediment cores along a latitudinal transect during the sampling period of May-2015-April-2010 at the Conowingo Reservoir. **(B)** Scatter plot showing all net ammonium flux data calculated for individual sediment cores along a latitudinal transect during the sampling period of May-2015-April-2010 at the Conowingo Reservoir. **(C)** Scatter plot showing all net nitrate flux data calculated for individual sediment cores along a latitudinal transect during the sampling period of May-2015-April-2010 at the Conowingo Reservoir. **(D)** Scatter plot showing all net  $N_2-N$  flux data calculated for individual cores along a latitudinal transect during the sampling period of May-2015-April-2016 at the Conowingo Reservoir.

## Discussion

### Stoichiometric relationship of net sediment fluxes

The Redfield ratio is a useful stoichiometric relationship based on the characteristic proportions of C, N and P in phytoplankton biomass, and remineralization results in a fixed proportion of N, P, and C. These ratios provide a better understanding of Conowingo Reservoir sediment processes and allow inferences on environmental processes that cause deviation from the predictable ratios.

Figure 25 shows a general tendency of points to be around the 100% stoichiometric line, suggesting that most of the remineralized nitrogen was denitrified (Figure 25A). A detailed analysis of points split by sampling months showed that during December and April, most of the nitrogen was denitrified. September appeared to be a transition month, where the sequestration or ammonium release was proportional to the denitrification. In May and July points were below the 100 % stoichiometric line, meaning that in these two latter months, remineralized nitrogen was sequestered in sediment or released as ammonium to the water column. In average, the ratios O: N<sub>2</sub>-N (7.9) and O: ΣN (6.7) were very similar to that predicted by the Redfield ratio.

This plot shows a strong and significant (Mann-Whitney Test,  $P < 0,05$ ) correlation between the NH<sub>4</sub><sup>+</sup> flux and DIN (NO<sub>x</sub><sup>-</sup> + NH<sub>4</sub><sup>+</sup> flux) with most of the points around the 1:1 stoichiometric line, indicating that the net sediment NO<sub>x</sub><sup>-</sup> efflux was negligible and denitrification was an important process in sediment nitrogen cycling (Figure 25B).

The net flux of sum of all inorganic nitrogen species, i.e. the sum of net flux of N<sub>2</sub>-N, NH<sub>4</sub><sup>+</sup>, and NO<sub>x</sub><sup>-</sup> (also referred to as ΣN), may be stoichiometrically related to the amount of oxygen consumed during the phytoplankton biomass remineralization (Fig. 25C). In this plot, it is shown a strong relationship with most of the points falling around the 100 % stoichiometric line, meaning that microbial metabolism was efficient in remineralizing nitrogen from the sediment to the water column. A more detailed examination of the points showed that May (87 %), July (75 %), and April (70 %) showed the highest percentage of points falling around or above the 100 % stoichiometric line, while nitrogen remineralization in sediment in September (20 %) and December (50 %) was less effective. By subtracting the net flux of nitrate to the net N<sub>2</sub>-N flux, we can evaluate how these two processes are coupled in sediment at the Conowingo Reservoir. As it is shown, most of the nitrate for denitrification was supplied by the sediment nitrification (Figure 25D).

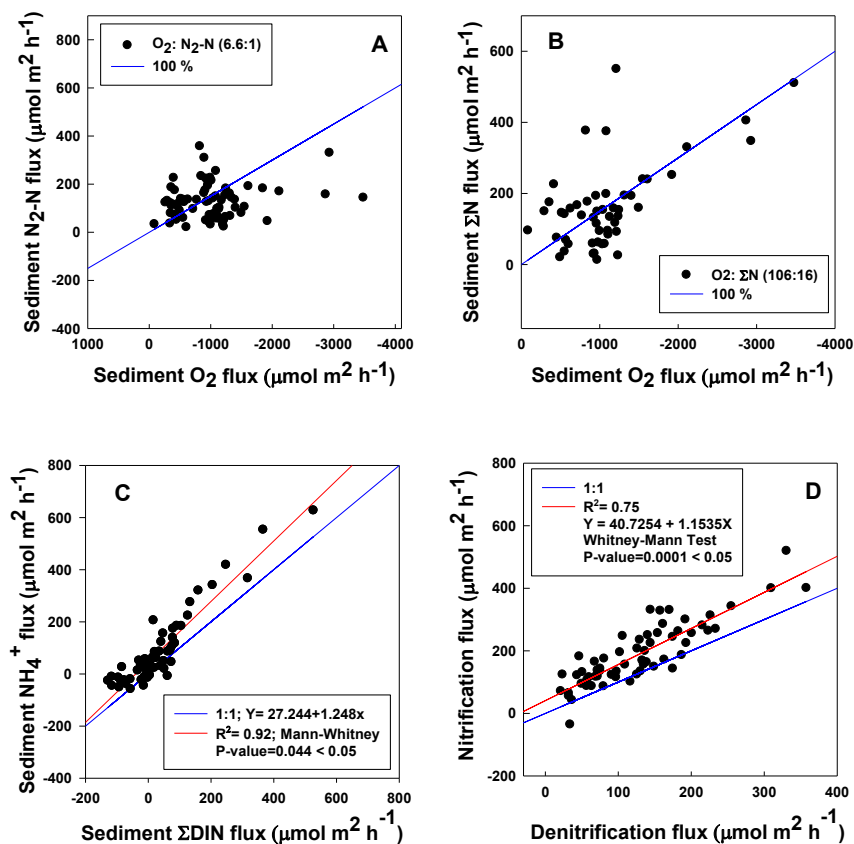


**Figure 25. Sediment Flux Property Plots.** (A) Relationship between net sediment  $N_2-N$  flux and net sediment oxygen flux for the individual cores. The 100 % line represents a Redfield ratio of  $O_2:N$  (6.6:1). (B) Relationship between the sum of all net sediment N flux ( $N_2-N+NH_4^++NO_3^- = \Sigma N$ ) and net sediment oxygen flux for the individual cores. The blue line represents Redfield ratio of C:N (106:16), assuming to be identical to the  $O^2:N$  ratio. (C) Relationship between the net sediment dissolved inorganic nitrogen (DIN =  $NH_4^++NO_3^-$ ) flux versus net sediment ammonium flux. Most of the individual cores are around the 1:1 blue line, meaning both that sediment  $NO_3^-$  fluxes were about zero or negative with a net loss to denitrification ( $N_2-N$ ). This figure also shows a strong positive Spearman correlation fit (red line) between net sediment ammonium flux and net dissolved DIN flux. (D) Relationship between denitrification (net sediment  $N_2-N$  flux) and nitrification (net sediment  $N_2-N$  flux minus net sediment  $NO_3^-$  flux).

## Effects of Reservoir Processes on Nutrient Balances

Given the importance of climate on water discharge, sediment types and transport, and water quality downstream to the Conowingo reservoir (Langland 2014, Hirsch 2012, Langland and Hainly 1997), we first put in a historical context the water discharges reported for Marietta Monitoring Site (USGS Identification Number 01576000), Pennsylvania, USA, (Marietta MS) for the Lower Susquehanna River subbasin, which is the nearest upstream monitoring site to the our study sites at the Conowingo Reservoir. Overall, the average water discharge ( $890 \pm 676 \text{ m}^3 \text{ s}^{-1}$ ) during our study period was similar to that calculated for the 1960-1970 decade ( $855 \pm 667 \text{ m}^3 \text{ s}^{-1}$ ), which was one of the periods with lowest water discharge ever reported for Marietta MS (Figure 26). Such low flows likely result in very low rates of scour. The average water discharge reported for Marietta MS for 2015, according to Scott (2012), would predict a residence time of water in the Conowingo Reservoir of about 4 days during our study. Under this residence time, Scott (2012) also estimated that only 5 percent of the “total annual sediment load” is transported from the upper Susquehanna River reaches to the downstream reservoirs, including Conowingo Reservoir. The hydrologic conditions that there was a relatively low sediment flux from the upstream reaches during the sampling period of this study and the water residence time in Conowingo Reservoir was enough to retain and remineralize the labile organic matter *in situ*. In this study, the water temperature at Conowingo Reservoir reflected normal seasonal variations, and non-significant differences between surface and bottom water temperatures, DO, and conductivity suggested a well mixed water column. Contrasting with our results, Mathur et al. (1988) reported DO stratification during the summer and attributed it to meteorological factors. More recently, Steffy (2013) did not find any stratification at the Conowingo Reservoir. Even at the deepest part of the Conwingo Reservoir (20 m), the latter author reported a relative very small changes between surface and bottom waters in both temperature ( $0.37^\circ\text{C}$ ) and DO ( $0.26 \text{ mg/L}$ ). Further discussion on the benthic flux data is included in the “Conowingo Biogeochemistry In Perspective” section of this report.

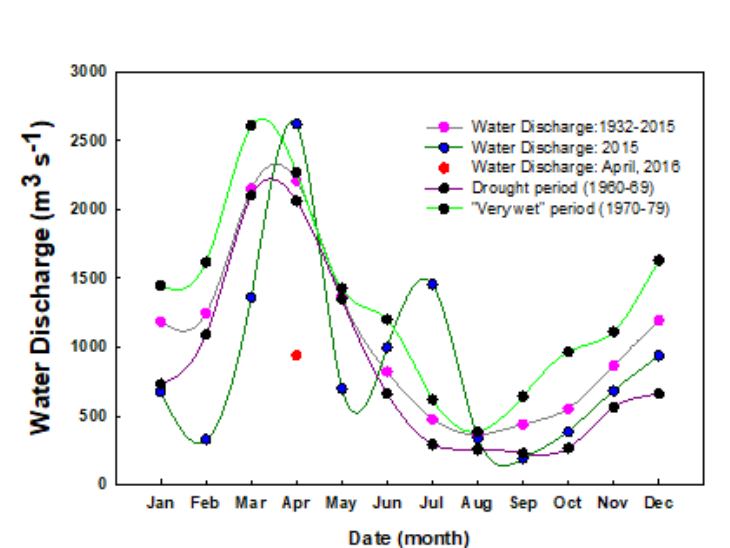


Figure 26. Conowingo water discharge (USGS monitoring data).

# Lake Clarke and Lake Aldred Sediment Biogeochemical Measurements

## Introduction

Together Lake Clarke and Lake Aldred have a similar area as the Conowingo Reservoir. The same concerns for the deposition and erosion of materials derived from the watershed that have driven this program are also present in these two reservoirs. Three stations were sampled in each reservoir on April 27, 2016 using the same procedures for coring, incubation and chemical analysis as in the Conowingo Reservoir. The sampling time was chosen for a period immediately after the April 13, 2016 Conowingo Reservoir sampling, but because April is a period of maximum temperature change, the upper reservoir temperatures were 18°C versus 9.6°C in the Conowingo Reservoir. Thus, biogeochemical rate processes are not easily compared between these three systems because of potentially large changes in microbial processing rates.

## Solid Phase and Pore Water Chemistry

The carbon and nitrogen concentrations in the cores from Lake Clarke and Aldred were similar to observations in the Conowingo Reservoir (Figure 27), with C concentrations ranging from 31-69 mg g<sup>-1</sup> and N concentrations ranging from 1.4-4.2 mg g<sup>-1</sup>. The molar ratio had values that ranged from 11.6-29.0, suggesting either different organic matter sources or some low N coal in the samples.

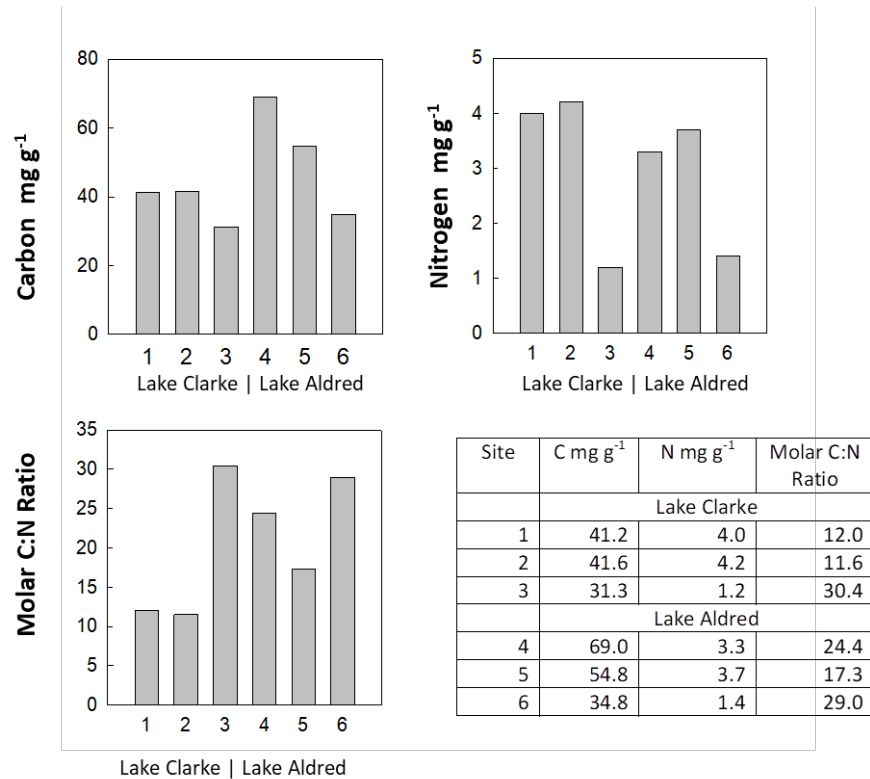


Figure 27. Solid phase C and N concentrations and the molar C:N ratio of surficial (0-1 cm) deposits.

Pore water concentrations were determined on all cores, but as with the long cores and some short cores from the Conowingo Reservoir, not all sections had recoverable water for analysis. High variability in ammonium concentrations were observed, with the expected downward increase in most cores (Figure 28). Core 2 in Lake Clarke had exceptionally high ammonium concentrations ( $> 3,000 \mu\text{mol L}^{-1}$ ), while few observations in Lake Aldred had concentrations in excess of  $100 \mu\text{mol L}^{-1}$ . The presence of dissolved iron in all cores was consistent with Conowingo observations.

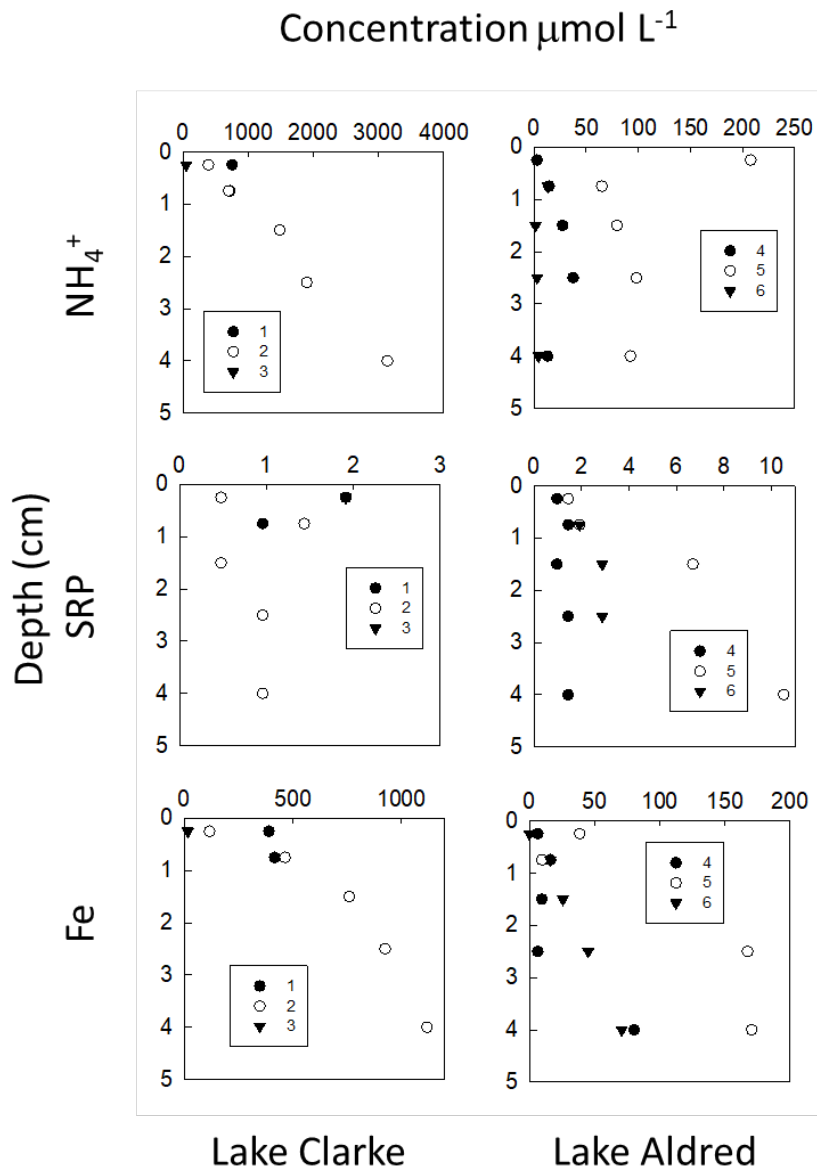


Figure 28. Pore water chemistry of Lake Clarke and Lake Aldred sediments.

## Sediment-Water Exchange Rates

The sediment-water exchange rates in Lake Clarke and Lake Aldred (Figure 29) were generally similar to Conowingo Reservoir rates. Oxygen flux rates in the two reservoirs averaged  $-983 \pm 316 \mu\text{mol m}^{-2} \text{h}^{-1}$ , with the highest uptake rates at site 3 in Lake Clarke and site 4 in Lake Aldred. Rates of  $\text{N}_2\text{-N}$  production averaged  $115 \pm 68 \mu\text{mol m}^{-2} \text{h}^{-1}$  in the two reservoirs, with the highest rates in Lake Aldred. Ammonium fluxes were higher in Lake Clarke, with sites 1 and 2 exceeding  $100 \mu\text{mol m}^{-2} \text{h}^{-1}$ . Rates at the other sites were much lower and in Lake Aldred there were two observations of ammonium uptake. The  $\text{NO}_x^-$  flux rates were lower in Lake Clarke, with one core having a substitution production rate. In Lake Aldred, most cores had a large  $\text{NO}_x^-$  uptake rate.

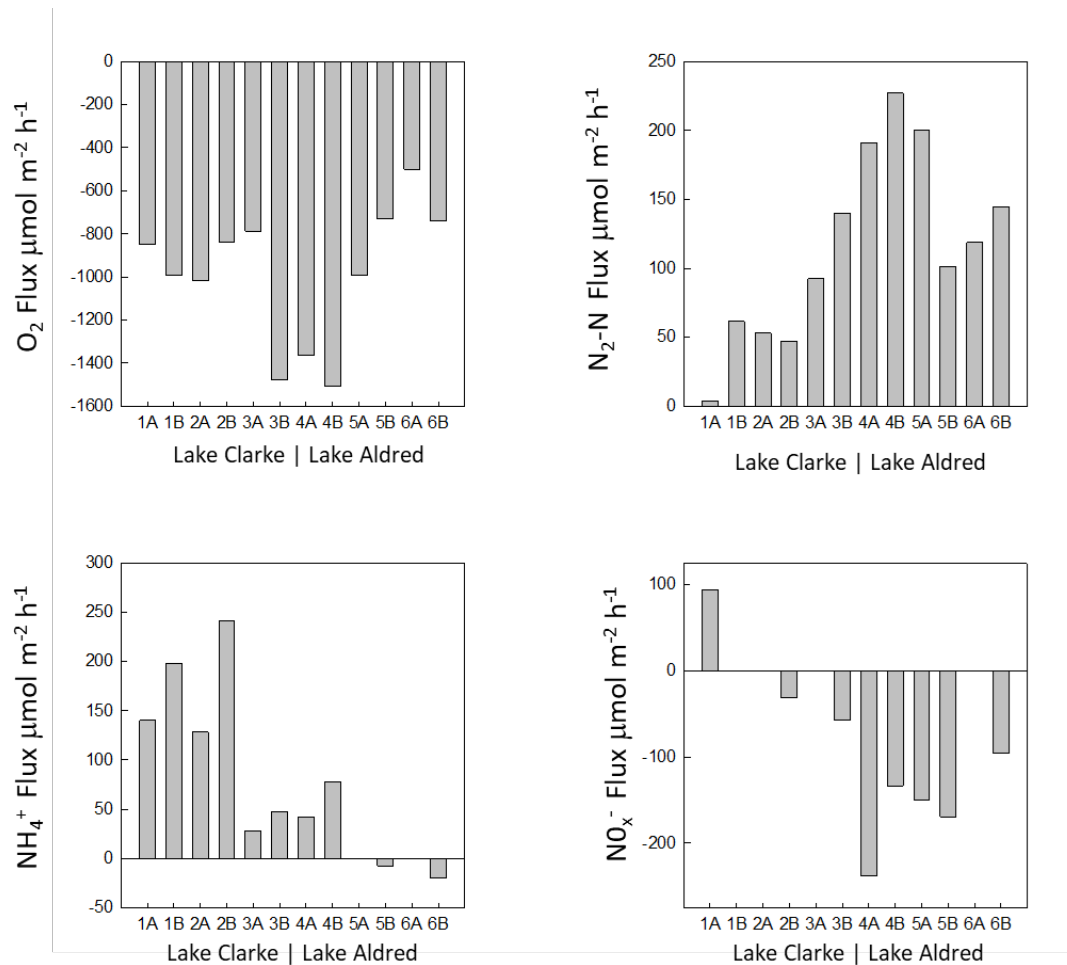


Figure 29. Sediment-water exchange rates of Lake Clarke and Lake Aldred sediments.

## Sediment-Water Exchange Rates – Chesapeake Bay Fluxes

Although sediment-water exchange rate data are abundant in the upper Chesapeake Bay (Cornwell and Boynton 1999, Boynton and Bailey 2008), there are mostly restricted to measurements of the fluxes of oxygen, ammonium,  $\text{NO}_x^-$  and SRP. Data was collected for sediment-water exchange on two occasions (August 2015, April 2016) in conjunction with 1) experiments on Conowingo sediment additions and 2) the measurement of radionuclide inventories (Palinkas et al. 2014) by Dr. Cindy Palinkas for baseline measurements prior to high flow events (which never occurred). The SRP flux data from the August 2015 fluxes are used as the initial flux data prior to sediment manipulations. The April 2016 data are used in a comparison of fluxes from the upper reservoirs into the upper bay (“Nitrogen Cycling – Reservoirs to the Bay” report section). The data are briefly presented and discussed here, with a particular emphasis on denitrification and SRP fluxes. Station locations are tabulated in Table 3.

Upper bay sediment oxygen demand and  $\text{N}_2\text{-N}$  effluxes in August 2015 (Figure 30) were similar to average summer rates in the Conowingo Reservoir. Rates of ammonium efflux were variable but 4 of 6 rates were similar to average July rates in the Conowingo Reservoir. September rates in the Conowingo were negligible, and were thus much lower than these bay sites. The uptake of  $\text{NO}_x^-$  was similar in the upper bay and in the Conowingo Reservoir. Only the Lee 5A/Still Pond site had SRP effluxes, much higher than reservoir observations.

In April 2016, the most northern site had similar rates as the Conowingo Reservoir (Figure 31), with higher rates observed toward the south. Denitrification rates ( $\text{N}_2\text{-N}$ ) were generally similar in the reservoir and bay, though in this case the more southerly sites were closer to average reservoir rates ( $96 \mu\text{mol m}^{-2} \text{h}^{-1}$ ). Ammonium efflux rates were about half of reservoir rate observations in April, with one lower bay site having high rates in one core. In the bay, nitrate fluxes were low or not significant, with one site at the top of the bay having a core with high effluxes. SRP fluxes were negligible in the reservoir and in the bay. The overall picture of upper bay sediments is one of generally similar behavior to observations in the Conowino Reservoir.

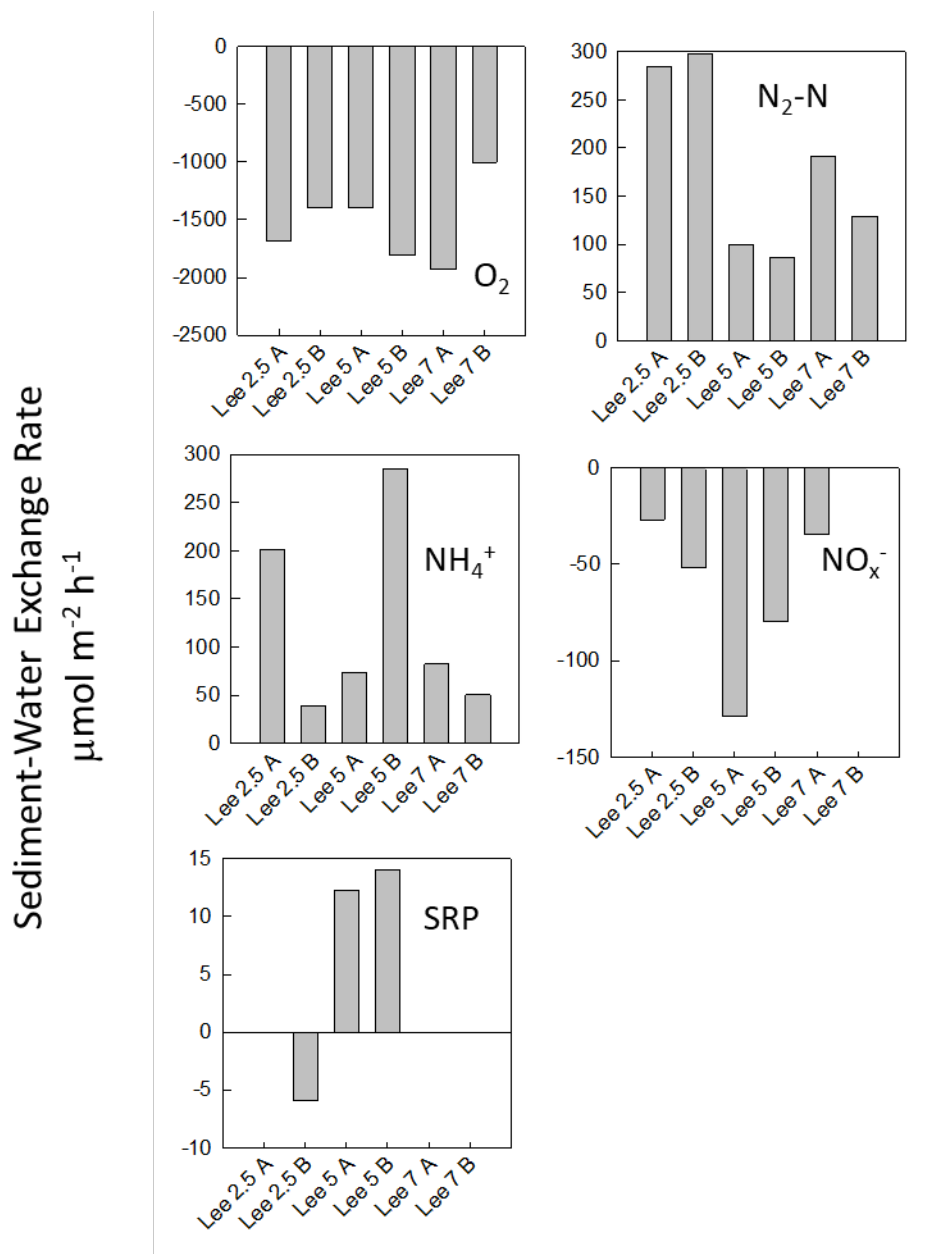


Figure 30. Sediment-water exchange rates from Chesapeake Bay sites, August 15, 2015. Samples were incubated at 26.4°C. Lee 3 is co-located with the long-term station Still Pond. For reference, the station locations (left to right) represent a south to north transect.

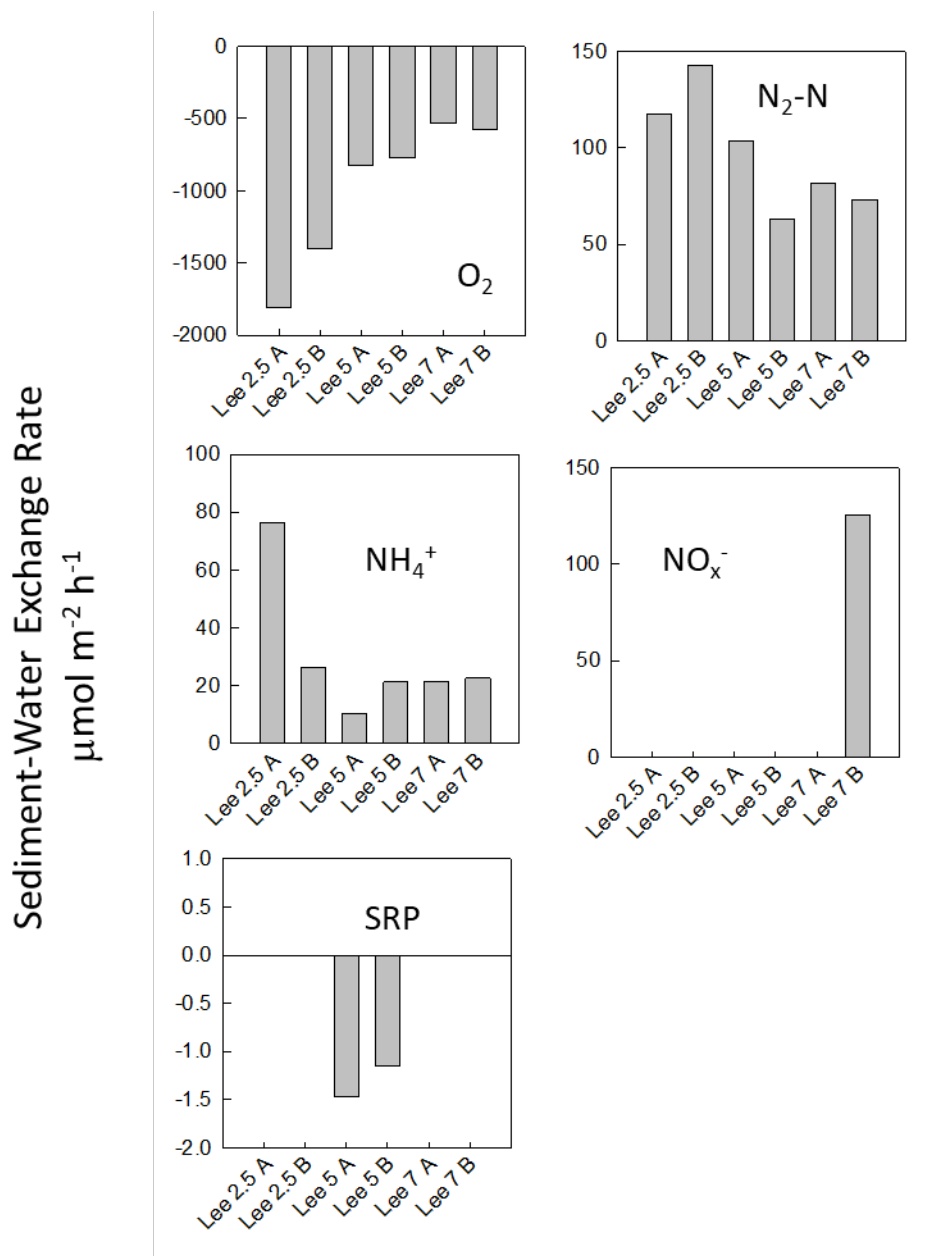


Figure 31. Sediment-water exchange rates from Chesapeake Bay sites, April 28, 2016. Samples were incubated at 14.5°C. For reference, the station locations (left to right) represent a south to north transect.

# Reservoir scour as a major source of bioavailable phosphorus to a coastal plain estuary? (Zoe Vulgaropulos)

## Introduction

Eutrophication due to anthropogenic nutrient enrichment often is a major problem in estuarine and coastal systems. Large increases in phytoplankton production and biomass, as well as other effects such as anoxia and loss of benthic photosynthesis, occur with high inputs of nitrogen (N) and phosphorus (P). While nitrogen can be removed as  $N_2$  gas through denitrification, phosphorus gaseous losses are negligible so burial and transport out of the system are the main outputs. Another key difference between N and P cycles is that most of the N load in rivers is dissolved, while about 95% of the P load is particulate (Follmi, 1996); not all of this particulate P will necessarily be released as dissolved, bioavailable phosphate. Primary production is usually limited by P in freshwater and N in coastal seawater (Howarth and Paerl 2008), where fresh and saline water mix, are often characterized by spatial and seasonal variation in N and P limitation (Fisher et al. 1992). Phosphorus is typically limiting in the spring due to inflowing fresh water high in dissolved N, while N limitation dominates in summer when DIN is depleted and phosphate is released from anoxic sediments (Fisher et al. 1999, Conley 2000, Kemp et al. 2005). Due to the dynamic nature of estuarine systems, both N and P must be considered in nutrient management strategies.

Particulate inorganic P, which makes up nearly 60% of fluvial particulate P loads (Follmi 1996), can be converted to bioavailable dissolved inorganic P through processes enhanced by increased salinity (Caraco et al. 1990, Jordan et al. 2008). Phosphorus bound to iron oxyhydroxides (FeOOH), a significant fraction of the P load, can be released to solution when FeOOH is reduced in anoxic sediment layers (Figure 32). Under aerobic freshwater conditions, reduced dissolved Fe(II) can diffuse upward to aerobic sediments and become re-oxidized to FeOOH, which has a high surface area and affinity for inorganic P. Phosphorus can also be immobilized under anaerobic freshwater conditions due to sorption to Fe(II) hydroxides and/or precipitation of ferrous-phosphate minerals such as vivianite (Cornwell 1987, Roden and Edmonds 1997). In contrast, in more sulfate-rich saltwater sediment, sulfides formed by sulfate reduction in anoxic sediment layers chemically reduce Fe(III) to iron sulfides; this immobilizes iron in the sediment, enhancing the efflux of iron-bound phosphorus to the water column (Krom and Berner 1981, Lehtoranta et al. 2009). Significant phosphate mobilization through this pathway requires high inputs of labile organic carbon, which decreases the redox potential and allows the dominance of sulfate reduction (Cornwell and Sampou 1995, Lehtoranta et al. 2009). Even when the water column is re-oxidized, the burial of iron as iron sulfides minimizes resorption of phosphate to iron oxides (Krom and Berner 1980).

Various extraction techniques have been used to differentiate pools of particulate P and assess the bioavailable fraction. Citrate-dithionite-bicarbonate (CDB) solutions are often used in sequential extractions to extract P bound to FeOOH (Ruttenberg 1992). However, since this strong reducing agent dissolves crystalline iron oxides, it may overestimate the amount of Fe-bound P that is bioavailable (Kostka and Luther 1994, Jordan et al. 2008). Alternatively, more moderate reducing agents such as ascorbate can also be used to extract potentially mobile Fe-bound P (Scicluna et al. 2015). However,

ascorbate only reduces amorphous FeOOH and may not include the potentially mobile P associated with crystalline Fe oxides (Anschutz et al. 1998). Because sequential extraction methods often have overlaps between the pools of P extracted in each step, the extraction categories are often operationally defined.

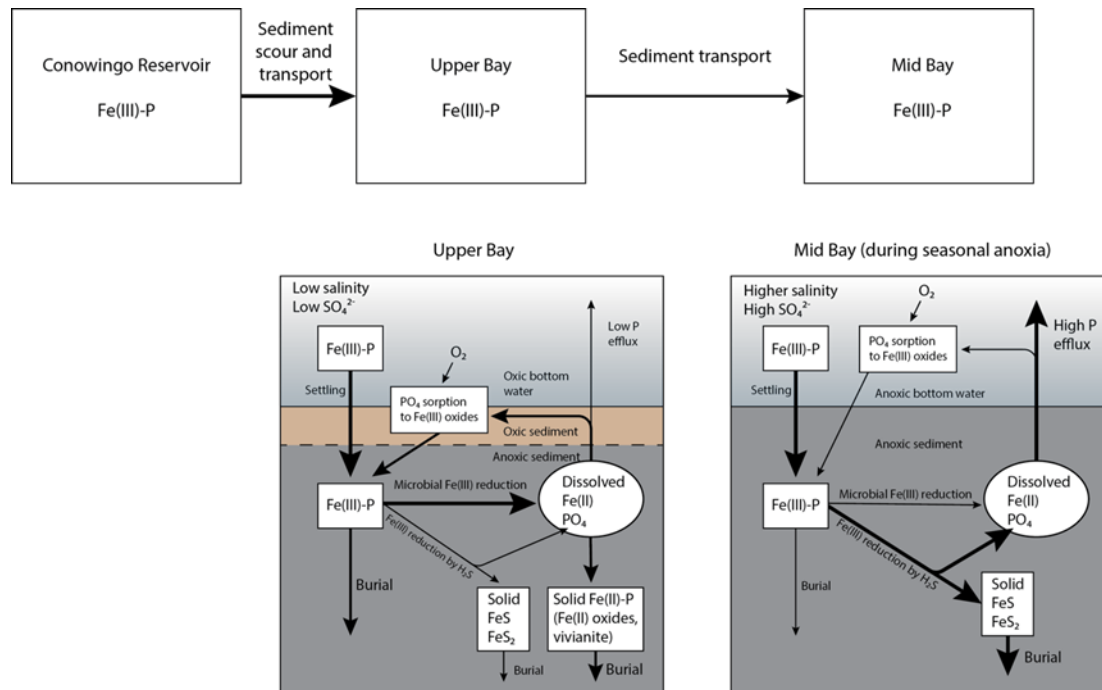


**Figure 32. Sedimentary iron (Fe), phosphorus (P), and sulfur (S) cycling in the Upper vs. Mid Chesapeake Bay. In the Upper Bay and similar oligohaline systems, iron reduction is the dominant anaerobic metabolic pathway, and P efflux is limited due to sorption to Fe oxides and precipitation of Fe(II) minerals. In contrast, in higher salinity regions such as the Mid Bay where sulfate reduction dominates, Fe is reduced by sulfides to Fe sulfides, burying Fe and allowing greater P efflux.**

While nutrient loading contributes to eutrophication and harmful algal blooms in Chesapeake Bay, the role of suspended fluvial sediments has largely been relegated to concerns about light attenuation. The Susquehanna River is responsible for nearly half the freshwater input to the Bay as well as a large portion of the sediment and nutrient loads, although a significant portion of these loads are trapped in reservoirs behind three hydroelectric dams near the mouth of the river. The two upstream reservoirs were filled with sediment by the mid-1900s, a few decades after their construction. Conowingo Reservoir, the farthest downstream, has reached about 92% of its storage capacity (Langland, 2015). Recent reports suggest that outputs of sediment, phosphorus, and nitrogen from the reservoir have increased due to reservoir infilling and event-driven scour (Hirsch 2012, Langland 2015, Zhang et al. 2015). This increased flux of sediment and nutrients complicates the attainment of water quality goals established by the Total Maximum Daily Loads (TMDLs; Linker et al. 2016), which target watershed nitrogen, phosphorus, and sediment reductions from the Chesapeake Bay watershed. Although Conowingo Dam construction in 1928 resulted in a trapping efficiency of 70-75% of sediment inputs to

the reservoir, current trapping efficiency has been reduced to 45-50% (Langland 2015). Flow-normalized loads of suspended sediment and particulate nutrients have increased at Conowingo Dam since the 1990s, while inputs to the reservoir system have decreased (Zhang et al., 2013). This decrease in net deposition of sediment and nutrients has a greater effect on Chesapeake Bay P loading than N loading, since most P is particulate (Zhang et al., 2013, 2016). A large fraction of sediment transport across the dam occurs during high-flow events due to scouring of reservoir deposits. Although scoured sediment itself is not a significant threat in terms of long term water clarity, nutrients associated with sediment are detrimental to water quality (Cercio and Noel 2016).

The reactivity of particulate P transported from Conowingo Reservoir to the Chesapeake Bay during a scour event is strongly dependent on where sediments are deposited along the Bay salinity gradient. In subestuaries of the Chesapeake Bay, mobilization of Fe-bound P is enhanced with increasing salinity due to the conversion of Fe oxides to Fe sulfides (Hartzell et al. 2010). In the Bay mainstem, soluble reactive P (SRP) efflux from sediment is most pronounced in the mesohaline mid Bay relative to the upper and lower Bay (Cowan and Boynton 1996). Iron sulfide formation and burial is highest in the mid Bay due to the greater availability of sulfate and organic matter and the fine-grained nature of the deposits (Cornwell and Sampou 1995).

Although storm scour is likely to transport increased loads of particulate P from the Lower Susquehanna reservoir system to the Chesapeake Bay, it is unclear what fraction of this scoured P is likely to be reactive. The objective of this study is to assess the potential bioavailability of P in reservoir sediments. First, we examine benthic SRP flux along the Chesapeake Bay salinity gradient and the reservoir system in order to evaluate differences in P reactivity depending on environmental conditions at the site of deposition. Then, we characterize reservoir sediments using extractions of P and Fe, including P extraction through the addition of a sulfide solution as described in Chapter 1. Results are combined with recent studies of Bay sediment transport and deposition to estimate the water quality impact of a large storm event in terms of scoured P.

## Materials and Methods

### Study Site

The Chesapeake Bay is a 300 km long coastal plain estuary with an average depth of ~7 m, and depths exceeding 25 m in the central channel in the mid (mesohaline) portion of the Bay. An average of 2300 m<sup>3</sup> s<sup>-1</sup> of freshwater flows into the Bay from its 167,000 km<sup>2</sup> watershed, with the Susquehanna River at the head of the Bay supplying over half of the flow (Schubel and Pritchard 1986). Water discharge from the Susquehanna River to the Chesapeake is controlled by the Conowingo Dam, 14 km upstream of the mouth of the river, which is the last of three dams forming the Lower Susquehanna Reservoir System (Figure 33). Above Conowingo Reservoir is Lake Aldred (formed by Holtwood Dam) and Lake Clarke (formed by Safe Harbor Dam). The reservoirs total over 50 km in length and up to about 2 km in width.

### Reservoir Sampling

Three-meter-long cores were collected in August 2015 at five sites along the length of the Conowingo Reservoir (Figure 6). Cores were collected in 61 cm long thin walled Shelby tubes using a piston tub sampler (ASTM 1587) deployed from a barge. From the 5 Shelby tubes, eight 10-cm long sections were taken from each core, homogenized, and dried for solid phase analyses.

In addition, short cores were collected on five occasions during 2015 and 2016 at a total of 13 stations throughout the Conowingo Reservoir. Three short cores were also collected in April 2016 from each of the two upper reservoirs (Lake Clarke and Lake Aldred). Intact surface sediment was collected using a box corer or pole corer, then subcored with 7-cm i.d. acrylic cores, with ~15 cm of sediment and ~15 cm of overlying water. The cores were incubated for sediment-water exchange measurements, after which the top 1 cm of sediment was dried for solid phase analysis.

### Sediment-Water Exchange Methods

Short cores were transported to the Horn Point Laboratory, submerged in water from the reservoir, and bubbled overnight in the dark at field temperatures. Sediment-water SRP exchange was measured using intact 7 cm i.d. cores with a magnetic stirring mechanism (Owens and Cornwell 2016); samples were collected over 4 time points. Colorimetric analysis of SRP followed Parsons et al. (1984) and fluxes were estimated from regression of SRP concentrations over time.

### Solid Phase Analyses

Total and inorganic phosphorus were measured using a 1 N HCl extraction of ashed and unashed sediment, respectively (Aspila et al., 1976). Phosphorus concentrations in the extract were determined by the molybdate blue technique using a UV/VIS spectrophotometer for colorimetric analysis (Parsons et al., 1984). Organic P was estimated as the difference between total and inorganic P. Iron was determined by analysis of the unashed 1 N HCl extract using flame atomic absorption spectroscopy (Leventhal and Taylor 1990).

Phosphorus was also extracted from sediment using a sulfide solution (Vulgaropoulos, M.S. Thesis, 2017). Briefly, a 24 mM  $\text{H}_2\text{S}/\text{HS}^-$  solution was added to dry sediment samples in centrifuge tubes, which were then shaken for 24 hours. The resulting extract was dried and the residue was re-dissolved with 1 N HCl, then analyzed by colorimetry using the molybdate blue technique.

### Flux Data Synthesis

Patterns of benthic P flux along the salinity gradient of the Chesapeake Bay utilized a sediment-water exchange database maintained at the Chesapeake Biological Laboratory (Boynton and Bailey 2008). Data were collected at 82 stations along the mainstem Bay from 1980 to 1998 using core flux incubations (Cowan and Boynton 1996). For this study, we utilized summer (June-August) SRP fluxes from these stations, totaling 227 measurements. These data were augmented by sediment flux measurements made in summer 2014 and 2015 in the Susquehanna Flats area of the upper Bay (Gurbisz et al.,

accepted), and in the Conowingo Reservoir (this report). The locations of all of the sediment-water flux sites are shown in Figure 33.

In this study, we examined dissolved inorganic P flux rates in relation to latitude as well as various water quality parameters. To assess spatial variation, the stations were separated by latitude into four regions: the Conowingo Reservoir, the Upper Bay, the Mid Bay, and the Lower Bay. The boundaries between the three Bay regions were set at 39 N (near the Bay Bridge) and 38 N (at the mouth of the Potomac estuary).

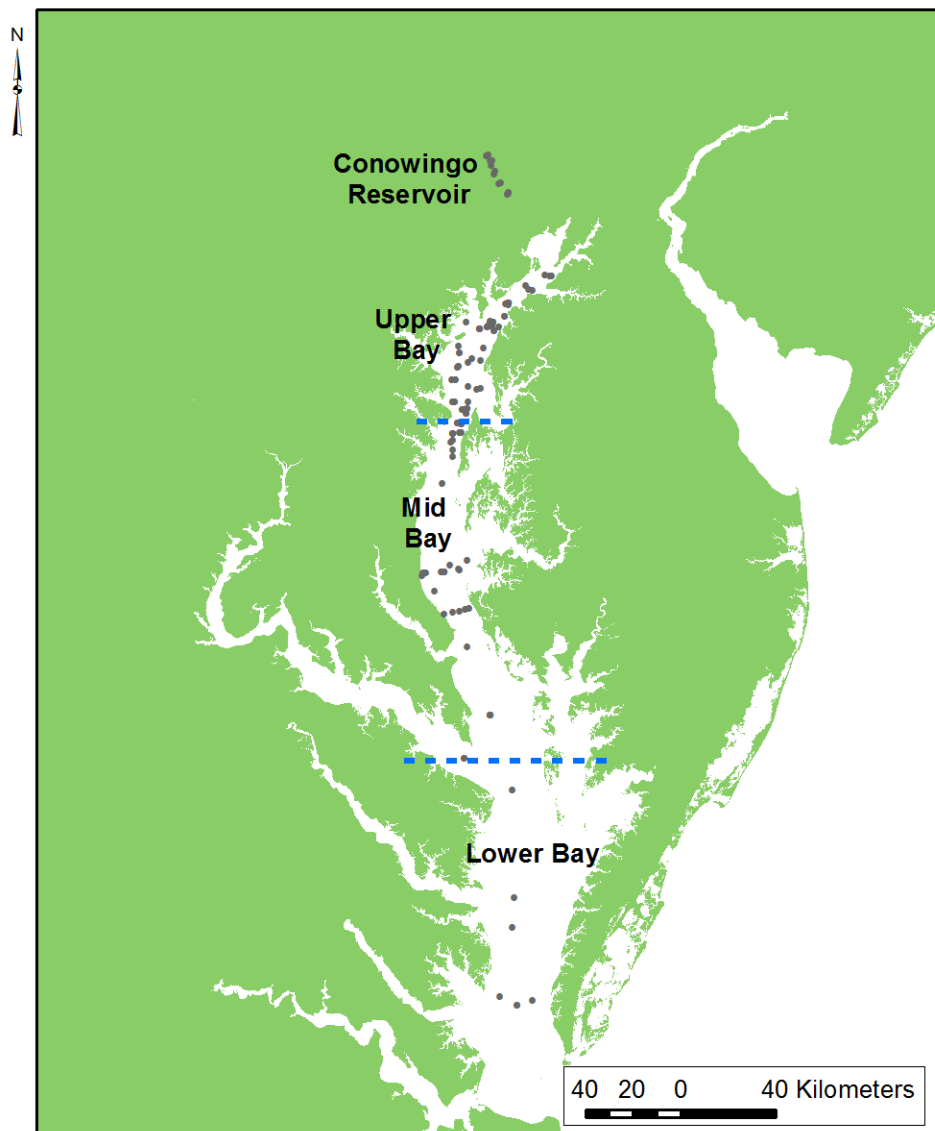
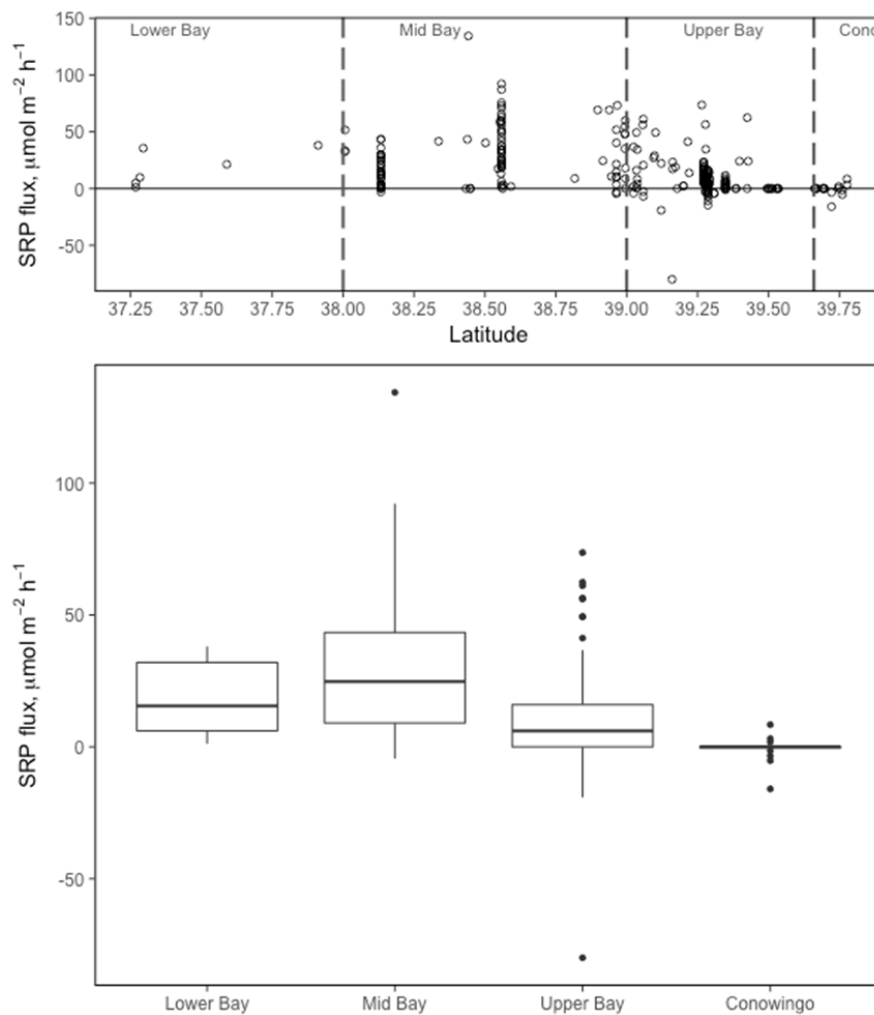


Figure 33. Site locations for sediment-water exchange measurements.

## Results

Observed summer SRP effluxes were highest in the Mid Bay region, and lower in the Upper Bay with occasional high outliers (Figure 34). Fluxes of SRP in the Conowingo Reservoir were very low or negative. The upper two reservoirs were not sampled for sediment-water exchange during the summer, but April measurements yielded no detectable SRP flux. The Mid Bay and Upper Bay SRP flux rates were significantly different ( $p \leq 0.01$ ). Significant ( $p \leq 0.01$ ) relationships were observed between SRP flux and bottom water salinity, station depth, and bottom water dissolved oxygen (Figure 35). Given the vertical stratification in the bay, some of these relationships are likely driven by the low oxygen concentrations of deeper, more saline water masses. Indeed, oxygen was the strongest predictor of SRP efflux.



**Figure 34. Summer SRP fluxes along the Chesapeake Bay salinity gradient and Conowingo Reservoir (A) and box plots of the same flux data for each region (B).**

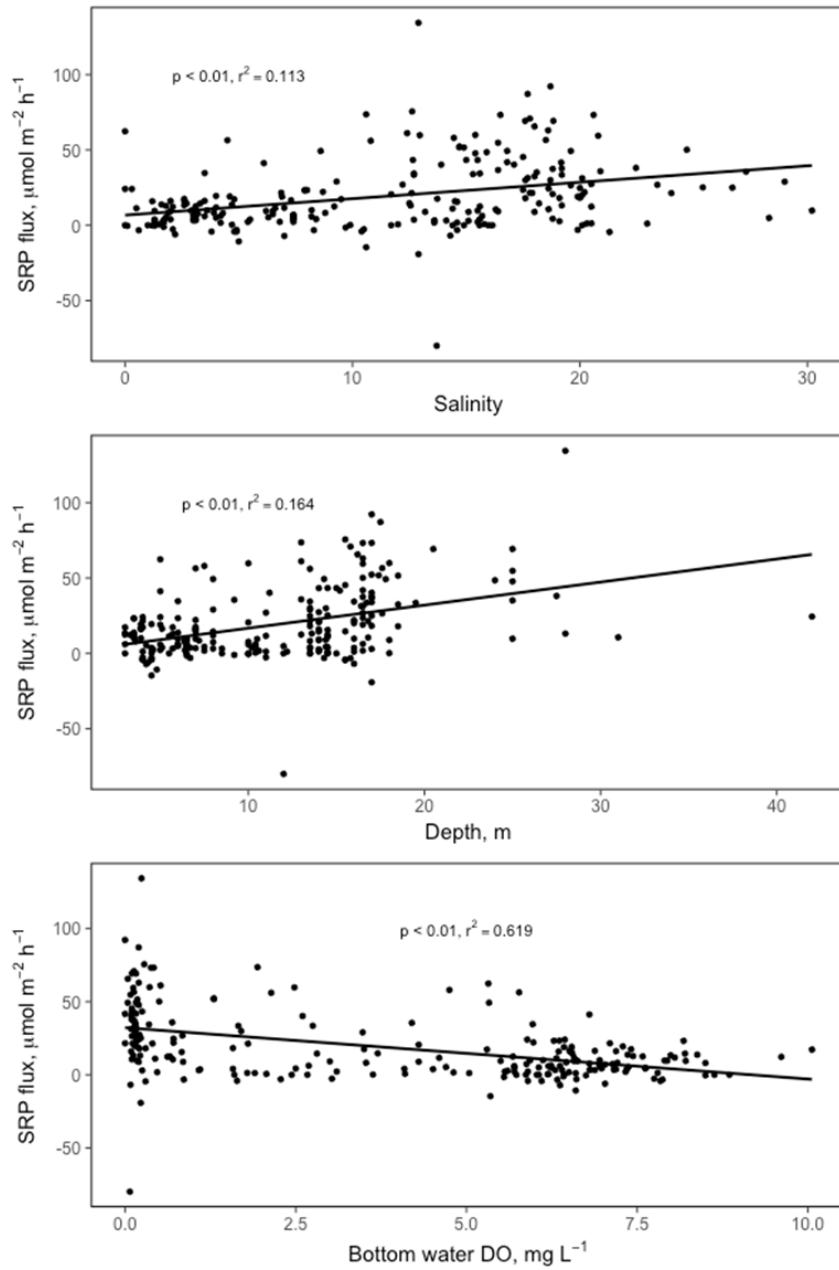


**Figure 35. Relationships between summer SRP flux in the Bay mainstem and different water quality parameters: salinity, station depth, and bottom water dissolved oxygen (DO).**

Inorganic P made up most of the particulate P in all of 5 vertical profiles in the Conowingo Reservoir, especially at the upper two stations (Figure 36). Inorganic P varied with depth and was generally higher at the stations closest to the dam (8, 9, and 13). Inorganic P and Fe were positively correlated ( $p \leq 0.05$ ) in all of the profiles except station 5 (Figure 37). The overall higher P concentrations and more significant correlations with iron closer to the dam were likely related to finer grain size; average grain size at stations 2 and 5 was higher than at stations 8, 9, and 13 (Palinkas and Russ, unpublished data).

Sulfide-extractable P did not vary with depth as much as inorganic P, and ranged from about 0.01 to 0.37 mg g<sup>-1</sup>, or 5 to 33% of total P (median 22%). As with inorganic P, sulfide-P concentrations were higher closer to the dam (stations 8, 9, and 13) compared to stations 2 and 5 (Figure 36). Sulfide-P was not correlated with Fe in the long core profiles (Figure 37).

In surface sediment collected over multiple seasons in the three reservoirs, inorganic P again made up most of total P (Figure 38). Inorganic P, organic P and Fe increased in concentration closer to each of the three dams. Sulfide-extractable P concentrations increased slightly as well (Figure 39). Both inorganic P and sulfide-P were correlated with Fe ( $p \leq 0.01$ ) (Figure 40).

The seasonal variability of inorganic P was low at the lower end of the Conowingo Reservoir, and higher at the upper stations (Fig. 11). Different stations showed different seasonal patterns, likely reflecting spatial heterogeneity of sediment erosion and deposition. Iron was seasonally variable throughout the reservoir, tending to be highest in late spring and summer (Figure 38). The variability of iron concentrations drove the IP:Fe molar ratio to be lowest during late spring and summer (May and July) and highest from fall through early spring (September, December, and April) (Figure 41).

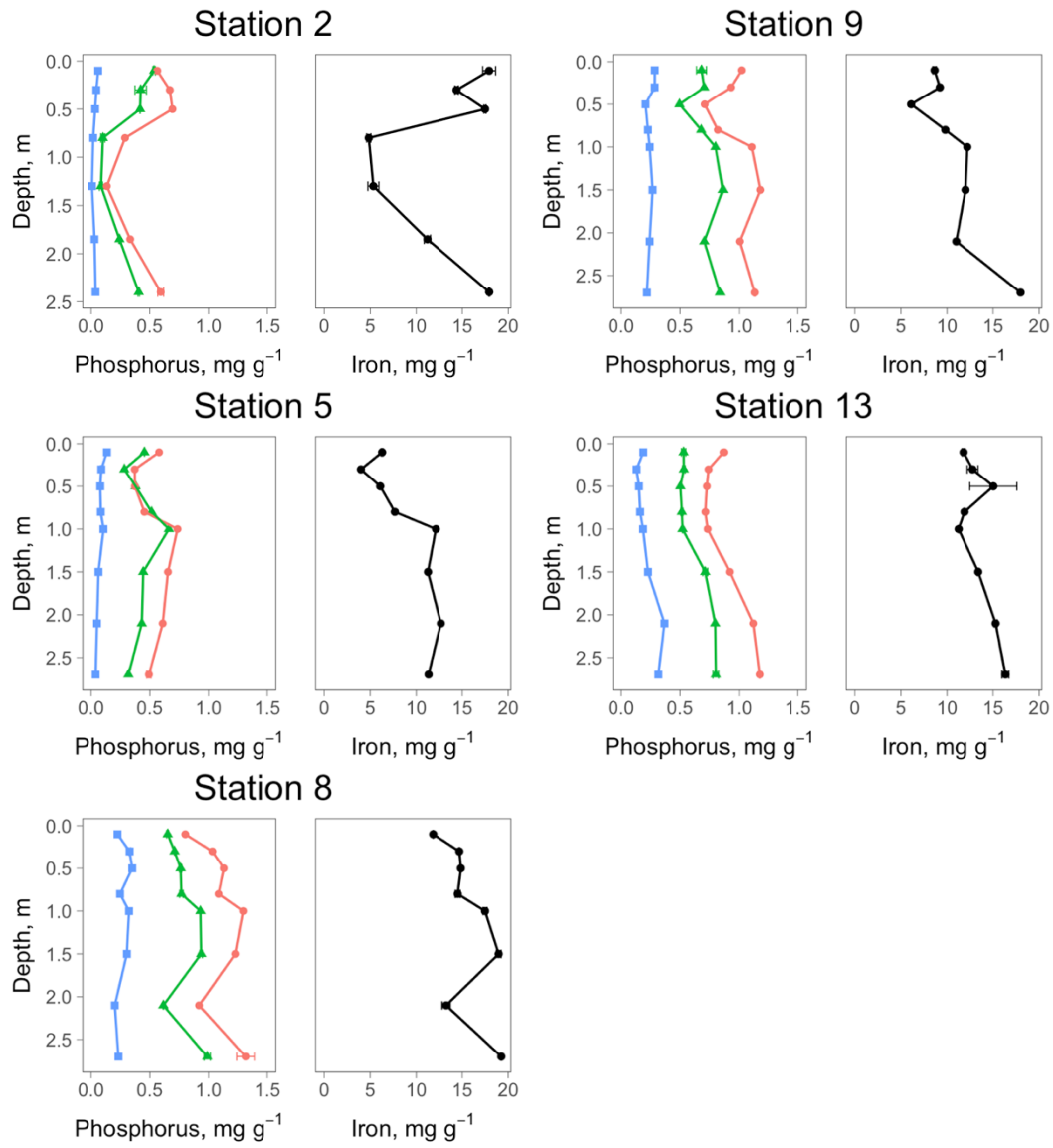


**Figure 36. Concentration depth profiles of different phosphorus forms and iron in Conowingo Reservoir sediments.**

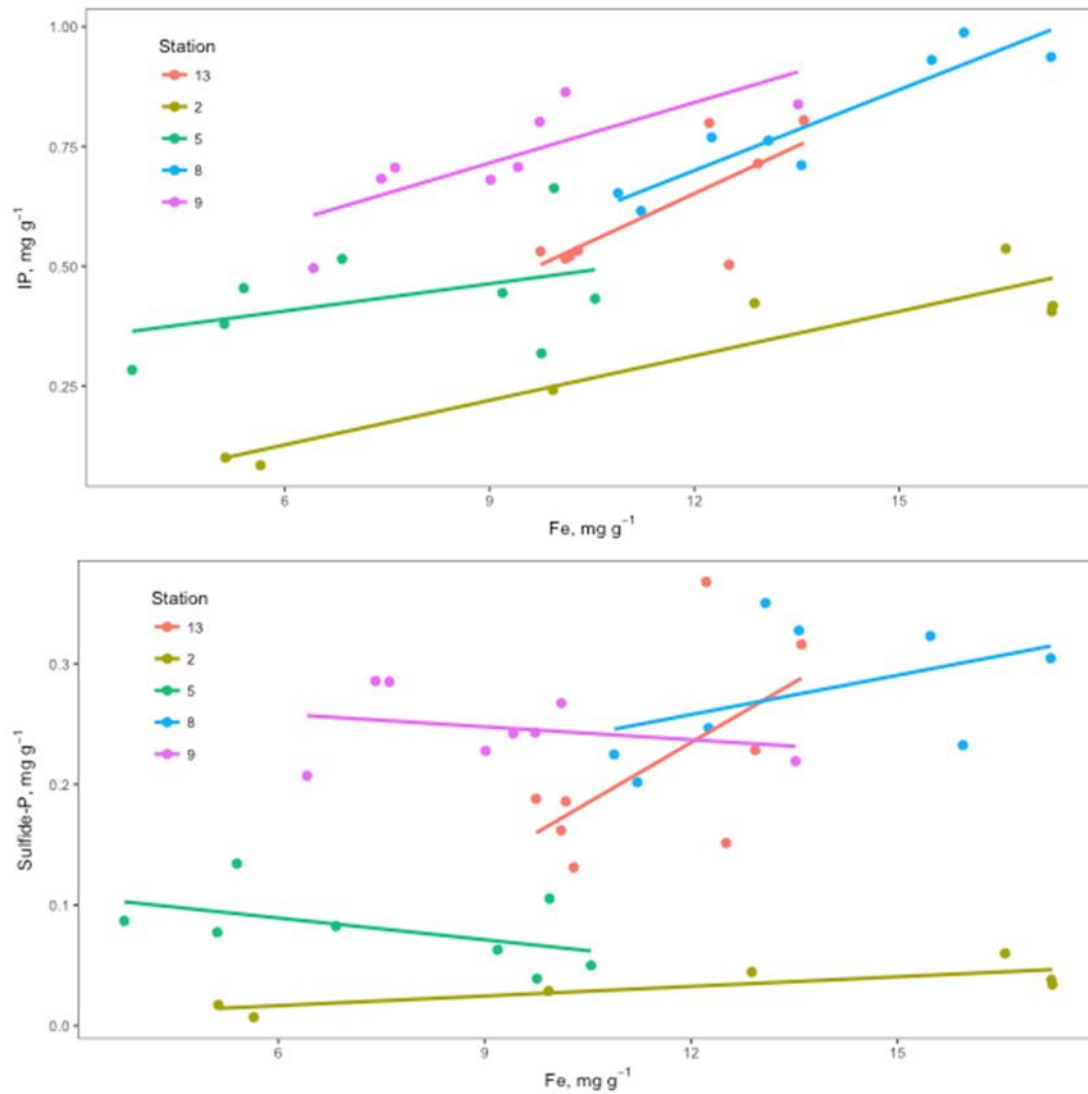


Figure 37. Relationship between concentrations of iron (Fe) and inorganic phosphorus (IP) (A) and sulfide-extractable phosphorus (sulfide-P) (B) in Conowingo Reservoir long cores.

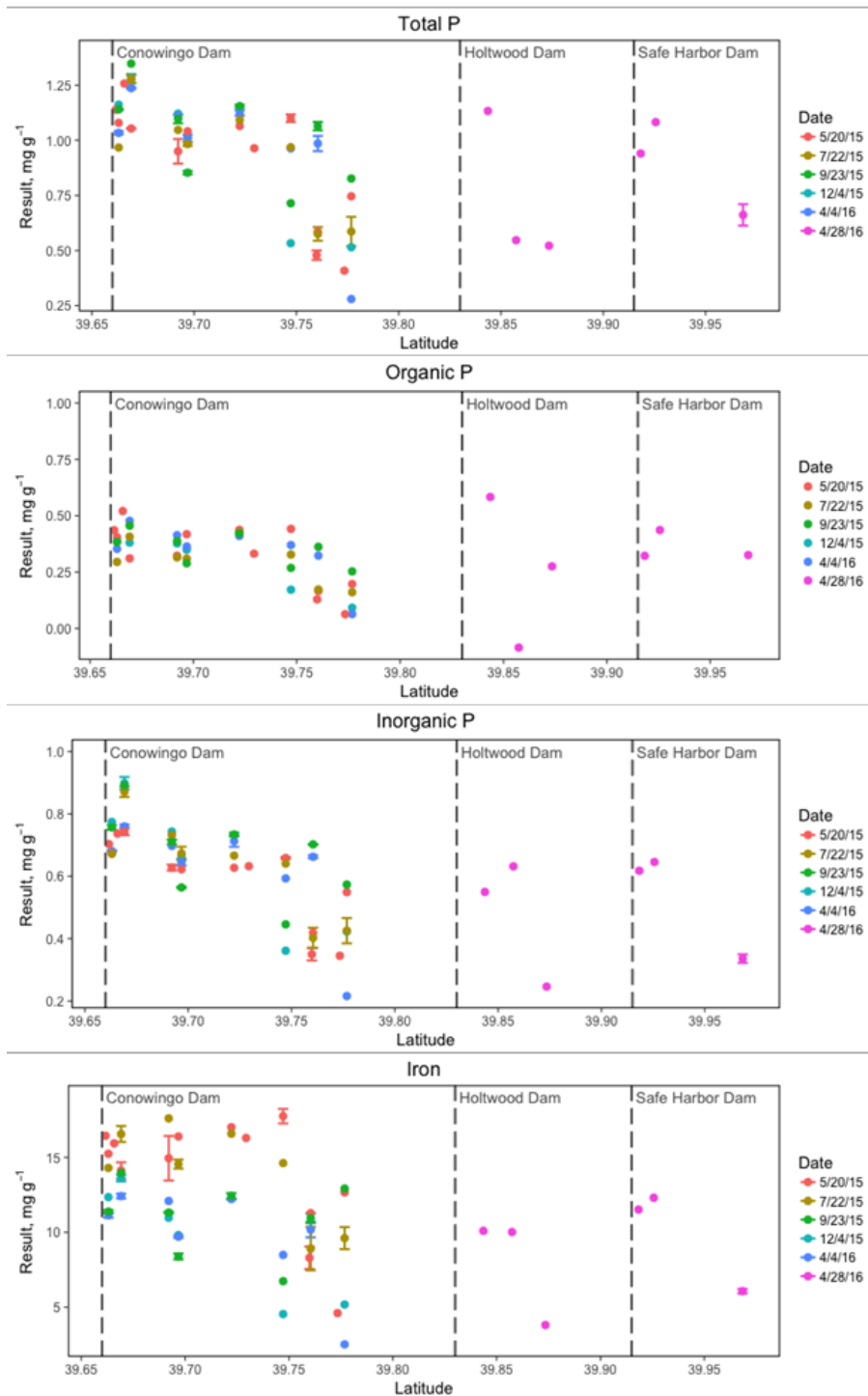
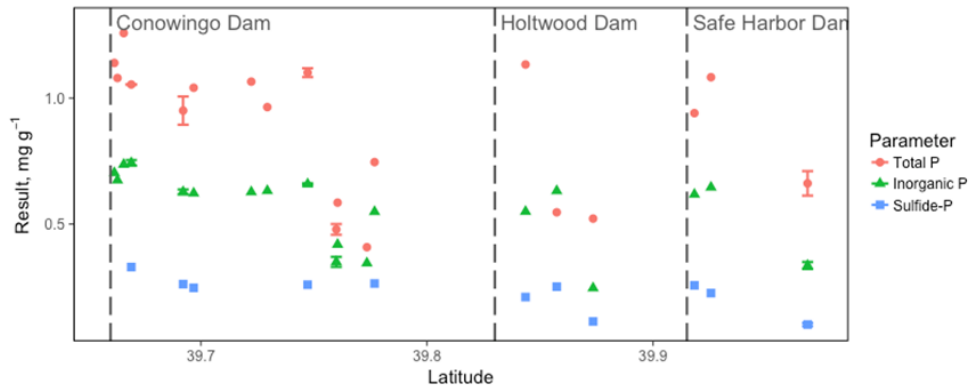
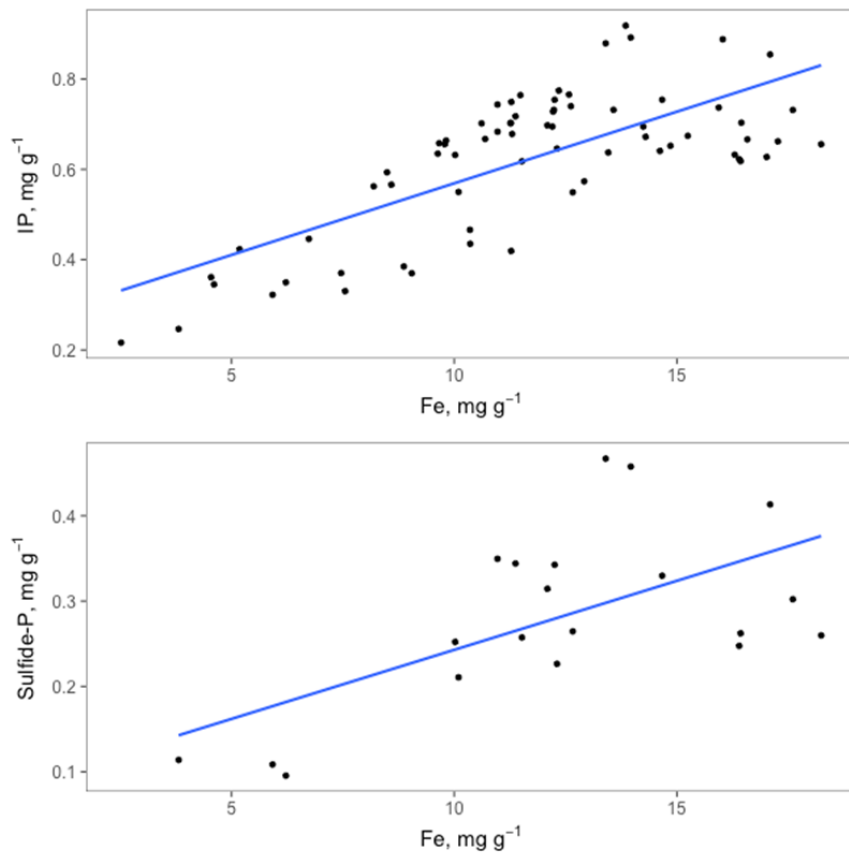


Figure 38. Surface sediment concentrations of different P forms and iron during different seasons along the length of the Lower Susquehanna Reservoir System.



**Figure 39. Spring surface sediment concentrations of total, inorganic, and sulfide-extractable P along the length of the Lower Susquehanna Reservoir System.**



**Figure 40. Relationship between concentrations of iron (Fe) and inorganic phosphorus (IP) (A) and sulfide-extractable phosphorus (sulfide-P) (B) in surface sediment from the Lower Susquehanna Reservoir System**

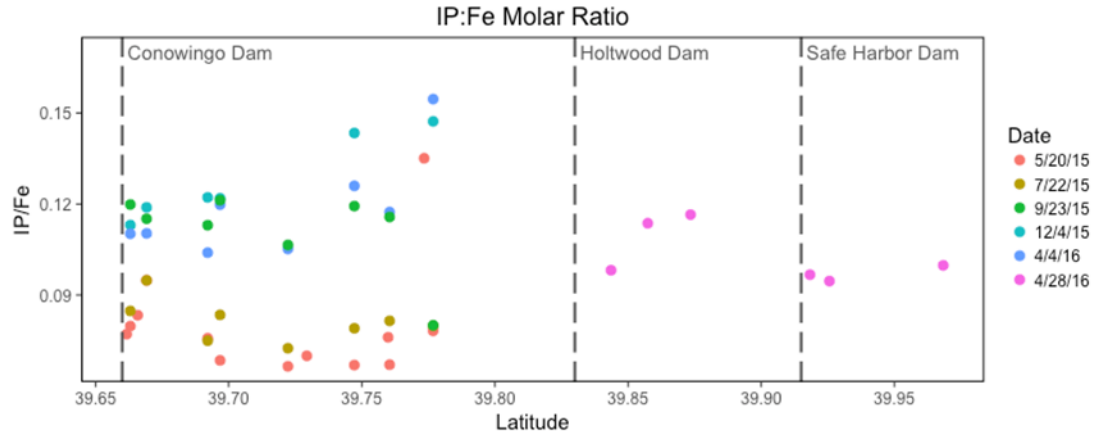


**Figure 41. Molar ratios of inorganic P/Fe during different seasons along the length of the Lower Susquehanna Reservoir System.**

## Discussion

Analysis of the comprehensive sediment-water exchange data indicated that P efflux from scoured reservoir sediment would most likely occur if the sediment is transported to the mesohaline Mid Bay. Previous studies have suggested that enhanced P efflux in deeper saline environments is due to the formation and burial of iron sulfides and release of iron-bound P (Hartzell et al., 2010, 2017; Jordan et al., 2008; Roden and Edmonds, 1997). In this study, the addition of a sulfide solution to reservoir sediment samples yielded a portion of the particulate P pool ranging from ~5-30% of total HCl-extractable P and ~8-45% of inorganic P. Within reservoirs, P concentrations were higher close to each of the three dams and lower farther up the reservoirs, likely due to grain size distributions. Inorganic P and sulfide-extractable P in surface sediment were significantly correlated with iron. Findings suggested that only a fraction of particulate P from a scour event would likely be bioavailable, depending on environmental conditions at the site of deposition.

Summer SRP fluxes along the salinity gradient from the Lower Susquehanna reservoirs through the Chesapeake Bay mainstem were variable but generally highest in the mid-Bay. Previous studies of sediment-water exchange in the Bay have also reported that SRP fluxes are highest in the mid-Bay relative to the upper and lower Bay, and are enhanced by high temperatures and hypoxia (Boynton et al. 1991). Salinity transition zones in estuaries are likely to be areas with high levels of P mobilization because the availability of sulfate and organic matter allows enhanced sulfate reduction and iron sulfide formation (Kemp and Boynton 1984, Capone and Kiene 1988). Sulfate reduction is not limited by sulfate concentrations at higher salinities, but sulfide re-oxidation by bioturbation in the limits iron sulfide burial efficiencies (Cornwell and Sampou 1995). Algal production and net deposition of organic matter is

highest in the mesohaline zone of the Chesapeake (Kemp and Boynton 1984, Cowan and Boynton 1996, O'Keefe 2007) while refractory terrestrial organic material, combined with low sulfate concentrations, limits sulfate reduction in the oligohaline zone (Marvin-DiPasquale et al. 2003). In general it is observed that Fe-bound P decreases with increasing salinity (Hartzell et al., 2010, 2017; Jordan et al., 2008). The observed high P fluxes in the mid-Bay, and the positive correlation between salinity and P efflux, are consistent with particulate P conversion to bioavailable SRP in the mid-Bay due to iron sulfide formation. It is clear that this process is enhanced by hypoxia and anoxia, since SRP flux decreased with increasing bottom water dissolved oxygen, and the highest fluxes were found in deeper water where seasonal stratification and oxygen depletion is more likely (Kemp et al. 2005).

Various extraction methods have been used to differentiate iron-associated P from other P forms, but it is difficult to determine what fraction of this iron is reducible and likely to release dissolved phosphate. In sequential extraction techniques such as SEDEX, a citrate-dithionite-bicarbonate solution is used to extract P bound to Fe oxyhydroxides (Ruttenberg, 1992). However, this strong reducing agent may include the more crystalline forms of FeOOH, so P bioavailability may be poorly predicted (Jordan et al. 2008, Kostka and Luther III 1994, Scicluna et al. 2015). Alternatively, other studies have used the more moderate reducing agent ascorbate (Kostka and Luther III 1994, Scicluna et al. 2015), but this reduces only amorphous FeOOH and may underestimate the amount of P that could be mobilized. Since P release from iron oxides in the Chesapeake Bay is predominantly caused by iron sulfide formation (Jordan et al., 2008; Roden & Edmonds, 1997), an extraction using a sulfide solution should more directly represent the fraction of iron-bound P that is potentially bioavailable in the Bay. We found that up to ~30% of total HCl-extractable P could be extracted using a 24 mmol L<sup>-1</sup> sulfide solution, which is a significantly higher sulfide concentration than would be found in the mid-Bay (Roden and Tuttle 1992). Li et al. (2016) also found that P could be released from sediment through the addition of a sulfide solution, with P concentrations in the overlying water increasing with increasing concentrations of added sulfide.

Total particulate P concentrations in the reservoir sediment ranged from about 0.5 to 1.3 mg g<sup>-1</sup>, and generally over two thirds of it was inorganic. The concentrations were similar to those found in tidal freshwater deposits in various Chesapeake Bay subestuaries (Hartzell et al., 2010, 2017; Jordan et al., 2008). Sulfide-extractable P made up ~20-30% of total P. The amount of inorganic P not extracted by the sulfide solution averaged about 0.4 mg g<sup>-1</sup>, which is similar to IP concentrations measured in sediment at 15 cm depth in the mid-Bay (Cornwell, unpublished data). This suggests that sulfide-extractable P is a realistic representation of the amount of P that is released from sediment under sulfidic conditions in the Bay.

The positive correlation between inorganic P and iron in Conowingo Reservoir sediments was likely a reflection of the iron-bound P fraction as well as grain size differences, since both iron and phosphorus are preferentially associated with smaller particles. Iron oxides are strongly associated with surfaces and increase with increasing relative surface area (Pacini and Gächter 1999, Poulton and Raiswell 2005). Concentrations of various fractions of particulate P have been shown to increase with decreasing grain size (Pacini & Gächter, 1999; Stone & English, 1993; Yao et al., 2016). Small particles provide more

surface area not only due to their size, but also due to the laminated structure of clay minerals, which provides many internal surfaces for interactions with iron oxides and phosphorus (Pacini & Gächter, 1999; Poulton, 2005). Sulfide-extractable P was also moderately well correlated with HCl-Fe in surface sediment from the three reservoirs. Interestingly, however, sulfide-P generally did not correlate with Fe in the deep cores from Conowingo Pond, and was more constant with depth than TP and IP. This likely points to the presence of less reactive forms of iron-associated P that cannot be released through iron sulfide formation.

The increase in inorganic P and sulfide-P with distance along each reservoir is also likely due to the prevalence of finer particles in the downstream areas of the reservoirs. In addition, the higher temporal variability of inorganic P at the upper end of the Conowingo Reservoir may be due to periodic erosion and deposition of sediment in these shallow environments.

Storm events can be responsible for a large fraction of the annual sediment load from the Susquehanna River, partly due to reservoir scour. An estimated 6.7 million tons of sediment were transported across the Conowingo Dam during Tropical Storm Lee in September 2011 (Palinkas et al., 2014), of which 3.5 million tons were scoured from the Lower Susquehanna reservoirs (Langland, 2015). The percent of the sediment load that is from scour increases with streamflow and also varies based on characteristics of different events (Cerco and Noel, 2016; Langland, 2015). For instance, a January 1996 flood event had a similar daily-mean streamflow as T.S. Lee, but over 80% of the sediment load was scoured material, likely because it was partly a snowmelt event with lower sediment loads from the watershed (Cerco & Noel, 2016). Assuming a total particulate P concentration of  $1 \text{ mg g}^{-1}$  based on core data, and a scoured sediment load of 3.5 million tons, an event similar to T.S. Lee would deposit 3,500 tons of particulate P in the Bay. With sulfide-extractable P comprising up to about 30% of total P, this would mean up to 1,050 tons of scoured P could be converted to bioavailable SRP through Fe sulfide formation. As previous studies and historical flux data have shown, P mobilization is more likely to occur in the mid Bay than the upper Bay due to enhanced sulfate reduction. After T.S. Lee, flood deposits of at least 1 cm thickness reached as far south as  $38.7^\circ \text{ N}$ , near station R-64, where the highest benthic SRP fluxes are generally found. However, most of the sediment is deposited in the upper Bay, where it is more likely to be buried in the solid phase.

Findings from this study suggested that although event-driven reservoir scour is increasingly likely to cause greater P loading to Chesapeake Bay, not all of this scoured P is likely to be bioavailable. Future work may further constrain the water quality impact of particulate P transported from the reservoir system during a storm. The analysis of P pools in reservoir sediment could be combined with studies of sediment deposition from T.S. Lee for a more thorough spatial analysis of P loading and bioavailability. In addition, these extraction methods could be applied to suspended sediment or size-fractionated samples to control for grain size, since finer particles are more likely to be scoured and transported to the Bay.

The P extracted from reservoir sediments using a sulfide solution is likely a conservative estimate of potentially mobile Fe-bound P, since most scoured sediment would be deposited in the Upper Bay

where Fe sulfide formation is limited. Flux data analysis and sediment characterizations indicate that the majority of scoured particulate P transported to the Chesapeake Bay during a storm event is unlikely to be bioavailable.

## Experimental Addition of Conowingo Sediment to Bay Sediments

The addition of Conowingo sediment to the surface of Chesapeake Bay sediment cores can be used as a short-term analogue to the addition of scour sediment during a high flow event. Salinity, redox conditions (i.e. aerobic versus anaerobic overlying water), the lability of organic matter and the amount and form of inorganic P in the sediment are likely controls on sediment P release (Caraco et al. 1989, Lehtoranta et al. 2009). Experiments with unamended cores in the Chesapeake mid-bay region showed a high rate of SRP release with anoxia, followed by a relaxation in flux rates as the inorganic P was depleted (Jasinski 1996). Experiment with addition of upper bay dredged sediments (Cornwell et al. 2000) showed the release of added sediments from the upper bay, sediments that were likely derived from the Susquehanna River watershed.

## 2015 Experiment

### Methods

Sediment cores were collected from 3 sites (3, 2.5, S2) along a salinity gradient in the mainstem Chesapeake Bay on August 11, 2015 (Figure 42). Site S3 is also known as Still Pond and has been the site of many sediment-water flux measurements (Boynton and Bailey 2008). Six replicate cores were collected from each site and transported to the lab for initial flux measurements and porewater extraction. Bottom water at site S2 had low  $O_2$  ( $\sim 3 \text{ mg L}^{-1}$ ) and was not anoxic at the time of coring. The initial measurements were conducted under aerobic on 2 replicate cores from each site for fluxes and 1 porewater core on August 12, 2015. Surface sediment (0-2 cm) from Conowingo Pond collected July 21 was homogenized, slurried and added to the Bay on August 14, 2015. The amounts of added sediment were chosen to mimic sediment deposition from tropical storm Lee. Approximate sediment amendments for replicate cores A-E are listed in Table 9. Cores were allowed to equilibrate for 23 days under aerobic conditions for sites 3 and 2.5 and anaerobic conditions for site S2. Sediment water fluxes were measured at a day 10 and again at day 23. A single core from each site was initially sectioned for pore water and following each flux incubation. All incubations were carried out at 26°C.

Photographs of cores immediately after the sediment amendment and after long-term incubations are shown in Figures 43 and 44. Stations Lee 3/Still Pond and Lee 2.5 had a deeper iron oxide hue after time. Station S2 developed a jet-black color in the top layers, with layer at the junction of the original sediment and the added sediment that had the appearance of iron oxide.

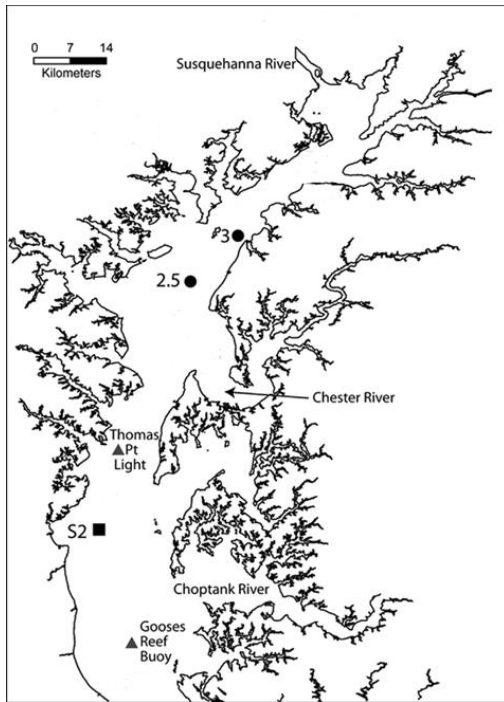
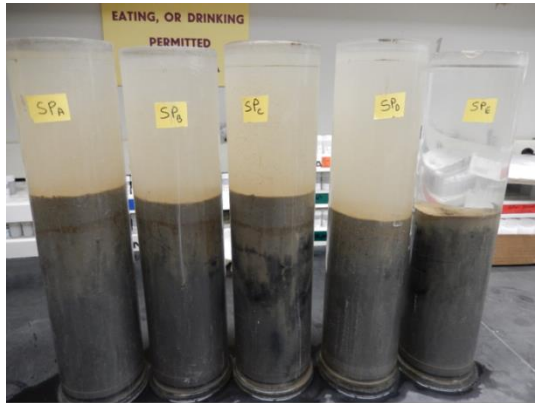


Figure 42. Site locations for the experimental cores collected August 11, 2015.

Table 9. Sediment amendments to Chesapeake Bay cores in cm. Bottom water salinity for each site is shown.

Site	Core A cm	Core B cm	Core C cm	Core D cm	Core E cm	Salinity
Lee 5 “Still Pond”	3	3	3	1	0	4.2
Lee 2.5	1	1	1	0	0	6.4
S2	0.5	0.5	0.5	0	0	12.9



**Figure 43. Cores on August 14 2015 after sediment addition. The upper cores are from Still Pond, the middle cores from Lee 2.5, and the bottom cores from S2.**

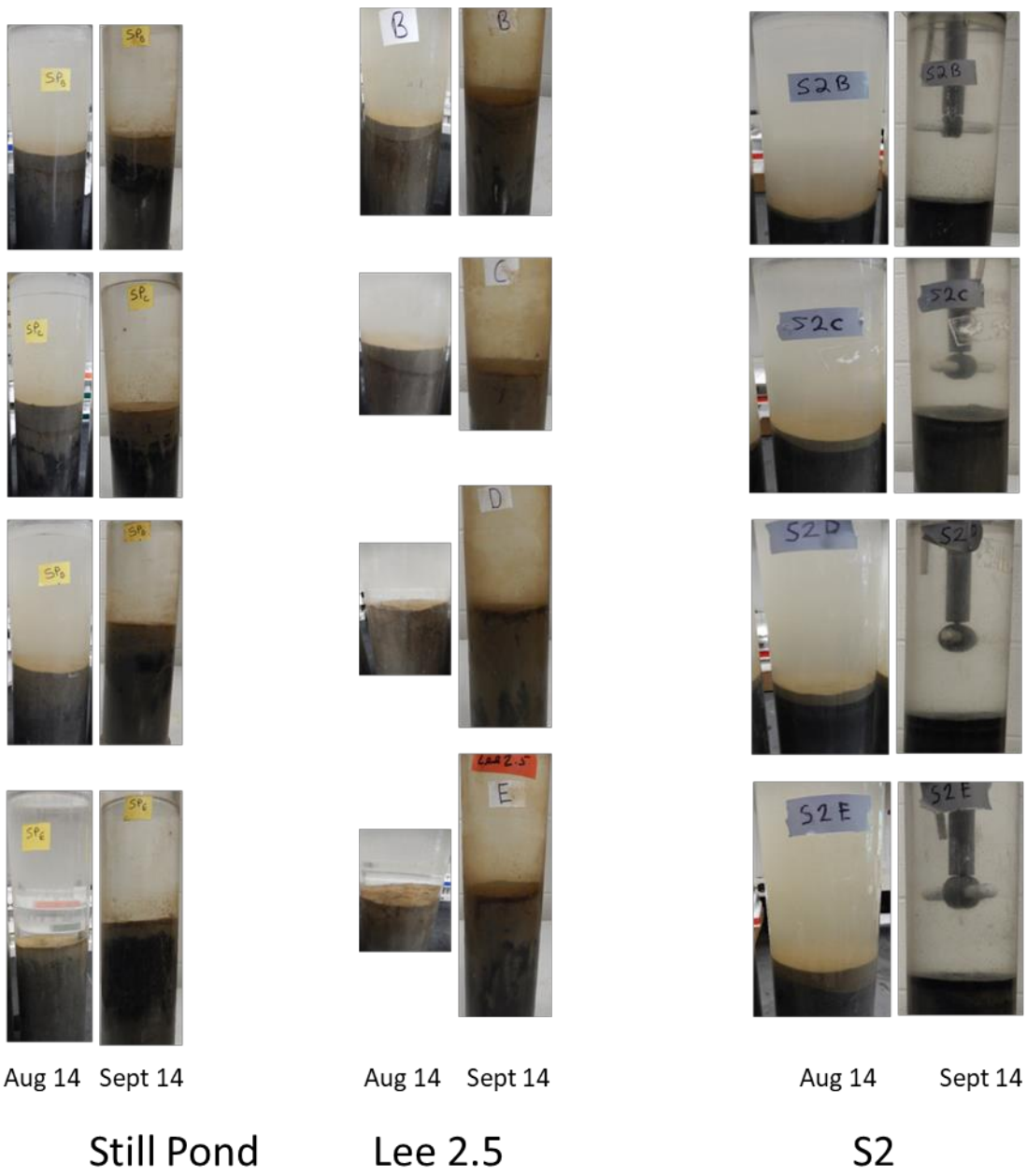
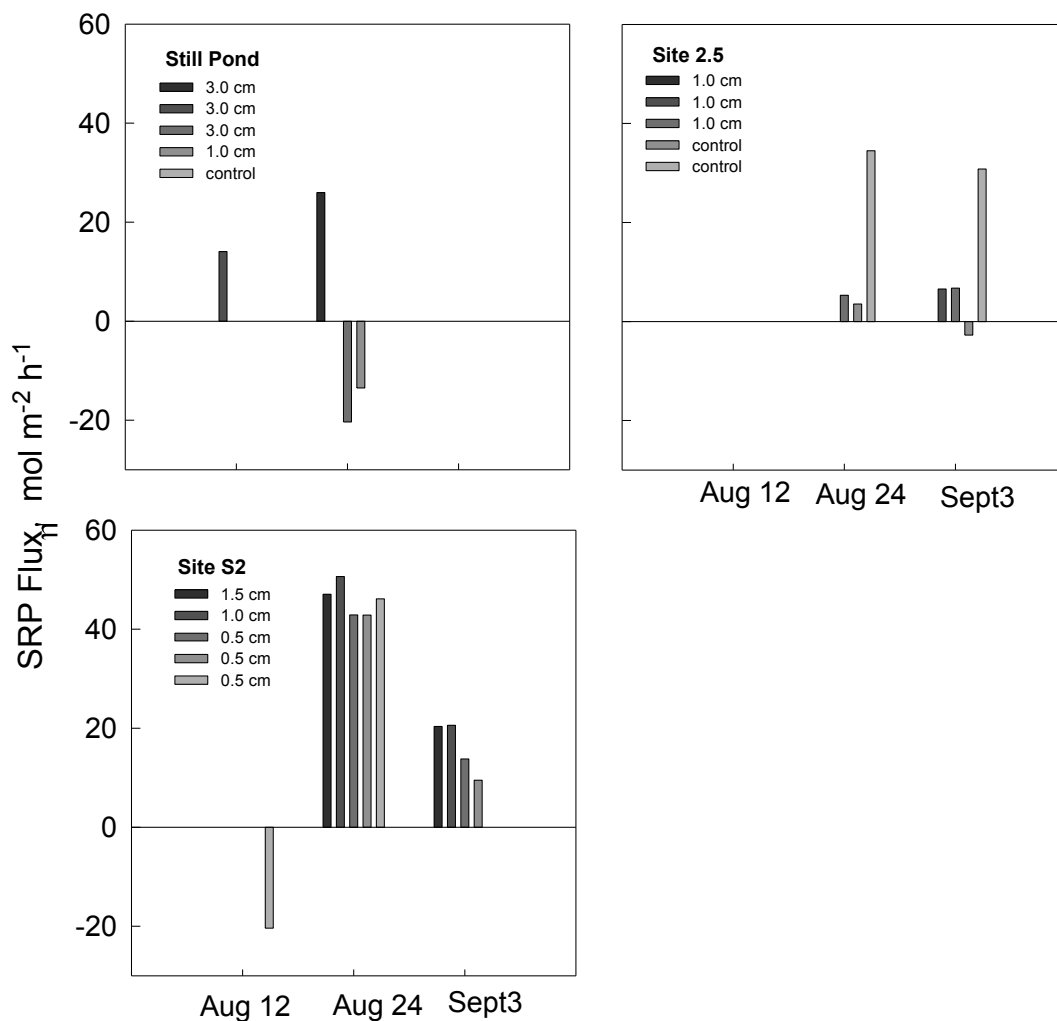


Figure 44. Core comparison between the initiation of the experiment on August 14 and the end on September 14.

## Results and Discussion

The initial rates of SRP release from the Chesapeake Bay cores were undetectable at sites 2.5 and S2 with the exception of one S2 core which had uptake of  $-20 \mu\text{mol m}^{-2} \text{h}^{-1}$  (Figure 45). One core from site 3 had a measureable SRP flux directed out of the sediment of  $14 \mu\text{mol m}^{-2} \text{h}^{-1}$  prior to the Conowingo sediment amendment.



**Figure 45. Time course of SRP flux from Chesapeake Bay sediment amended and control cores.**

At day 10 of the experiment one amended core from site 2.5 had SRP release of  $5.3 \mu\text{mol m}^{-2} \text{h}^{-1}$  with the control cores showing similar or higher SRP fluxes. Core A from site 3 had a SRP release of  $26 \mu\text{mol m}^{-2} \text{h}^{-1}$  with the remaining amended cores having either non detectable or negative SRP flux. High SRP release was measured from all amended cores from site S2 which averaged  $45.9 \pm 3.2 \mu\text{mol m}^{-2} \text{h}^{-1}$  after

10 days under anaerobic conditions. No SRP flux was measured from site 3 and only low fluxes ( $<7 \mu\text{mol m}^{-2} \text{h}^{-1}$ ) from site 2.5 after 23 days of equilibration. SRP flux from site S2 decreased to an average flux of  $16.1 \pm 5.4 \mu\text{mol m}^{-2} \text{h}^{-1}$  by day 23. The molar ratio of dissolved inorganic carbon to SRP flux on August 24 ranged between 52 and 24 with the lowest values occurring in cores with thicker deposits of Conowingo sediment (Figure 46). These ratios would suggest  $\sim 2$  to 4 times greater SRP being released than would be predicted from remineralization. The molar ratio in all treatments shifted closer to redfield by September 3 as the SRP release from the sediment decreased. The shifting of the DIC/SRP ratio at the end of the experiment provides some evidence that inorganic P was being extracted from the surface layer. Porewater profiles of SRP at all 3 sites increased at depth over the 23 day experiment (Figure 47). Site S2 was the only site where SRP increased in the 0-0.5 cm surface sediment layer. The presence of worm tubes at sites 3 and 2.5 suggest that sediment irrigation may have played a role in oxidizing surface sediments and preventing SRP release.

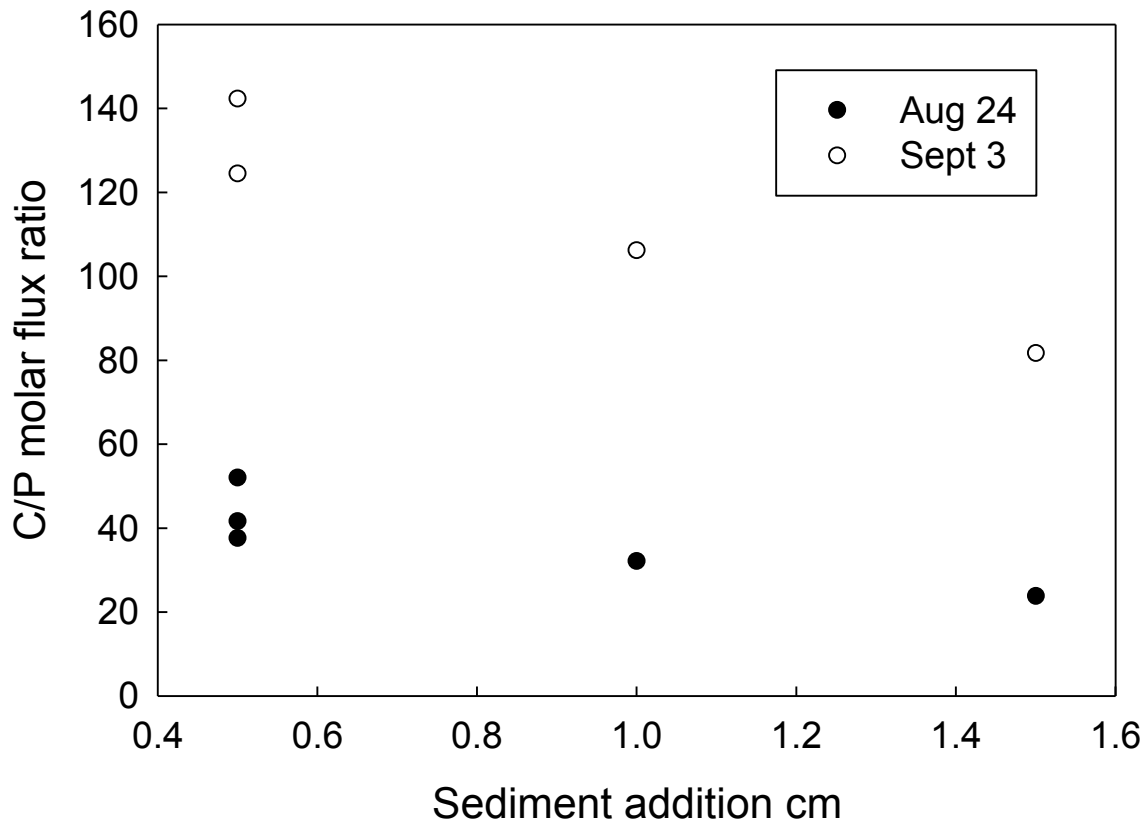


Figure 46. Molar dissolved inorganic carbon to SRP flux ratio versus depth of added Conowingo sediment for site S2.

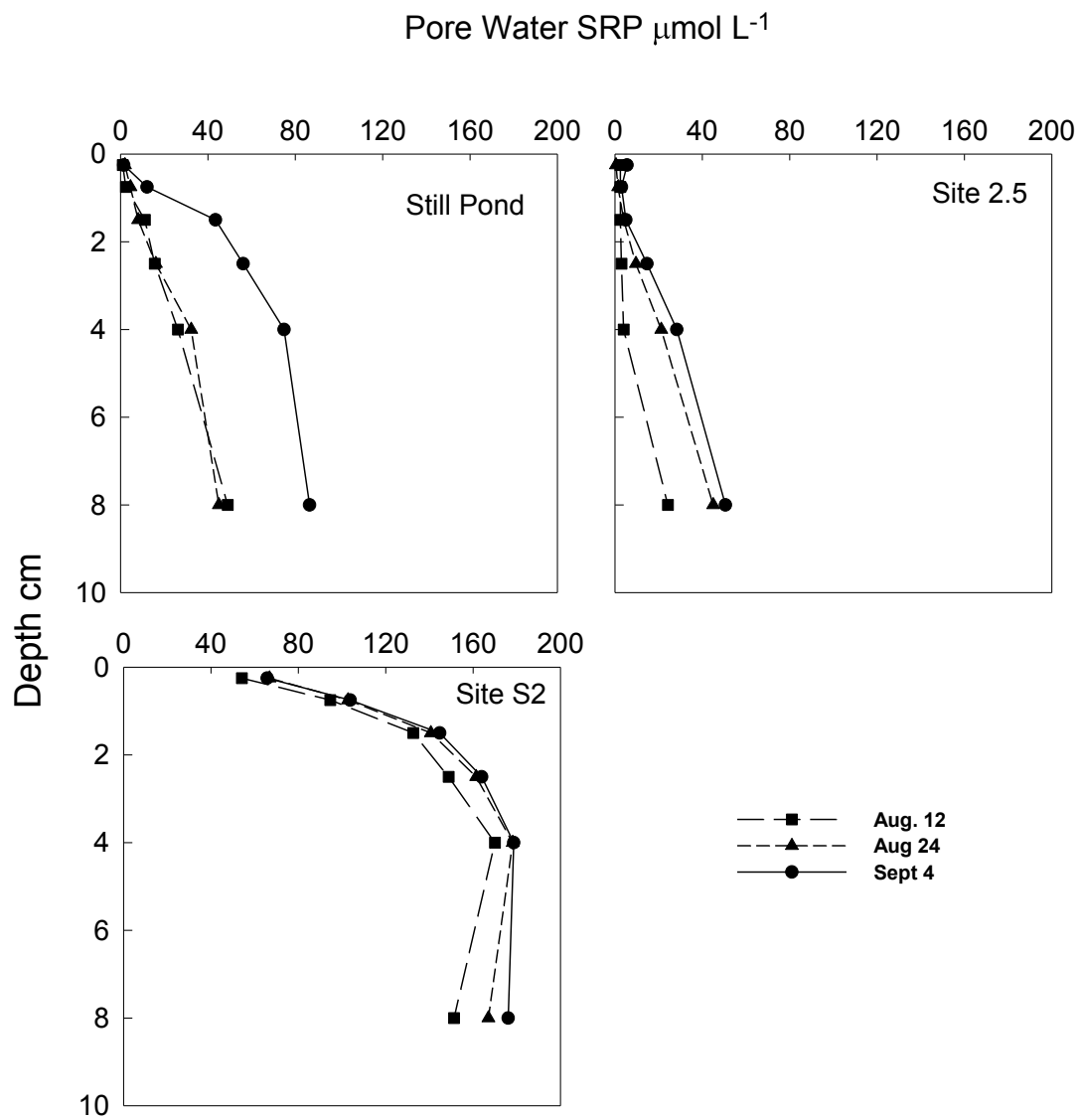


Figure 47. Time course of SRP porewater profiles.

## Carbon and Nitrogen Production Rates - Anaerobic Diagenesis

The review of sediment biogeochemical rates processes by Reeburgh (1983) evaluated jar experiments, sediment flux experiments, modeling of pore water and the use of tracers to estimate biogeochemical rate processes. For the purposes of the Conowingo biogeochemical assessment, the key rate processes in this program are the rates of areal sediment-water exchange documented earlier in this document, and “diagenesis” experiments, otherwise known as jar experiments or slurry experiments. Conceptually the reactivity of a parcel of sediment over time, such as CO<sub>2</sub> or NH<sub>4</sub><sup>+</sup> generation, allows a better comparison of the intrinsic reactivity of organic matter. These rates may be expressed on a volumetric or dry mass basis.

Early models of organic matter diagenesis (Berner 1981) generally had a relatively simple formulation where the rate of organic matter breakdown was a function of the metabolizable organic matter and a first order rates constant (k):

$$dG/dt = -kG$$

This formulation assumes one class of organic matter and one rate coefficient. An improvement in this model was made that included 3 classes of organic matter:

$$G_t = G_1 + G_2 + G_3$$

Where G<sub>1</sub> is very labile organic matter, G<sub>2</sub> is less labile, and G<sub>3</sub> is relatively inert (Berner 1980). Thus total organic matter diagenesis may be represented:

$$dG_t/dt = -(k_1G_1 + k_2G_2 + k_3G_3)$$

Alternative formulations have also been developed in which K is not a constant (Middelburg 1989). In a perfect incubation, over many years, different components of fresh organic matter with different reaction rates would be identified by increases in the concentrations of the products of diagenesis. In the Chesapeake Bay and elsewhere, such incubations have long informed models of organic matter reactivity (Burdige 1991, Cornwell and Owens 1999, DiToro 2001). As with any encapsulation of sediments, intact or slurried, incubation artifacts are important considerations (Burdige 1989).

In this program, incubations were carried out on sediments from all reservoirs, the Chesapeake Bay, and suspended sediment. Rates are expressed on a dry mass basis. Here we present representative results of the experimental program, more detailed data interpretation has been carried out by the modelers using this data.

**The data generated in this program has been used by Exelon contractors to inform bay modeling efforts and it will not be heavily interpreted here. Limited examples of some of the rate measurements will be presented.**

## Methods

For short core sediments, samples were collected in the field from the top 2 cm of sediment, and in one instance, over several depths. Samples were kept at ambient temperature in a 50 mL centrifuge without a headspace. For the long cores (10'), sections were collected in 50 mL cutoff syringes that were inserted vertically and then capped. In the laboratory, sediments were placed in a glove bag filled with N<sub>2</sub> to minimize oxidation, emptied into a 140 mL plastic bottle, and homogenized. Using a cutoff syringe, 5 mL of sediment was measured into 6-8 27 mL serum vials. A total of 15 mL of N<sub>2</sub>-bubbled water was added to each vial and the vial was bubbled for 15 seconds, capped with a rubber septum, and crimped with an aluminum seal. All diagenesis samples in this program were incubated at 20°C to allow a comparison of sites and sample times. Vials were sacrificed over time to develop a concentration time course for NH<sub>4</sub><sup>+</sup> and DIC. For each sediment section, a 5 mL sample was placed on a pre-weighed aluminum pan and the percent dry mass was determined by drying at 65°C.

For most incubations, the added water consisted of a solution similar to the composition of Conowingo Reservoir water, using average water quality data from USGS site 1578310. We added extra sulfate to make DIC the final end product for diagenesis via suppression of methanogenesis (Capone and Kiene 1988). The solution consisted of 40 μmol L<sup>-1</sup> KCl, 80 μmol L<sup>-1</sup> MgCl<sub>2</sub>, 200 μmol L<sup>-1</sup> NaHCO<sub>3</sub>, 220 μmol L<sup>-1</sup> MgSO<sub>4</sub> and 870 μmol L<sup>-1</sup> CaSO<sub>4</sub>. A second solution was used on some sections, without sulfate, but these data did not appear to generate different results and have not been used.

For the analysis of diagenetic rates in samples collected from the dam by AECOM, 20L carboys were allowed to settle for ~3 days and all but ~3 L was siphoned off. The suspension was placed in a 8 L USGS sampling churn (Bel-Art Scienceware 37805-0008) and mixed. Samples were drawn for TSS analysis via filtration of GF/F glass fiber filters to determine sediment mass on a volumetric basis, and multiple filters were collected for the diagenesis experiments. Two or more filters were added to 125 mL serum bottles and filled with 100 mL of N<sub>2</sub>-sparged water as outlined above. Samples were collected over time for chemical analysis.

For the small vial incubations, samples were put in 15 mL centrifuges, spun at 2500 rpm for 10 minutes, and filtered using a 25 mm diameter 0.4 μm syringe filter. Samples were collected for ammonium analysis with preservation by freezing and samples for DIC analysis were placed in vials for subsequent analysis via TCD gas chromatography (Stainton 1973). Ammonium was analyzed colorimetrically (Parsons et al. 1984).

Part way through the program, the sediment diagenesis program switched to a single large vial that was sampled repeatedly over time. The small vials appeared to have a higher degree of vial to vial variability, likely due to the difficulties of putting 5 mL of sediment in each vial with a consistent grain size. This was particularly an issue in upper Conowingo Reservoir sites and in the deep cores. We used a 250 mL vial with 40 mL of wet sediment and 120 mL of incubation water, maintaining the same ratio as the small vials.

## Results and Discussion

Examples of time course incubations are shown in Figures 48-50. These data are expressed on the basis of dry mass that was estimated by dried sediment or filters. The Conowingo sediments from September 2015 showed substantial increases in both ammonium and DIC concentrations over the course of 2/3 of a year. These incubations showed little indication of rate changes in the samples over time. In Lake Clarke, the time course showed a good increase in DIC concentration over time, with the ammonium time course showing excess variability. DIC slopes were similar to the September 2015 Conowingo time course. The water column particulate diagenesis example shown here, with sampling from a higher flow event in February 2016, showed linear increases in DIC and ammonium. The slope of the DIC regression is much higher than observed for sediment incubations and was > 20 times that observed for the sediment examples shown here from the Conowingo Reservoir and Lake Clarke. The suspended sediment ammonium slope similarly was > 15 times higher than sediment slopes. The deep core incubations showed generally slow rates of diagenesis, with a high degree of variability in the time courses.

One of the key conclusions of this study is that, as expected, water column organic matter reactivity is much higher than the reactivity of sediments from the surface of the reservoirs. Our incubations of the 0-2 cm horizon may include sediments that are relatively “new” to materials that are more than one year old. Moreover, in comparison to work in algal-dominated systems (Burdige 1991, DiToro 2001), the organic matter in the lower Susquehanna is a mixture of terrestrial and aquatic organic matter, with different reactivity rates and pools sizes. The material deposited in the Conowingo Reservoir may have a strong seasonal variability; the high respiration and ammonium effluxes observed in May 2015 may have been driven by a large input of labile organic materials.

This program provides insights into processes in the reservoirs, as well as information useful for future diagenesis studies. The use of small vials has worked well in many studies (Cornwell and Owens 1999), but the mixed grain sizes and the extremely long periods of incubation proved challenging. The many hundreds of vial incubated here resulted in a massive analytical program with consequent large and diverse data analyses. The use of larger incubation vessels added toward the end of the program is likely a better approach, and has been used successfully in short term incubations of highly reactive Everglades sediments (M. Owens and J.C. Cornwell, unpublished).

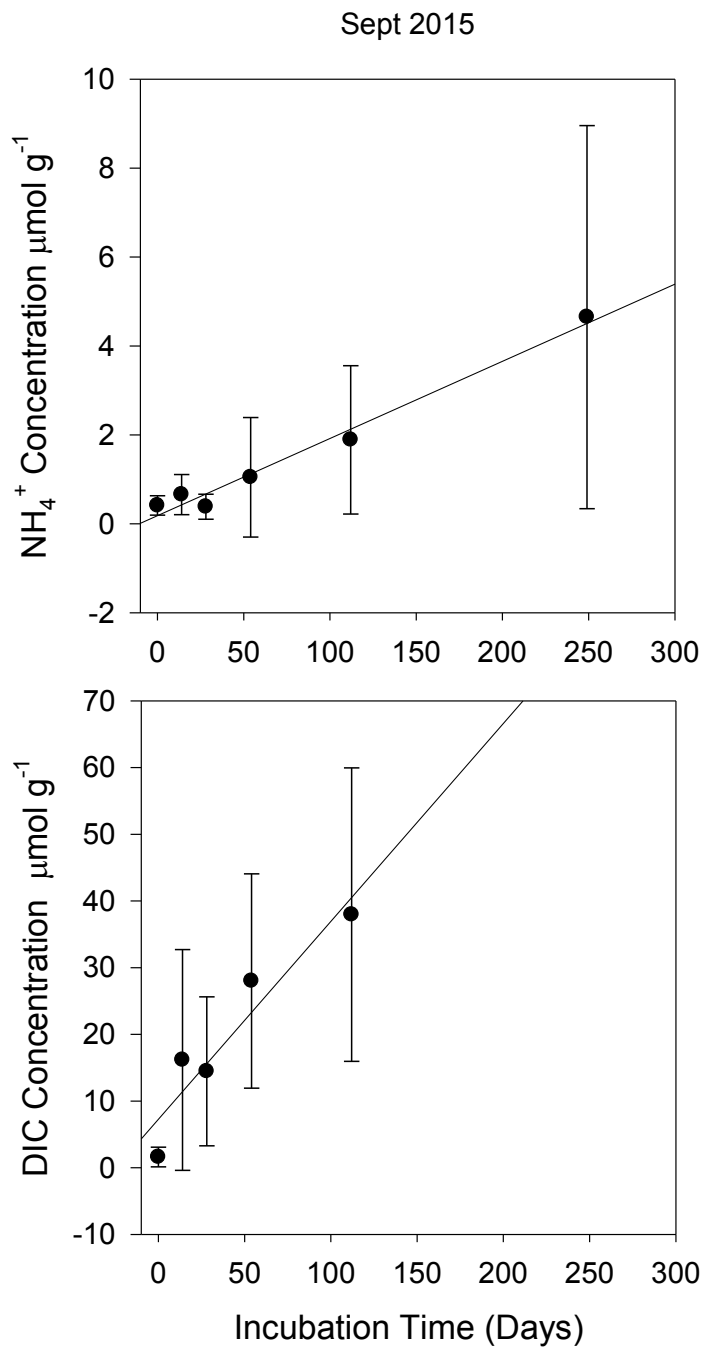


**Figure 48. Ammonium and DIC diagenesis time courses from surficial sediments (0-2 cm) collected from the Conowingo Reservoir in September 2015. Concentrations are expressed on the basis of dry mass in the incubation and are the average  $\pm$  S.D. of 4 samples. The four samples came from Sites 2, 5, 8, and 13**

Lake Clarke April 2016

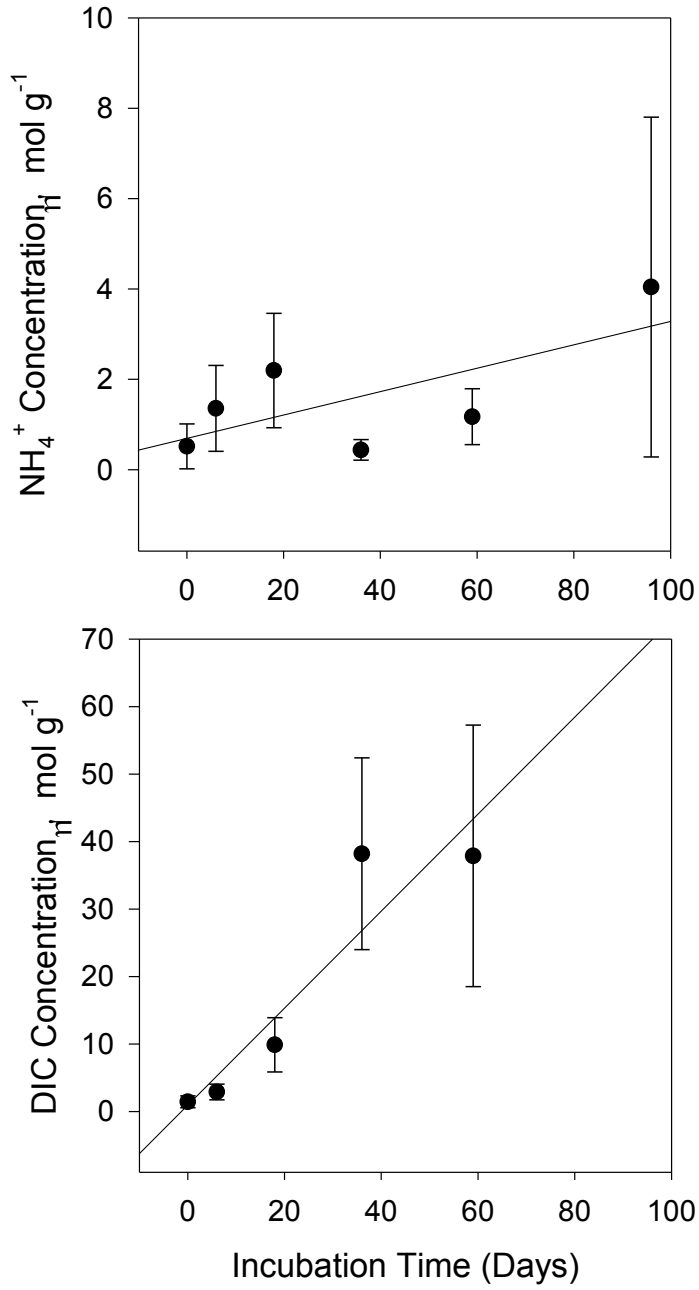


**Figure 49. Ammonium and DIC diagenesis time courses from surficial sediments (0-2 cm) collected from Lake Clarke in April 2016. Concentrations are expressed on the basis of dry mass in the incubation and are the average  $\pm$  S.D. of 3 samples, one from each sample location.**

Conowingo Outflow February 2016

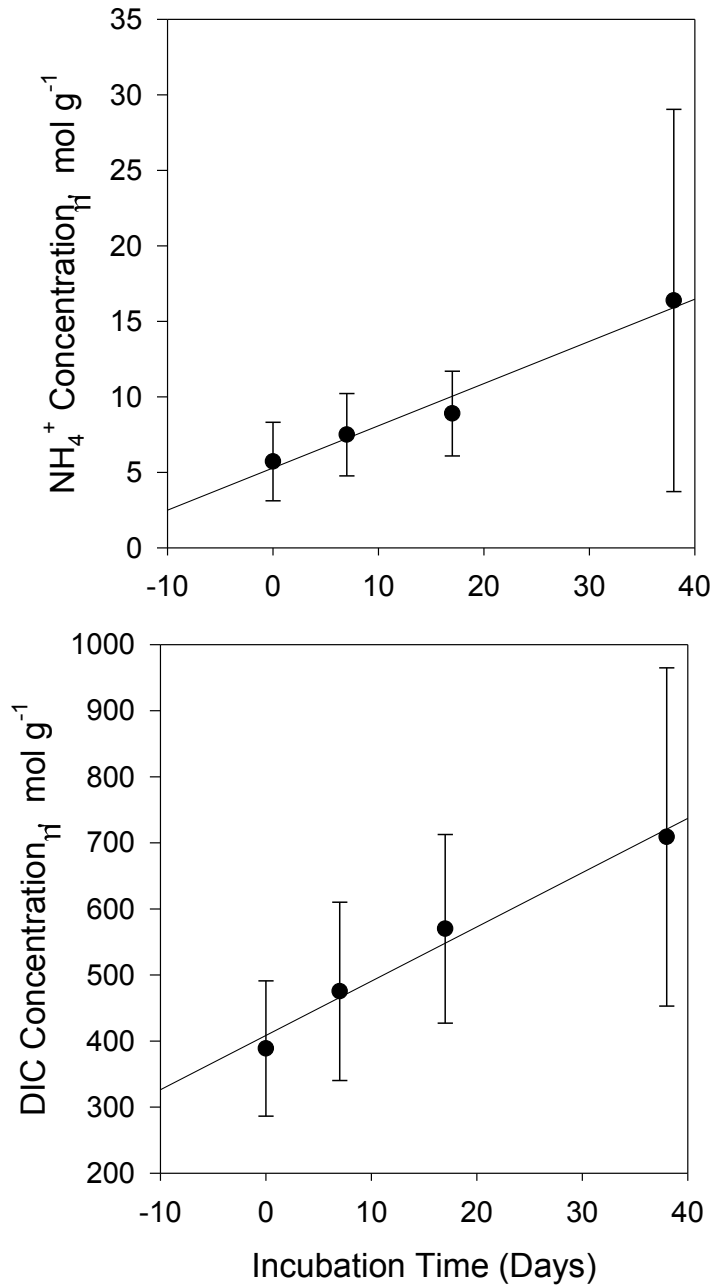


Figure 50. Time course of average  $\pm$  S.D. concentrations of ammonium and DIC concentrations from seven suspended samples collected in February 2016. Concentrations are expressed on the basis of dry mass in the incubation. The much higher concentrations per gram relative to sediment incubations reflects the much higher water volumes relative to the amount of sediment.

# Conowingo Biogeochemistry in Perspective

## Comparison to other studies

The data from this study were identical to studies carried out in three other Maryland reservoirs, as well as reservoirs/flowing waters in Indiana, Minnesota, Utah and Washington State (Table 10). These studies have been separated into aerobic and anoxic studies. The characteristics of the lower Susquehanna River reservoirs are somewhat different than these other studies in that the residence time in these other reservoirs are likely much longer. In the Maryland reservoirs (Tridelphia, Lake Linganore, Lake Anita Louise), reservoirs are thermally stratified in the summer and high algal biomass is observed, with cyanobacteria as major concerns in Lake Linganore and Lake Anita Louise. Similarly, the reservoirs in Utah, Minnesota and Washington State have issues with cyanobacteria (specifically *Microcystis* spp.). Consequently, sediments in these systems may have autochthonous organic matter inputs from algae and cyanobacteria.

The highest effluxes of soluble reactive phosphorus in reservoirs are generally found under anoxia, with rates that can approach  $100 \mu\text{mol m}^{-2} \text{h}^{-1}$ . The co-release of P with the reduction of iron oxides is a well-documented phenomena (Einsele 1936, Mortimer 1941). Aerobic rates were generally similar to observations in this study, though rates in rates up to  $28 \mu\text{mol m}^{-2} \text{h}^{-1}$  were observed in Minnesota. Elevated pH's are an alternative pathway for high P releases from sediments (Seitzinger 1991, Gao et al. 2012). The low levels of P efflux from the lower Susquehanna reservoirs are consistent with the high concentrations of extractable Fe and the aerobic conditions observed during the course of this study. These data do not indicate that the increased P flux from the Conowingo Reservoir to the Chesapeake Bay (Zhang et al. 2016) could be derived via efflux of dissolved P from bed deposits.

The fluxes of  $\text{N}_2\text{-N}$ , generally from the process of denitrification, are not especially high for the reservoirs listed in Table 10. Many reservoirs have much higher concentrations of water column  $\text{NO}_x^-$ , with the higher concentrations driving higher rates of denitrification. Similarly, Conowingo Reservoir rates for uptake of  $\text{NO}_x^-$ , release of  $\text{NH}_4^+$  and consumption of oxygen are not at the higher end of reservoir observations.

While oxygen concentrations in bottom water were not low enough to change biogeochemical pathways in the Conowingo Reservoir, previous observations in the reservoir suggest that bottom water hypoxia has occurred in the past. The lack of hypoxic conditions in this study may be a function of the hydrological conditions in the lower Susquehanna during the period of study, or a result of lower inputs of labile organic matter. Improvements in P releases in waste water and consequently lower algal biomass would result in lower bottom water oxygen depletion. In the past, such low oxygen events would likely increase SRP releases from sediment, increase  $\text{NO}_x^-$  uptake by sediment, and increase rates of denitrification.

**Table 10. Reservoir and river sediment-water exchange rates using techniques identical to this study. The studies were carried out by UMCES and Chesapeake Biogeochemical Associates (Cornwell and Owens 2002, Cornwell and Owens 2004, Owens and Cornwell 2006, 2008a, Owens and Cornwell 2008b, Owens and Cornwell 2009, Cornwell et al. 2017).**

Site	Type	SRP	NH <sub>4</sub> <sup>+</sup>	NO <sub>x</sub> <sup>-</sup>	N <sub>2</sub> -N	O <sub>2</sub>
		$\mu\text{mol m}^{-2} \text{h}^{-1}$				
Tridelphia July 2001 (MD)	Anoxic	6 - 7	133 - 255			
Tridelphia May 1999 (MD)	Aerobic	0	0 - 194	-92 - -104	84 - 240	-1,089 - -1,293
East Canyon (UT)	Anoxic	4 - 7	79 - 181			
Byllesby (MN)	Anoxic	6 - 37				
Byllesby (MN)	Aerobic	3 - 28			351 - 519	-1,403 - -1,881
Spokane Lake (WA)	Aerobic	0 - 10	-162 - 213	-39 - -799	70 - 562	-1,962 - -3,315
Grand Calumet River (IN)	Aerobic	-58 - 0	-188 - 851	-2,036 - 277	64 - 1,334	-1,215 - -3,354
Lake Linganore (MD)	Anoxic	17 - 66	54 - 114	-9 - 2		
Lake Linganore (MD)	Aerobic	-2 - 0	186 - 551	-236 - -575	42 - 572	-759 - -1,359
Lake Anita Louise (MD)	Anoxic	50-97	120	--1.9 - 0		
Conowingo Reservoir (this study)	Aerobic	-0.8±3.7	90±134	-52±53	128±72	-982±605
Lake Aldred + Lake Clarke	Aerobic	0	73±86	-98±101	115±68	-983±317

## Nitrogen Cycling – Reservoirs to the Bay

The scaling of Conowingo biogeochemical measurements to bay nutrient mass balances can provide some insight on its importance to nutrient balances (Table 11). The most obvious scaling is the size of the reservoir relative to the upper Chesapeake Bay. If we define the Maryland mainstem Chesapeake Bay as Boynton et al. (1995) did, it includes the Chesapeake Bay from the north shore of the Potomac River mouth and all tributary areas other than the Choptank and Patuxent Rivers. The Conowingo reservoir is 0.9% of the area of the MD mainstem bay, and the three reservoirs combined cover an area equivalent to 1.8 % of the MD mainstem bay.

April 2016 is the only month in which we have measurements in all 3 reservoirs and the upper Chesapeake Bay. Temperatures increase rapidly during April averaging 9.6°C in the Conowingo Reservoir, 14.5°C at Bay sites, and 18.0°C at Lakes Clarke/Aldred at the time of sediment collection and incubation. Direct comparison of benthic fluxes across a latitudinal gradient with a large temperature range would result in the lower temperatures having lower metabolic rates and the last site sampled having higher rates. Models use  $Q_{10}$ 's to estimate the expected differences as a function of temperature. Such efforts may be useful for “normalizing” sediment oxygen uptake, but may not be effective at predicting a multi-step process such as denitrification.

Over the latitudinal gradient from the bay to the upper reservoirs, oxygen demand ranged from  $< 100 \mu\text{mol m}^{-2} \text{h}^{-1}$  in the upper Conowingo reservoir to  $> 1,800 \mu\text{mol m}^{-2} \text{h}^{-1}$  at Lee 2.5 in the Chesapeake Bay near the Patapsco River entrance (Figure 51). Higher rates in the Lake Aldred and Lake Clarke may result from higher temperatures found later in April. In the Conowingo Reservoir, if the May 2015 data are not used, we find that there is an increase of  $\sim 40 \mu\text{mol m}^{-2} \text{h}^{-1}$  of sediment oxygen demand with each 1 °C increase in temperature (Figure 52). The upper reservoir oxygen uptake data appear consistent with the Conowingo data if the temperature differences are considered.

The  $\text{N}_2\text{-N}$  efflux data (Figure 53) were highly variable within each reservoir and in the bay, though rates of denitrification increase in the southern site Lee 2.5. The highest rates of ammonium efflux were observed in Lake Clarke where two sites (4 cores) had rates in excess of  $100 \mu\text{mol m}^{-2} \text{h}^{-1}$ . Nitrate uptake and release were also variable throughout.

The upper bay sites, in spring, likely have similar biogeochemical rates as Conowingo sediments. Sediment  $^{13}\text{C}$  stable isotopic data (Cornwell and Sampou 1995) suggest that the upper Chesapeake Bay sediment organic matter is a mixture of fluvial/terrestrial materials. Despite modest upper bay salinities, upper bay nitrogen processing looks similar to the reservoirs.

**Table 11. Scaling of Conowingo Nitrogen Fluxes to Chesapeake Bay Fluxes**

Parameter or Measurement	Value	
Reservoir area, upper mainstem bay area, MD mid bay area	Lake Clarke	24.6 x 10 <sup>6</sup> m <sup>2</sup>
	Lake Aldred	10.4 x 10 <sup>6</sup> m <sup>2</sup>
	Conowingo	34.7 x 10 <sup>6</sup> m <sup>2</sup>
	MD Mainstem Bay	3,942 x 10 <sup>6</sup> m <sup>2</sup>
Total N input from Chesapeake Bay, 2002-2011 (Hirsch 2012)	5,124 x 10 <sup>6</sup> moles y <sup>-1</sup>	
Average NH <sub>4</sub> <sup>+</sup> flux in reservoir	90 umol m <sup>-2</sup> h <sup>-1</sup> , 0.79 mol m <sup>-2</sup> y <sup>-1</sup>	
Average NH <sub>4</sub> <sup>+</sup> production based on O <sub>2</sub> stoichiometry	150 umol m <sup>-2</sup> h <sup>-1</sup> , 1.314 mol m <sup>-2</sup> y <sup>-1</sup>	
Conowingo NH <sub>4</sub> <sup>+</sup> flux as percent annual MD mainstem bay DIN flux	MD Mainstem Bay	0.75 %
Moles of N produced from flux.  Mainstem Din efflux data from previous mass balance estimates (Boynton et al. 1995).	Conowingo	26.8 x 10 <sup>6</sup> moles y <sup>-1</sup>
	MD Mainstem Bay	3,550 x 10 <sup>6</sup> moles y <sup>-1</sup>
Adsorbed NH <sub>4</sub> <sup>+</sup> - mean of all depths	38.7 mmol L <sup>-1</sup> , 38.7 mol m <sup>-3</sup> , 50.6 moles yd <sup>-3</sup> , 1.19 lb N yd <sup>-3</sup>	
Adsorbed NH <sub>4</sub> <sup>+</sup> - mean of 0-50 cm	12.1 mmol L <sup>-1</sup> , 12.1 mol m <sup>-3</sup> , 15.8 moles yd <sup>-3</sup> , 0.37 lb N yd <sup>-3</sup>	
Adsorbed ammonium in scoured sediment if half the reservoir erodes 0.5 m. Average ammonium in top 0.5 cm used in calculation.	Conowingo	105 x 10 <sup>6</sup> moles
Adsorbed NH <sub>4</sub> <sup>+</sup> in 10 <sup>6</sup> yd <sup>3</sup> to 10'	Conowingo	50.6 x 10 <sup>6</sup> moles
1 x 10 <sup>6</sup> yd <sup>3</sup> adsorbed NH <sub>4</sub> <sup>+</sup> as percent average annual Conowingo NH <sub>4</sub> <sup>+</sup> flux	Conowingo	189 %

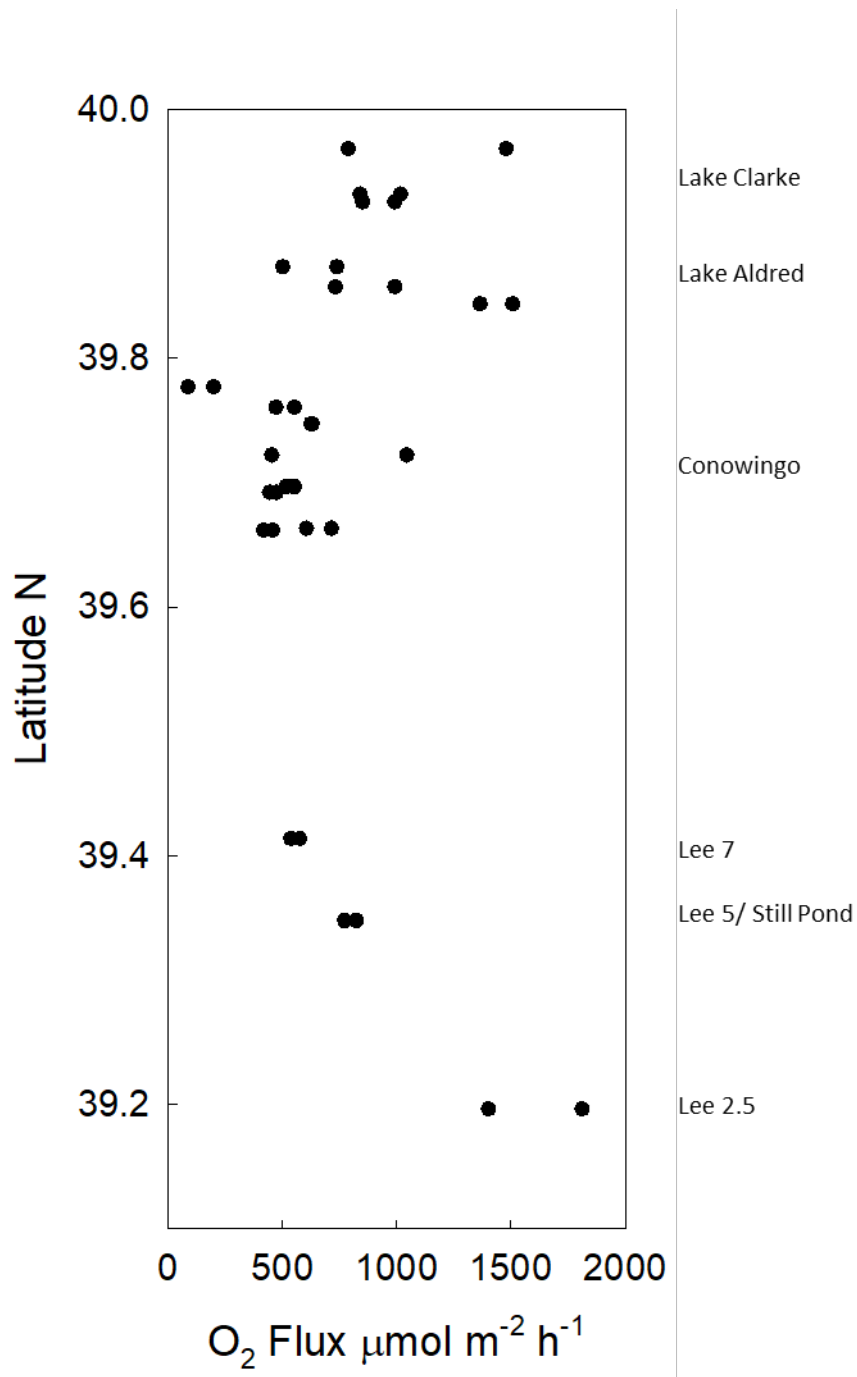


Figure 51. Sediment oxygen demand as a function of latitude in April 2016. Note the sign reversal from previous oxygen flux plots. The average rate at all sites was  $763 \pm 387 \mu\text{mol m}^{-2} \text{h}^{-1}$ . Though all measurements were made in April, temperatures were different at the time of sampling, with  $T = 9.6^\circ\text{C}$  in the Conowingo Reservoir,  $T = 14.5^\circ\text{C}$  at Bay sites, and  $T = 18.0^\circ\text{C}$  at Lakes Clarke/Aldred.

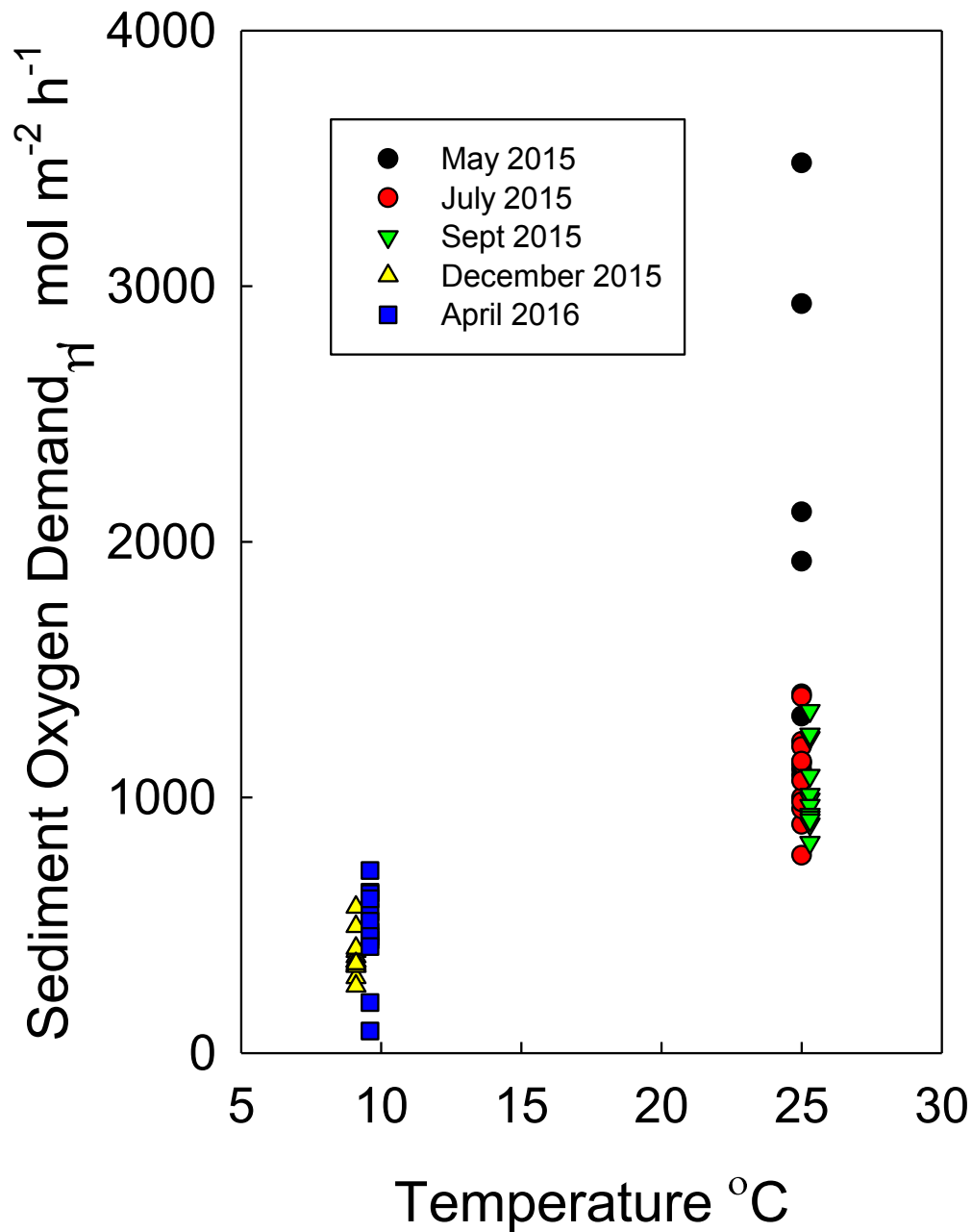
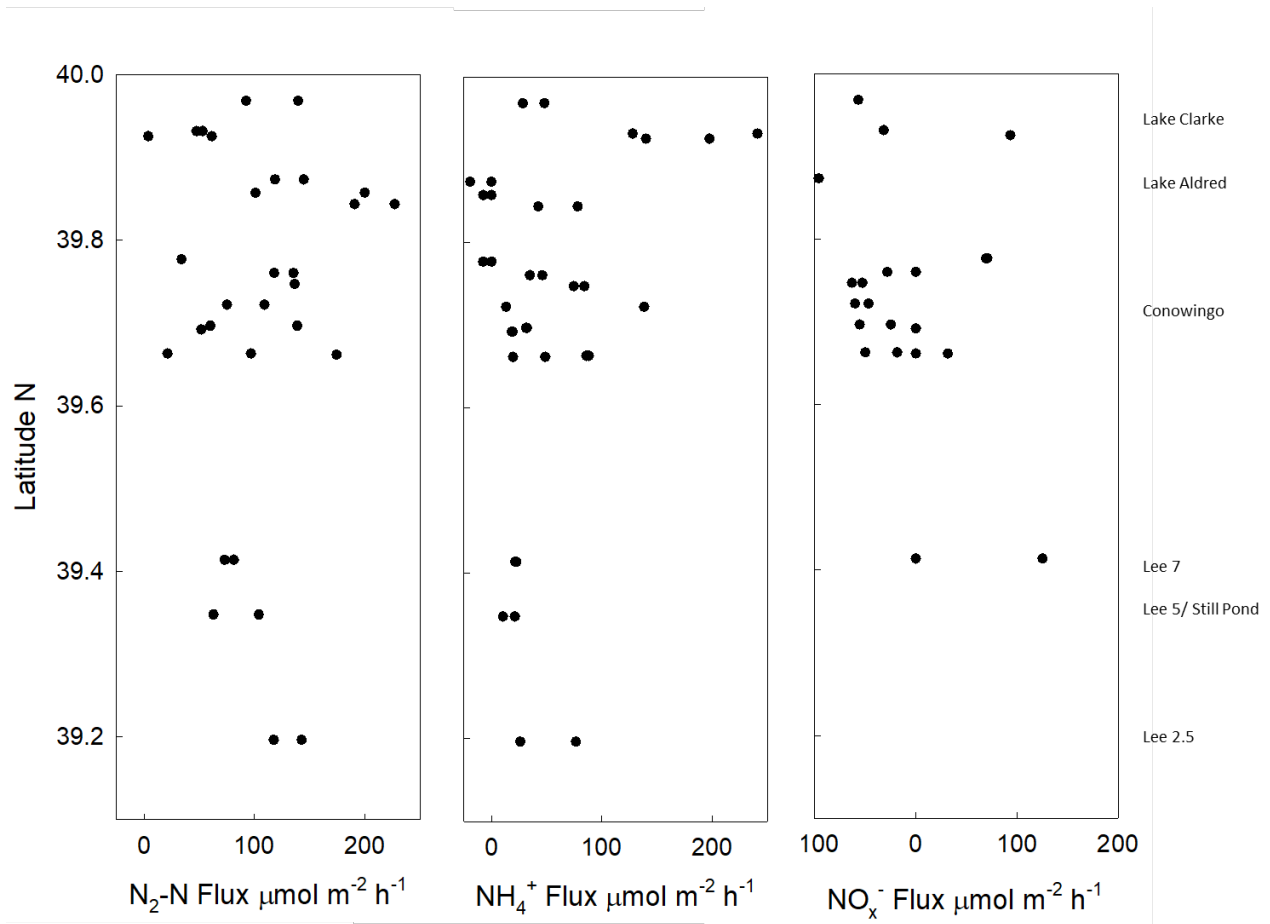


Figure 52. Conowingo sediment oxygen demand as a function of incubation temperature. Only sites with data from all 5 dates were used in the analysis. Each individual core is plotted. Average rates in May 2015 are almost twice the other rates at similar temperatures.



**Figure 53. Spring 2016 sediment-water nitrogen exchange rates as a function of latitude. The average  $\text{N}_2\text{-N}$ ,  $\text{NH}_4^+$  and  $\text{NO}_x^-$  flux rates were  $104 \pm 54$ ,  $52 \pm 59$  and  $-34 \pm 81 \mu\text{mol m}^{-2} \text{h}^{-1}$  respectively. Though all measurements were made in April, temperatures were different at the time of sampling, with  $T = 9.6^\circ\text{C}$  in the Conowingo Reservoir,  $T = 14.5^\circ\text{C}$  at Bay sites, and  $T = 18.0^\circ\text{C}$  at Lakes Clarke/Aldred.**

## Comparative Rates

In Table 11, the rates of N transformation and the pools of adsorbed ammonium are presented in a number of different ways. If we do a simple comparison of mean ammonium effluxes from the Conowingo reservoir to that of the upper Chesapeake Bay, we see that the Conowingo Reservoir fluxes are ~ 0.75% of MD mainstem bay N fluxes (Figure 54), with the contribution of all reservoirs of ~1.5%. These results suggest that:

- 1) With a complete washout of the sediment in the Conowingo Reservoir, along with much of the potential metabolism of all the sediment producing ammonium, the effect of the Conowingo nitrogen regeneration to the Chesapeake Bay has only a minimal impact on Chesapeake Bay nutrient balances.
- 2) Sediment in the Conowingo Reservoir behaves very similar to upper bay sediments, and there likely is little difference between the efflux of ammonium into the flowing waters leaving the Conowingo and the tidal waters of the upper bay.
- 3) The release of adsorbed ammonium needs more detailed assessment, but if half the bottom of the Conowingo Reservoir was eroded to 0.5 m, those releases would be equivalent to ~3% of the ammonium plus nitrate efflux into the Chesapeake Bay (Table 11), or 2% of total N inputs.

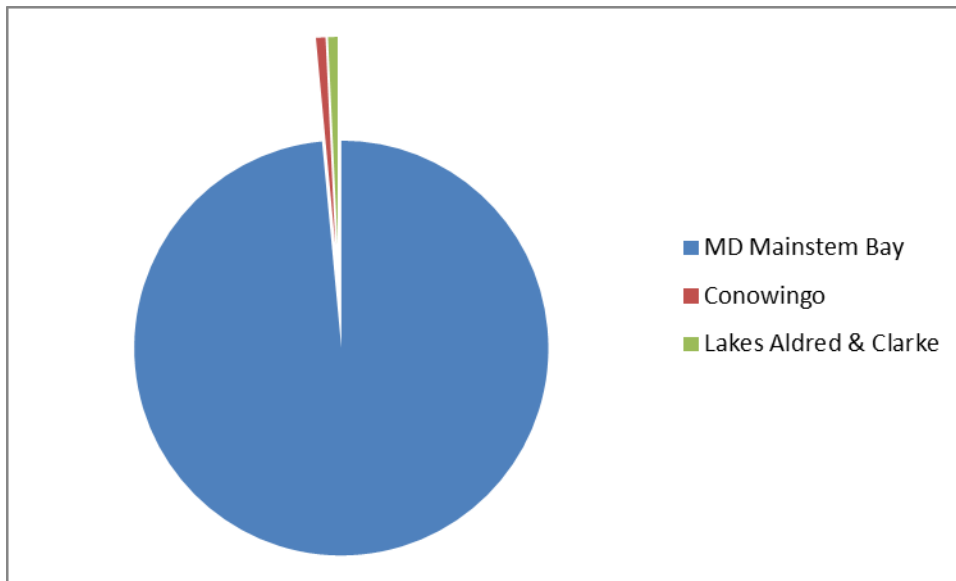


**Figure 54. Pie chart of sediment-water ammonium fluxes from reservoirs and the Maryland mainstem bay. The sum of all fluxes is  $3,604 \times 10^6$  moles  $y^{-1}$ , or 111,136,564 lbs N per year. In this plot, it is assumed that the annual ammonium flux per  $m^2$  in Lakes Clarke and Aldred are the same as in the Conowingo reservoir.**

## Dredging - Biogeochemical Considerations

The purpose of this assessment program was to determine the biogeochemical characteristics of Conowingo sediment deposits and inform bay modeling efforts by supplying better calibration data. Any decisions regarding dredging the Conowingo Reservoir will be informed by the results of USEPA's modeling output, particularly the effect of episodic loading of sediments in the mid bay region. Previous modeling suggests nitrogen, rather than phosphorus, might fuel a very small incremental loss of dissolved oxygen in several bay segments. Our long-core data may be useful in consideration of potential biogeochemical impacts of dredging.

The release of soluble reactive phosphorus during dredging and sediment placement is likely a minor process. Moderate to high concentrations of pore water iron, when exposed to oxygen during dredging operation, will oxidize to form high surface area iron oxide minerals. These surfaces will be highly efficient at removing any soluble phosphorus and it is likely that any environment effect would be related to the movement of particulate phosphorus. Further assessment of phosphorus mobility would not appear to be warranted.

Adsorbed ammonium in Conowingo sediment deposits presents the same challenges faced by the Maryland Port Administration and US Army Corps of Engineers in the dredging of navigation channels in the upper Chesapeake Bay. The elutriation of adsorbed ammonium by the addition of water for sediment slurring will likely result in the release of high concentrations of ammonium to the water. In the case of dredged channels, concentrations of ammonium were high but the overall effect on bay nitrogen balances were small (Cornwell and Owens 2011). The data in this report (Table 9) likely is a maximum release number. Our estimate of the amount of adsorbed  $\text{NH}_4^+$  in  $1 \times 10^6 \text{ yd}^3$  is  $\sim 50.6 \times 10^6$  moles of N, or  $1.56 \times 10^6$  lbs N. This number is equivalent to almost 2 years of ammonium efflux.

We can compare potential effects, both positive and negative, to observations made previously for Chesapeake Bay navigation channels:

- 1) The concentration of adsorbed ammonium is much higher in Conowingo sediments, possibly leading to greater releases when slurring sediments
- 2) Conversely, freshwater sediments are much more adsorptive of ammonium (Seitzinger et al. 1991) and elutriation of adsorbed ammonium with low potassium river water might result in a low proportion of adsorbed ammonium release.

In order to assess the potential release of ammonium by dredging, cores from the specific areas to be dredged should be collected and subjected to dilution by water in the same proportions used to pump sediment slurries in pipes to the point of deposition. During the dewatering phase, the ponded dilution water should be assessed for ammonium concentrations and the potential production of high concentrations of algae. In addition, if algae raise pH dramatically (Seitzinger 1991, Gao et al. 2014b) there is the potential of  $\text{NH}_3(\text{g})$  release to the atmosphere (Larsen et al. 2001) and release of SRP from iron oxide bound forms (Bailey et al. 2006).

## Monitoring Recommendations

The sediment assessment program presented here presents a detailed examination of benthic processes over a period of roughly one year. In particular, the project period was a period of relative quiescent conditions in the reservoir, with flows well below those in which scour is likely to occur. Improvement in our understanding would come from:

- Measurement of sediment biogeochemical processes before and after large scale flow events, along with characterization of the suspended material.
- A better understanding of the linkage between all three reservoirs. Our program was focused on the Conowingo pool, but the same process of deposition/scour of bottom sediments is clearly in place in the upper two reservoirs. In a large scale event, the upper two reservoirs are also potential contributors of sediment and nutrient inputs to the Chesapeake Bay.
- A dynamic physical/biogeochemical model of these reservoirs is needed to better predict 1) how reservoirs affect current nutrient and sediment inputs to the Chesapeake Bay and 2) to allow prediction of future inputs based on improved land use, infill of reservoirs, etc.
- There is little water column biogeochemical data. Understanding the balance between allochthonous and autochthonous organic matter inputs and biogeochemical controls of nutrient recycling would provide a better understanding of the interception and release of biogeochemical constituents.

## Summary

This biogeochemical assessment program has provided the first comprehensive look at biogeochemical processes in the sediments of the Conowingo Reservoir, as well as additional information on biogeochemical processes in Lake Clarke, Lake Aldred and the upper Chesapeake Bay. In general, the biogeochemical behavior of reservoir sediments is similar to comprehensive sediment observations in the upper Chesapeake Bay. These data are also consistent with previous modeling efforts (Linker et al. 2016) that suggest that the potential biogeochemical effects of the bay are relatively small.

The input of phosphorus from scour could greatly increase the input of P to the Chesapeake Bay. However, the effects of such extra P inputs appear to be minimal because it is likely to mostly deposited in the upper bay where sediment P retention is high. The potential mobility of iron-bound P is thus limited by location; experiments with sulfide addition suggest that ~30% of total P might enter the active Chesapeake Bay biogeochemical P cycle when deposited in deep, anoxic Chesapeake Bay environments.

If in a scour event all Conowingo Reservoir sediment metabolism was moved to the sediments of the upper Chesapeake Bay, the likely increase in sediment nitrogen regeneration in the bay would be < 1%. In the total environmental context, this likely has a minimal biogeochemical effect on Chesapeake Bay nitrogen cycling. However, any conclusions about the importance of this additional N loading needs to be put in the context of meeting TMDL goals; for this, ongoing modeling by the USEPA Bay Program,

rather than our biogeochemical measurements alone, will provide the final conclusions on TMDL compliance.

The key unexpected result of this study is that there is a substantial amount of adsorbed ammonium in Conowingo Reservoir deposits. Although originally this work was not an emphasis, it may have implications for estimates of N release from scour and from dredging activities.

## **Acknowledgements**

This project was initiated as a joint effort by Exelon Corporation and the State of Maryland to expand our understanding of the biogeochemical implications of Conowingo scour on Chesapeake Bay processes. Bruce Michael at the Maryland Department of Natural Resources and Lee Curry at the Maryland Department of the Environment made important contributions to the scope of this project. Project management was largely carried out by Tim Sullivan and Tom Sullivan at Gomez and Sullivan Engineers. Bryan Strawn at AECOM provided helpful guidance on sampling events and Marjie Zeff was key to the long core sampling program.

Emily Russ, from Cindy Palinkas' laboratory, helped with all coring activities and with Cindy Palinkas has provided sediment grain size data. Alison Sanford provided key laboratory and organizational help with the diagenesis program. The Analytical Services group at Horn Point Laboratory provided C and N analyses. We are grateful for input and discussions with our UMCES investigators: Larry Sanford, Cindy Palinkas, Michael Kemp, Jeremy Testa, and Ming Li. Jim Fitzpatrick of HDR provided valuable discussions of data and interpretation. The multi-decade work of Walter Boynton and colleagues has provided a strong biogeochemical context for this research.

## Literature Cited

- Anschutz, P., S. Zhong, B. Sundby, A. Mucci, and C. Gobeil. 1998. Burial efficiency of phosphorus and the geochemistry of iron in continental margin sediments. *Limnology and Oceanography* **43**:53-64.
- Anthony, R. S. 1977. Iron-rich rhythmically laminated sediments in Lake of the Clouds, northeastern Minnesota. *Limnology and Oceanography* **22**:45-54.
- Aspila, K. I., H. Agemian, and A. S. Y. Chau. 1976. A semi-automated method for the determination of inorganic, organic and total phosphate in sediments. *Analyst* **101**:187-197.
- Bailey, E. M., M. S. Owens, W. R. Boynton, J. Cornwell, E. Kiss, P. W. Smail, H. Soulen, E. Buck, and M. Ceballos. 2006. Sediment phosphorus flux: pH interactions in the tidal freshwater Potomac River estuary. TS-505-06-CBL, UMCES Final Report to the Interstate Commission on the Potomac River Basin.
- Berner, R. A. 1980. *Early Diagenesis A Theoretical Approach*. Princeton University Press, Princeton, NJ.
- Berner, R. A. 1981. A rate model for organic matter decomposition during sulfate reduction in marine sediments. Pages 35-44 *Biogeochimie de la Matiere Organique a l'Interface Eau-Sediment Marin*. CNRS, Paris.
- Boynton, W. R. 2000. Impact of nutrient inflows on Chesapeake Bay. Pages 23-40 *in* A. N. Sharpley, editor. *Agriculture and Phosphorus Management: The Chesapeake Bay*. Lewis Publishers, Boca Raton.
- Boynton, W. R., and E. M. Bailey. 2008. Sediment Oxygen and Nutrient Exchange Measurements from Chesapeake Bay, Tributary Rivers and Maryland Coastal Bays: Development of a Comprehensive Database & Analysis of Factors Controlling Patterns and Magnitude of Sediment-Water Exchanges. UMCES Technical Report Series No. TS-542-08. University of Maryland Center for Environmental Science.
- Boynton, W. R., J. H. Garber, R. Summers, and W. M. Kemp. 1995. Inputs, Transformations, and Transport of Nitrogen and Phosphorus in Chesapeake Bay and Selected Tributaries. *Estuaries* **18**:285-314.
- Boynton, W. R., W. M. Kemp, J. M. Barnes, J. L. W. Cowan, S. E. Stammerjohn, L. L. Matteson, F. M. Rohland, M. Marvin, and J. H. Garber. 1991. Long-term characteristics and trends of benthic oxygen and nutrient fluxes in the Maryland portion of the Chesapeake Bay. Pages 339-354 *in* J. A. Mihursky and A. Chaney, editors. *New Perspectives in the Chesapeake System: A Research and Management Partnership*. Proceedings of a Conference. Chesapeake Research Consortium, Solomons, Maryland.
- Bray, J. T., O. P. Bricker, and B. N. Troup. 1973. Phosphate in interstitial waters of anoxic sediments: oxidation effects during the sampling procedure. *Science* **180**:1362-1364.
- Burdige, D. J. 1989. THE EFFECTS OF SEDIMENT SLURRYING ON MICROBIAL PROCESSES, AND THE ROLE OF AMINO-ACIDS AS SUBSTRATES FOR SULFATE REDUCTION IN ANOXIC MARINE-SEDIMENTS. *Biogeochemistry* **8**:1-23.
- Burdige, D. J. 1991. The kinetics of organic matter mineralization in anoxic marine sediments. *Journal of Marine Research* **49**:727-761.
- Burford, M. A., S. A. Green, A. J. Cook, S. A. Johnson, J. G. Kerr, and K. R. O'Brien. 2012. Sources and fate of nutrients in a subtropical reservoir. *Aquatic Sciences* **74**:179-190.
- Burgin, A. J., and S. K. Hamilton. 2007. Have we overemphasized the role of denitrification in aquatic ecosystems? A review of nitrate removal pathways. *Frontiers in Ecology and the Environment* **5**:89-96.

- Callender, E. 1982. Benthic phosphorus regeneration in the Potomac River estuary. *Hydrobiologia* **92**:431-446.
- Capone, D. G., and R. P. Kiene. 1988. Comparison of Microbial Dynamics in Marine and Fresh-Water Sediments - Contrasts in Anaerobic Carbon Catabolism. *Limnology and Oceanography* **33**:725-749.
- Caraco, N., J. Cole, and G. E. Likens. 1990. A comparison of phosphorus immobilization in sediments of freshwater and coastal marine systems. *Biogeochemistry* **9**:277-290.
- Caraco, N. F., J. J. Cole, and G. E. Likens. 1989. Evidence for sulphate-controlled phosphorus release from sediments of aquatic systems. *Nature* **341**:316-318.
- Cerco, C. F. 2016. Conowingo Reservoir Sedimentation and Chesapeake Bay: State of the Science. *Journal of Environmental Quality* **45**:882-886.
- Cerco, C. F., and M. R. Noel. 2016. Impact of Reservoir Sediment Scour on Water Quality in a Downstream Estuary. *Journal of Environmental Quality* **45**:894-905.
- Conley, D. J. 2000. Biogeochemical nutrient cycles and nutrient management strategies. *Hydrobiologia* **410**:87-96.
- Conley, D. J., W. M. Smith, J. C. Cornwell, and T. R. Fisher. 1995. Transformation of particle-bound phosphorus at the land-sea interface. *Estuarine, Coastal and Shelf Science* **40**:161-176.
- Cook, P. L. M., K. T. Aldridge, S. Lamontagne, and J. D. Brookes. 2010. Retention of nitrogen, phosphorus and silicon in a large semi-arid riverine lake system. *Biogeochemistry* **99**:49-63.
- Cornwell, J. C. 1987. Phosphorus cycling in arctic lake sediment: adsorption and authigenic minerals. *Archiv fur Hydrobiologia* **109**:161-179.
- Cornwell, J. C., and W. R. Boynton. 1999. Sediment Water Oxygen and Nutrient Exchanges at Shoal and Channel Stations in the Upper Bay. Report to Maryland Port Administration. TS-186-99, University of Maryland Center for Environmental Sciences, Cambridge, Maryland.
- Cornwell, J. C., P. M. Glibert, and M. S. Owens. 2014. Nutrient Fluxes from Sediments in the San Francisco Bay Delta. *Estuaries and Coasts* **37**:1120-1133.
- Cornwell, J. C., W. M. Kemp, and T. M. Kana. 1999. Denitrification in coastal ecosystems: environmental controls and aspects of spatial and temporal scale. *Aquatic Ecology* **33**:41-54.
- Cornwell, J. C., and G. W. Kipphut. 1992. Biogeochemistry of manganese- and iron-rich sediments in Toolik Lake, Alaska. *Hydrobiologia* **240**:45-59.
- Cornwell, J. C., and M. Owens. 2004. A Study of Sediment Phosphorus Release from Lake Byllesby, July 2004. Final Report to the cities of Faribault and Owatonna, Minnesota. Chesapeake Biogeochemical Associates.
- Cornwell, J. C., and M. S. Owens. 1999. Benthic Phosphorus Cycling in Lake Champlain: Results of an Integrated Field Sampling/Water Quality Modeling Study. Part B: Field Studies. June 1999. 34B, UMCES Horn Point Laboratory, Cambridge Maryland.
- Cornwell, J. C., and M. S. Owens. 2002. Triadelphia Sediment-Water Exchange Study: Final Report for Washington Suburban Sanitary Commission. TS-364-02, UMCES Horn Point Laboratory, Cambridge MD.
- Cornwell, J. C., and M. S. Owens. 2011. Quantifying Sediment Nitrogen Releases Associated with Estuarine Dredging. *Aquatic Geochemistry* **17**:499-517.
- Cornwell, J. C., M. S. Owens, and L. Pride. 2000. Nitrogen and Phosphorus Releases During Dredging: Assessing Potential Phosphorus Releases and Refinement of Ammonium Release Estimates. TS-230-00, University of Maryland Center for Environmental Science, Cambridge, Maryland.
- Cornwell, J. C., H. Perez-Villalona, M. S. Owens, K. G. Sellner, and D. Ferrier. 2017. Lake Linganore biogeochemical measurements: sediment-water exchange rates of oxygen and nutrients from September 2016. Final Report to MDE.

- Cornwell, J. C., and P. A. Sampou. 1995. Environmental controls on iron sulfide mineral formation in a coastal plain estuary. Pages 224-242 in M. A. Vairavamurthy and M. A. A. Schoonen, editors. *Geochemical Transformations of Sedimentary Sulfur*.
- Cornwell, J. C., J. C. Stevenson, D. J. Conley, and M. Owens. 1996. A sediment chronology of Chesapeake Bay eutrophication. *Estuaries* **19**:488-499.
- Cowan, J. L. W., and W. R. Boynton. 1996. Sediment-water oxygen and nutrient exchanges along the longitudinal axis of Chesapeake Bay: Seasonal patterns, controlling factors and ecological significance. *Estuaries* **19**:562-580.
- Daskalakis, K. D., and T. P. O'Connor. 1995. Normalization and elemental sediment contamination in the coastal United States. *Environmental Science and Technology* **29**:470-477.
- David, M. B., L. G. Wall, T. V. Royer, and J. L. Tank. 2006. Denitrification and the nitrogen budget of a reservoir in an agricultural landscape. *Ecological Applications* **16**:2177-2190.
- DiToro, D. M. 2001. *Sediment Flux Modeling*. Wiley-Interscience, New York.
- Downing, J. A., J. J. Cole, J. J. Middelburg, R. G. Striegl, C. M. Duarte, P. Kortelainen, Y. T. Prairie, and K. Laube. 2008. Sediment organic carbon burial in agriculturally eutrophic impoundments over the last century. *Global Biogeochemical Cycles* **22**.
- Edwards, R. E. 2006. Comprehensive analysis of the sediments retained behind hydroelectric dams of the lower Susquehanna River. Publication 239. Susquehanna River Basin Commission.
- Einsele, W. 1936. Ueber die Beziehungen des Eisenkreislaufes zum Phosphatkreislauf im Eutrophen See. *Archiv fur Hydrobiologia* **29**:664-686.
- Fisher, T. R., A. B. Gustafson, K. Sellner, R. Lacoutre, L. W. Haas, R. L. Wetzel, R. Magnien, D. Everitt, B. Michaels, and R. Karrh. 1999. Spatial and temporal variation of resource limitation in Chesapeake Bay. *Marine Biology* **133**:763-778.
- Fisher, T. R., E. R. Peele, J. W. Ammerman, and L. W. Harding, Jr. 1992. Nutrient limitation of phytoplankton in Chesapeake Bay. *Marine Ecology Progress Series* **82**:51-63.
- Follmi, K. B. 1996. The phosphorus cycle, phosphogenesis and marine phosphate-rich deposits. *Earth Science Reviews* **40**:55-124.
- Fox, L. E. 1990. Geochemistry of dissolved phosphate in the Sepik River and Estuary, New Guinea. *Geochimica Et Cosmochimica Acta* **54**:1019-1024.
- Friedl, G., and A. Wuest. 2002. Disrupting biogeochemical cycles - Consequences of damming. *Aquatic Sciences* **64**:55-65.
- Froelich, P. N. 1988. Kinetic control of dissolved phosphate in natural rivers and estuaries: a primer on the phosphate buffer mechanism. *Limnology and Oceanography* **33**:649-668.
- Gao, Y., J. C. Cornwell, D. K. Stoecker, and M. S. Owens. 2012. Effects of cyanobacterial-driven pH increases on sediment nutrient fluxes and coupled nitrification-denitrification in a shallow fresh water estuary. *Biogeosciences* **9**:2697-2710.
- Gao, Y., J. C. cornwell, D. K. Stoecker, and M. S. Owens. 2014a. Influence of cyanobacterial blooms on sediment biogeochemistry and nutrient fluxes. *Limnology and Oceanography* **59**:959-971.
- Gao, Y., J. M. O'Neil, D. K. Stoecker, and J. C. Cornwell. 2014b. Photosynthesis and nitrogen fixation during cyanobacteria blooms in an oligohaline and tidal freshwater estuary. *Aquatic Microbial Ecology* **72**:129-144.
- Garcia-Robledo, E., A. Corzo, and S. Papaspyrou. 2014. A fast and direct spectrophotometric method for the sequential determination of nitrate and nitrite at low concentrations in small volumes. *Marine Chemistry* **162**:30-36.
- Gardolinski, P., P. J. Worsfold, and I. D. McKelvie. 2004. Seawater induced release and transformation of organic and inorganic phosphorus from river sediments. *Water Research* **38**:688-692.

- Gibb, M. M. 1979. A simple method for the rapid determination of iron in natural waters. *Water Research* **13**:295-297.
- Giblin, A. E., C. R. Tobias, B. Song, N. Weston, G. T. Banta, and V. H. Rivera-Monroy. 2013. The Importance of Dissimilatory Nitrate Reduction to Ammonium (DNRA) in the Nitrogen Cycle of Coastal Ecosystems. *Oceanography* **26**:124-131.
- Grantz, E. M., A. Kogo, and J. T. Scott. 2012. Partitioning whole-lake denitrification using in situ dinitrogen gas accumulation and intact sediment core experiments. *Limnology and Oceanography* **57**:925-935.
- Harrison, J. A., R. J. Maranger, R. B. Alexander, A. E. Giblin, P.-A. Jacinthe, E. Mayorga, S. P. Seitzinger, D. J. Sobota, and W. M. Wollheim. 2009. The regional and global significance of nitrogen removal in lakes and reservoirs. *Biogeochemistry* **93**:143-157.
- Hartzell, J. L., T. E. Jordan, and J. C. Cornwell. 2010. Phosphorus Burial in Sediments Along the Salinity Gradient of the Patuxent River, a Subestuary of the Chesapeake Bay (USA). *Estuaries and Coasts* **33**:92-106.
- Hartzell, J. L., T. E. Jordan, and J. C. Cornwell. 2017. Phosphorus Sequestration in Sediments Along the Salinity Gradients of Chesapeake Bay Subestuaries. *Estuaries and Coasts*:1-19.
- Hearn, P. P., D. L. Parkhurst, and E. Callender. 1983. Authigenic vivianite in Potomac River sediments: control by ferric oxy-hydroxides. *Journal of Sedimentary Petrology* **53**:165-177.
- Hirsch, R. M. 2012. Flux of nitrogen, phosphorus, and suspended sediment from the Susquehanna River Basin to the Chesapeake Bay during Tropical Storm Lee, September 2011, as an indicator of the effects of reservoir sedimentation on water quality: U.S. Geological Survey Scientific Investigations Report 2012-5185. U.S. Geological Survey, Reston, Virginia.
- Howarth, R., and H. W. Paerl. 2008. Coastal marine eutrophication: Control of both nitrogen and phosphorus is necessary. *Proceedings of the National Academy of Sciences of the United States of America* **105**:E103-E103.
- Jasinski, D. A. 1996. Phosphorus dynamics of sediment in the mesohaline region of Chesapeake Bay. University of Maryland, College Park.
- Jordan, T. E., J. C. Cornwell, W. R. Boynton, and J. T. Anderson. 2008. Changes in phosphorus biogeochemistry along an estuarine salinity gradient: The iron conveyor belt. *Limnology and Oceanography* **53**:172-184.
- Joye, S. B., and I. C. Anderson. 2008. Nitrogen cycling in coastal sediments. Pages 868-915 *in* D. G. Capone, D. A. Bronk, M. R. Mulholland, and E. J. Carpenter, editors. *Nitrogen in the marine environment*. 2nd Edition. Academic Press, Amsterdam.
- Kana, T. M., C. Darkangelo, M. D. Hunt, J. B. Oldham, G. E. Bennett, and J. C. Cornwell. 1994. Membrane inlet mass spectrometer for rapid high-precision determination of N<sub>2</sub>, O<sub>2</sub>, and Ar in environmental water samples. *Analytical Chemistry* **66**:4166-4170.
- Kellogg, M. L., J. C. Cornwell, M. S. Owens, and K. T. Paynter. 2013. Denitrification and nutrient assimilation on a restored oyster reef. *Marine Ecology Progress Series* **480**:1-19.
- Kemp, W. M., and W. R. Boynton. 1984. Spatial and temporal coupling of nutrient inputs to estuarine primary production: the role of particulate transport and decomposition. *Bulletin of Marine Science* **35**:522-535.
- Kemp, W. M., W. R. Boynton, J. E. Adolf, D. F. Boesch, W. C. Boicourt, G. Brush, J. C. Cornwell, T. R. Fisher, P. M. Glibert, J. D. Hagy, L. W. Harding, E. D. Houde, D. G. Kimmel, W. D. Miller, R. I. E. Newell, M. R. Roman, E. M. Smith, and J. C. Stevenson. 2005. Eutrophication of Chesapeake Bay: historical trends and ecological interactions. *Marine Ecology-Progress Series* **303**:1-29.

- Kerhin, R. T., J. P. Halka, D. V. Wells, E. L. Hennessee, P. J. Blakeslee, N. Zoltan, and R. H. Cuthbertsen. 1988. Surficial Sediments of Chesapeake Bay, Maryland: Physical Characteristics and Sediment Budget.
- Kimmel, B., O. Lind, and L. Paulson. 1990. Reservoir primary production. IN: Reservoir Limnology: Ecological Perspectives. John Wiley & Sons, New York. 1990. p 133-193, 8 fig, 4 tab, 278 refs. U. S. DOE Contract.
- Koike, I., and A. Hattori. 1978. Denitrification and ammonia formation in anaerobic coastal sediments. *Applied and Environmental Microbiology* **35**:278-282.
- Kostka, J. E., and G. W. Luther, III. 1994. Partitioning and speciation of solid phase iron in saltmarsh sediments. *Geochimica Et Cosmochimica Acta* **58**:1701-1710.
- Kozelnik, P., J. A. Tomaszek, and R. Gruca-Rokosz. 2007. The significance of denitrification in relation to external loading and nitrogen retention in a mountain reservoir. *Marine and Freshwater Research* **58**:818-826.
- Krom, M. D., and R. A. Berner. 1980. Adsorption of phosphate in anoxic marine sediments. *Limnology and Oceanography* **25**:797-806.
- Krom, M. D., and R. A. Berner. 1981. The diagenesis of phosphorus in a nearshore marine sediment. *Geochimica Et Cosmochimica Acta* **45**:207-216.
- Langland, M. J. 2015. Sediment transport and capacity change in three reservoirs, Lower Susquehanna River Basin, Pennsylvania and Maryland, 1900-2012. 2331-1258, US Geological Survey.
- Larsen, R. K., J. C. Steinbacher, and J. E. Baker. 2001. Ammonia exchange between the atmosphere and the surface waters at two locations in the Chesapeake Bay. *Environmental Science & Technology* **35**:4731-4738.
- Lehtoranta, J., P. Ekholm, and H. Pitkanen. 2009. Coastal Eutrophication Thresholds: A Matter of Sediment Microbial Processes. *Ambio* **38**:303-308.
- Leventhal, J., and C. Taylor. 1990. Comparison of methods to determine degree of pyritization. *Geochimica Et Cosmochimica Acta* **54**:2621-2625.
- Li, Z., Y. Sheng, J. Yang, and E. D. Burton. 2016. Phosphorus release from coastal sediments: Impacts of the oxidation-reduction potential and sulfide. *Marine Pollution Bulletin* **113**:176-181.
- Limnotech, and UMCES. 2007. Development of a phosphorus dynamics sub-model for incorporation into the next-generation Potomac River environmental model. Prepared for Metropolitan Washington Council of Governments. Limnotech, Inc. and University of Maryland Center for Environmental Science.
- Linker, L. C., R. A. Batiuk, C. F. Cerco, G. W. Shenk, R. Tian, P. Wang, and G. Yactayo. 2016. Influence of Reservoir Infill on Coastal Deep Water Hypoxia. *Journal of Environmental Quality* **45**:887-893.
- Marvin-DiPasquale, M. C., W. R. Boynton, and D. G. Capone. 2003. Benthic sulfate reduction along the Chesapeake bay central channel. II. Temporal controls. *Marine Ecology-Progress Series* **260**:55-70.
- McLean, R. I., J. K. Summers, C. R. Olsen, S. L. Domotor, I. L. Larsen, and H. Wilson. 1991. Sediment Accumulation Rates In Conowingo Reservoir As Determined By Man-Made And Natural Radionuclides. *Estuaries* **14**:148-156.
- Middelburg, J. J. 1989. A simple rate model of organic matter decomposition in marine sediments. *Geochimica Et Cosmochimica Acta* **53**:1577-1581.
- Mortimer, C. H. 1941. The exchange of dissolved substances between mud and lake water. *Journal of Ecology* **29**:280-329.
- Nilsson, C., and K. Berggren. 2000. Alterations of Riparian Ecosystems Caused by River Regulation: Dam operations have caused global-scale ecological changes in riparian ecosystems. How to protect

- river environments and human needs of rivers remains one of the most important questions of our time. *Bioscience* **50**:783-792.
- Owens, M., and J. C. Cornwell. 2006. Spokane Lake Sediment Nutrient Fluxes. Final Report For Wastewater Management, City of Spokane, WA. Chesapeake Biogeochemical Associates.
- Owens, M., and J. C. Cornwell. 2008a. Spokane Lake Sediment: Elevated pH and SRP Release. Final Report to Wastewater Management, City of Spokane, WA. Chesapeake Biogeochemical Associates.
- Owens, M. S., and J. C. Cornwell. 2008b. East Canyon Reservoir Sediment Nutrient Fluxes. Final Report to Snyderville Basin Water Reclamation District (Utah).
- Owens, M. S., and J. C. Cornwell. 2009. Spokane Lake Phosphorus Biogeochemistry: Anoxic Fluxes from Plant Bed Sediments. 2008 Field and Experimental Studies. Final Report to Wastewater Management, City of Spokane WA. Chesapeake Biogeochemical Associates, Sharptown MD.
- Owens, M. S., and J. C. Cornwell. 2016. The Benthic Exchange of O<sub>2</sub>, N<sub>2</sub> and Dissolved Nutrients Using Small Core Incubations. *Journal of Visualized Experiments* **114**: e54098.
- Pacini, N., and R. Gachter. 1999. Speciation of riverine particulate phosphorus during rain events. *Biogeochemistry* **47**:87-109.
- Palinkas, C. M., J. P. Halka, M. Li, L. P. Sanford, and P. Cheng. 2014. Sediment deposition from tropical storms in the upper Chesapeake Bay: Field observations and model simulations. *Continental Shelf Research* **86**:6-16.
- Parsons, T. R., Y. Maita, and C. M. Lalli. 1984. *A Manual of Chemical and Biological Methods for Seawater Analysis*. Pergamon Press, New York.
- Perez-Villalona, H., J. C. Cornwell, J. R. Ortiz-Zayas, and E. Cuevas. 2015. Sediment Denitrification and Nutrient Fluxes in the San Jos, Lagoon, a Tropical Lagoon in the Highly Urbanized San Juan Bay Estuary, Puerto Rico. *Estuaries and Coasts* **38**:2259-2278.
- Poulton, S. W., and R. Raiswell. 2005. Chemical and physical characteristics of iron oxides in riverine and glacial meltwater sediments. *Chemical Geology* **218**:203-221.
- Rabalais, N. N., R. E. Turner, and W. J. Wiseman. 2002. Gulf of Mexico hypoxia, aka "The dead zone". *Annual Review of Ecology and Systematics* **33**:235-263.
- Reeburgh, W. S. 1983. Rates of biogeochemical processes in anoxic sediments. *Annual Review of Earth and Planetary Science* **11**:269-298.
- Rich, J. J., O. R. Dale, B. Song, and B. B. Ward. 2008. Anaerobic ammonium oxidation (Anammox) in Chesapeake Bay sediments. *Microbial Ecology* **55**:311-320.
- Risgaard-Petersen, N., R. L. Meyer, M. Schmid, M. S. M. Jetten, A. Enrich-Prast, S. Rysgaard, and N. P. Revsbech. 2004. Anaerobic ammonium oxidation in an estuarine sediment. *Aquatic Microbial Ecology* **36**:293-304.
- Roden, E. E., and J. W. Edmonds. 1997. Phosphate mobilization in iron-rich anaerobic sediments: Microbial Fe(III) oxide reduction versus iron-sulfide formation. *Archiv Fur Hydrobiologie* **139**:347-378.
- Roden, E. E., and J. H. Tuttle. 1992. Sulfide Release from Estuarine Sediments Underlying Anoxic Bottom Water. *Limnology and Oceanography* **37**:725-738.
- Ruttenberg, K. C. 1992. Development of a sequential extraction method for different forms of phosphorus in marine sediments. *Limnology and Oceanography* **37**:1460-1482.
- Schubel, J., and D. Pritchard. 1986. Responses of upper Chesapeake Bay to variations in discharge of the Susquehanna River. *Estuaries and Coasts* **9**:236-249.
- Scicluna, T. R., R. J. Woodland, Y. Zhu, M. R. Grace, and P. L. Cook. 2015. Deep dynamic pools of phosphorus in the sediment of a temperate lagoon with recurring blooms of diazotrophic cyanobacteria. *Limnology and Oceanography* **60**:2185-2196.

- Seitzinger, S. P. 1991. The effect of pH on the release of phosphorus from Potomac estuary sediments: implications for blue-green algal blooms. *Estuarine, Coastal and Shelf Science* **33**:409-418.
- Seitzinger, S. P., W. S. Gardner, and A. L. Spratt. 1991. The effect of salinity on ammonium sorption in aquatic sediments: Implications for benthic nutrient recycling. *Estuaries* **14**:167-174.
- Spiteri, C., P. Van Cappellen, and P. Regnier. 2008. Surface complexation effects on phosphate adsorption to ferric iron oxyhydroxides along pH and salinity gradients in estuaries and coastal aquifers. *Geochimica Et Cosmochimica Acta* **72**:3431-3445.
- Stainton, M. P. 1973. A syringe gas-stripping procedure for gas-chromatographic determination of dissolved inorganic and organic carbon in fresh water and carbonates in sediments. *Journal of the Fisheries Research Board of Canada* **30**:1441-1445.
- Stumm, W., and J. J. Morgan. 1981. *Aquatic Chemistry*. Second edition. John Wiley & Sons, Inc., New York.
- Testa, J. M., D. C. Brady, J. C. Cornwell, M. S. Owens, L. P. Sanford, C. R. Newell, S. E. Suttles, and R. I. E. Newell. 2015. Modeling the impact of floating oyster (*Crassostrea virginica*) aquaculture on sediment-water nutrient and oxygen fluxes. *Aquaculture Environment Interactions* **7**:205-222.
- Testa, J. M., D. C. Brady, D. M. Di Toro, W. R. Boynton, J. C. Cornwell, and W. M. Kemp. 2013. Sediment flux modeling: Simulating nitrogen, phosphorus, and silica cycles. *Estuarine Coastal and Shelf Science* **131**:245-263.
- Thornton, S. F., and J. McManus. 1994. Application of organic carbon and nitrogen isotope and C/N ratios as source indicators of organic matter provenance in estuarine ecosystems: Evidence from the Tay estuary, Scotland. *Estuarine, Coastal and Shelf Science* **38**:219-233.
- Weston, N. B., A. E. Giblin, G. T. Banta, C. S. Hopkinson, and J. Tucker. 2010. The Effects of Varying Salinity on Ammonium Exchange in Estuarine Sediments of the Parker River, Massachusetts. *Estuaries and Coasts* **33**:985-1003.
- Zhang, Q., D. C. Brady, and W. P. Ball. 2013. Long-term seasonal trends of nitrogen, phosphorus, and suspended sediment load from the non-tidal Susquehanna River Basin to Chesapeake Bay. *Sci Total Environ* **452-453**:208-221.
- Zhang, Q., D. C. Brady, W. R. Boynton, and W. P. Ball. 2015. Long-Term Trends of Nutrients and Sediment from the Nontidal Chesapeake Watershed: An Assessment of Progress by River and Season. *Journal of the American Water Resources Association* **51**:1534-1555.
- Zhang, Q., R. M. Hirsch, and W. P. Ball. 2016. Long-Term Changes in Sediment and Nutrient Delivery from Conowingo Dam to Chesapeake Bay: Effects of Reservoir Sedimentation. *Environmental Science & Technology* **50**:1877-1886.